AN INVESTIGATION OF CONSTANT VELOCITY GRADIENT EFFECTS IN SEISMIC ANALYSIS

DAHANAYAKE BANDULA
WICKRAMARATNA

AN INVESTIGATION OF CONSTANT VELOCITY GRADIENT EFFECTS IN SEISMIC ANALYSIS

BY

© Dahanayake Bandula Wickramaratna, B.Sc. Eng.(Hons)

A thesis submitted to the School of Graduate Studies in partial fulfillment of the requirements for the degree of Master of Engineering

Faculty of Engineering and Applied Science
Memorial University of Newfoundland

August 1983

St. John's Newfoundland Canada

TO MY FRIEND

YASAWATHIE MUNASINGHE

AN INVESTIGATION OF CONSTANT VELOCITY GRADIENT EFFECTS IN SEISMIC ANALYSIS

ABSTRACT

Information concerning acoustic velocities plays an important role in seismic analysis. Acoustic velocity of the medium can be approximated by a polynomial function of depth. The concept that velocity varies linearly with depth has been considered by many researchers as an appropriate assumption for developing the velocity profile for a medium.

In this study the linear velocity profile approach has been used to estimate the parameters of the medium. The normal moveout relationship for a single zero-dipping reflector has been derived. A methodology for obtaining the parameters such as the reflector geometry and the constant velocity gradient of the medium from the surface observable x - t data is presented.

Further, the linear velocity profile model for a sloping reflector has been derived based on the normal ray analysis. Based on the knowledge of the velocity profile the least squares technique has been used to identify the reflector geometry from reflection data. The x - t data has been obtained by shifting the shot/receiver position progressively. A comparative analysis has been made to obtain the effect of constant velocity gradient in seismic analysis.

ACKNOWLEDGEMENT

I wish to express my gratitude to Dr. W.J. Vetter, Professor in Electrical Engineering, Memorial University of Newfoundland, Canada, for providing me the opportunity to do research under his guidance. He has been instrumental in the initiation, conduct and completion of this research work.

My thanks are due to Dr. Ross Peters, Dean of Engineering and Dr. T.R. Chari, Associate Dean of Engineering for providing the necessary facilities for conducting this research work.

It is my duty to thank Dr. F. Aldrich, Dean of Graduate Studies for making it possible for me to persue studies at Memorial University of Newfoundland.

TABLE OF CONTENTS

LIST OF TABLES

LIST OF ILLUSTRATIONS

OVERVIEW

We present here a brief summary of the content of the subsequent chapters. Detailed references to the literature are not given here as they are presented at the appropriate points in the subsequent material.

In Chapter I, the seismic objectives are briefly discussed in order to facilitate the understanding of the problem. Data gathering, processing, migration and interpretation are the main points considered. Objectives of the thesis are also presented.

In Chapter II, the fundamentals of acoustic wave propagation and their relations to the parameters of the media are discussed. The different ray theoretical approaches to the wave equation are presented. The behaviour of the raypaths in a vertically inhomogeneous medium are considered. The analysis pertaining to the raypaths in a constant velocity medium and in an one-dimensionally continuous linear velocity gradient medium is presented.

In the concluding part of this chapter the analysis of reflection phenomena at an interface is considered. This analysis gives some understanding about the reflection coefficient and the acoustic impedance contrast relationship at medium boundaries. It shows the effect of incidence angle on reflection and transmission coefficients.

Chapter III is divided into two parts - A and B. In part A, the segment-wise constant velocity profile multilayered medium is considered. Also, the methods of estimating the reflector geometry from reflection data has been presented. Part B is devoted to the analysis pertaining to the linear

velocity profile model. A zero-dipping reflector is considered. The normal moveout relationship is derived in the form which is suitable for obtaining the parameters of the medium. The least squares technique is used to obtain the parameters. The simulation results are presented.

In Chapter IV, the linear velocity profile model for a dipping reflector has been considered, based on the normal ray analysis. A suitable mathematical model has been formulated for obtaining the reflector geometry from reflection data. A method of obtaining reflection data is presented.

Chapter V is devoted to an error analysis of using the constant velocity profile model to estimate the reflector geometry in a linear velocity profile medium. A linear velocity profile medium is considered in the forward computation, i.e. in obtaining the data. In the reverse computation, i.e. in estimating the parameters of the medium an assumption is made that the velocity of the medium is a constant, equal to the average velocity of the data generating system. The resultant errors of the estimates are obtained for the noise-free simulation data.

In Chapter VI, the main conclusions and further areas of research are presented.

CHAPTER - I

OBJECTIVES OF THE EXPORATION SEISMICS

1.1 SEISMIC OBJECTIVES

Seismic encompasses the broad range of phenomena involving natural or deliberate excitation of the earth or a local section of the earth's surface, the attendant wave propagation, and diverse signal and medium interactions involved in such phenomena. Seismic phenomena involve a broad range of physical principles, and a comprehension of the phenomena involves an interdisciplinary approach with aspects from geology, physical and mechanical properties of substances, rock mechanics, engineering, oceanography and sedimentology, data acquisition and processing, mathematics and signal theory, and others.

One generally makes a distinction between seismology and exploration seismics. Seismology is a branch of geophysics, which is concerned with deep-earth phenomena, strong ground motion and related earthquake hazard, volcanoes and related man-caused disturbances, etc. Exploration seismics is identified as pertains generally to the search for hydrocarbon and mineral resources, and involving very deliberate probing signal and extensive sensing and interpretation of the medium responses. Other applications in exploration seismics pertain to study of geological media in general, study of deep and shallow ocean sediments within the framework of oceanography, and geotechnical and engineering studies of media.

The broad objective of exploratory seismic analysis is to extract from the responses, estimates of medium geometry, composition, and parameters which are influential in the interaction of signal and media. Seismic analysis is associated with geophysical modeling (model building is a

systematic coordination of theoretical and empirical elements of the knowledge into a joint construct). In seismics, the real earth is approximated by a model in certain significant respects.

Our study is mainly concerned with the subsurface structure of the seabed and of deep media with hydrocarbon potential. Seismic methods have become indispensable in the search of oil and gas. They are utilized for the exploration of new reservoirs and also for the evaluation of discoveries and existing fields. Drilling activities for the search of hydrocarbon are generally guided by insight from the deep seismic data and from bore-hole information. The engineering criteria for design and siting of offshore structures involved in the drilling and extraction activities are based on the shallow seismic data.

The seismic reflection method is an acoustic imaging technique. The main objective is to collect information from the earth's subsurface by measuring and analysing the response to seismic excitations at the earth's surface. Most of the analysis deals with compressional waves (also known as p-waves). However, to obtain some further properties like rigidity modulus one must also consider the shear waves (called s-waves).

In exploration seismics, the disturbance created by a seismic energy source propagates through the earth and is reflected from the medium discontinuities. The reflected signal consists of the primary reflections as well as multiple reflections. The arrival time of the primary reflections at the surface contains information about propagation velocity

of the subsurface strata. Reflection strengths contain information about contrast in characteristic impedances at the discontinuities.

Seismic activities can be divided into four main sub classifications, namely,

. data acquisition
. data processing
. migration and
. interpretation.

In exploration seismics, arrays of transducers are used to collect the data. There are four principal types of trace gathers, namely, common-source gather, common-receiver gather, common-offset gather, and common-depth-point gather. The type of gather to be used depends on the objectives. Usually, a total of 24 or 48 sensors are used for each gather. These sensor signals are first multiplexed together and then recorded on magnetic tapes. In view of the above, the recorded responses have to be demultiplexed before processing. Subsequently, some time corrections for various phenomena are carried out. The time correction comprises static correction and dynamic correction. Through the static correction one attempts to remove the variations from anomalous conditions of the earth, specifically, the elevation effects and effects of greatly differing surface layer velocities. The static correction is not required for seismic recording at sea. The dynamic correction is the time correction applied for the path differences. It depends on geometry of spread and reflector depth.

The signal-to-noise ratio (SNR) of seismic responses can be enhanced

greatly through superposition or stacking of a gather. Stacking should be done after normal-move-out correction (i.e. the dynamic correction). In addition to the inherent enhancement of the signal-to-noise ratio, stacking reduces the effect of multiple reflections. Among these gathers, the common-depth-point gather is generally used for construction of the velocity spectra plot used for obtaining the estimates of velocities. It can also be used to obtain the interval velocities and the datum velocity. In addition, velocity spectra are used in applications like checking the presence of shale body or oil and gas reservoirs. Further, the amount of multiples present in the seismic gather can also be obtained using the velocity spectra.

Data processing is carried out by using a model, which is developed, based on the physical insight of the phenomena.

In exploration seismics, the reflection amplitudes, through their dependence on parameters for the media on the two sides of an interface can contribute to the interpretation of geological detail. In practice, large amplitude effects known as bright spots may indicate an interface between a porous gas-bearing medium and an oil-or water-bearing medium or a strongly reflecting cap rock. Such a phenomenon can sometimes be seen on reflection seismograms and on velocity spectra displays.

If it were possible to probe the medium with an ideal impulse, the reflection response would be the impulse response of the medium, and would contain impulses from the medium discontinuities. In practice, the probing pulse is at best impulse-like and the pulse shape may

frequently be unknown. In order to enhance the primary reflections, which contain the information of interest about the medium, one needs to remove the non-ideal pulse shape effects, as well as any strong reveberations, ghost and other multiple reflections. The method of predictive deconvolution introduced by Robinson (1967) has been successfully used for these tasks. A fundamental assumption for this method is that the reflectivity at the interfaces are statistically random so that the earth impulse response can be considered to be a random signal. With the additional assumptions that the source wavelet is minimum phase and that the layered earth is a linear system, it is then possible to effect a decomposition of the source wavelet and the (random) innovation signal representing the medium impulse response. The effectiveness of deconvolution filtering on actual data depends on the extent to which the inherent assumptions apply in the actual situation. In practice these assumptions may not be upheld. The widespread applications of predictive deconvolution have proved its ability for primary reflection enhancement. In a typical data processing sequence, the deconvolution procedure follows a number of additional digital filter applications to compress the source pulse and to provide a greater emphasis to the deeper reflections. This is achieved by Wiener shaping filters. The variation in source pulse shape with travel time can be accounted for by windowing the trace and applying the Wiener filter [Robinson et al (1980)].

Homomorphic filtering is a generalization of linear filtering for certain non-linear filtering problems. It can be applied for the

deconvolution. The results are satisfactory under high signal-to-noise ratios [Tribolet (1979)]. This method can be used if the frequency ranges of the excitation and the system response are significantly different. This technique has been considered as an alternative approach for seismic deconvolution. The results are generally unsatisfactory since the seismic signals have usually low signal-to-noise ratios (SNR).

The maximum entropy method (MEM) has been developed [Burg (1967)] for spectral analysis. This technique produces a power spectral estimate corresponding to the most random and least predictable time series. This estimation technique effects the minimization of the prediction error and of the hindsight or retrospection error. For a large number of data points the results by this technique are very similar to the results obtained by the Wiener-Levinson method. The maximum entropy representation of the observed data is an autoregressive process (AR) [Van den Bos (1971)]. This technique is applicable to the observed data to the extent that these satisfy the autoregressive model hypothesis. This technique is in general superior to the more conventional spectral analysis methods [Lacoss (1971)., Burg (1970)., Ulrych (1972)., Ulrych (1975)]. Most of the usual methods of spectral analysis have associated window functions which are independent of the data or of the properties of the random process. The maximum entropy method (MEM) and maximum likelihood method (MLM) [Capon (1969)., Lacoss (1971)] do not have fixed window functions. It has been shown that the reciprocal of the maximum likelihood spectrum is equal to the average

of the reciprocals of the maximum entropy spectra [Burg (1972). The maximum entropy method has not been widely applied in exploration seismics since in this method the data is matched with an autoregressive (AR) process whereas the medium response is more appropriately modelled as an autoregressive moving average (ARMA) process. The MEM technique may be suitable for earthquake seismic analysis where the data are reasonably consistent with an autoregressive process. The MEM is of considerable importance in situations where short time series are encountered. A principal difficulty in applying MEM is the choice of operator length. This technique has found many applications outside the seismic area.

The state space approach has been suggested for seismic signal analysis [Mendel (1978)., Bayless et al (1970)., Berkhout et al (1976)., Crump (1974)., Ott et al (1972)]. The autoregressive and moving average (ARMA) model can be represented in state space form [Mendel (1977)., Silvia et al (1979)]. In such a representation, since the system matrices are unknown, the task of estimating the medium impulse response becomes a state and parameter estimation problem. It seems that Ljung's corrected extended Kalman filter [Ljung (1979)] can be used as a state and parameter estimator in seismic applications. The Minimum Variance [Mendel (1981)] and Maximum Likelihood [Kormylo et al (1983)] techniques can also be used in seismic applications based on state space model. The main advantage in the state space approach is that the assumptions such as stationarity of the noise, the minimum delay concept, linearity and time invariance need not be made, as in other deconvolution

techniques.

In processing of marine seismic data, a typical sequence of procedures is as follows: [Robinson et al (1980)].

- demultiplexing
- reformatting
- sorting for relative amplitude scaling
- bandpass filtering
- predictive deconvolution
- Wiener filtering
- CDP sorting
- velocity analysis
- NMO correction
- CDP stacking
- Wiener filtering
- modeling
- migration
- interpretation.

Now, turning our attention to the migration, one of the basic problems in exploration seismology is to obtain the coordinates of the subsurface structures. The reflection seismogram does not give the information about the true reflection point. The seismogram shows as if the reflection occurs direct beneath the CDP point when in reality, unless the reflector is horizontal, the reflection would be located elsewhere. To obtain the true reflector point from the reflection seismogram, a knowledge of the velocity profile is necessary. If the velocity profile is known it is possible to trace the ray path and hence to determine

the true reflection point. In our study, we have made the assumption that the velocity of the medium is varying linearly to enable us to estimate the true reflection point. The true reflector geometry identification from the reflection data is known as migration. The migration can be divided into two main categories, namely, geometrical migration and wave equation migration. There are different techniques under these categories. These techniques are discussed in the following paragraphs.

There are two geometrical migration techniques, namely, maximum convexity migration and wavefront migration. In principle, both the migration techniques are the same for a given record section. The maximum convexity migration takes the values of the record section along a hyperbolic arc and puts their sum at its apex [Robinson (1982)]. Wavefront migration takes the value of the record section at a point and puts the value evenly along the circular arc that has this point as its deepest point [Hagendoorn (1954)., Hubral (1977)., Robinson et al (1980)., McQuillin et al (1979)., Robinson (1982)].

The wave equation migration is closely related to the problem of determining the wave field that exists in the propagating media. In wave equation migration it is assumed that the sources are positioned along the reflector surface with strength proportional to the reflection coefficients and all the sources are activated at time t = 0 [Berkhout (1980)]. The receivers are on the surface of the ground. The migration problem is considered as a depropagation from time t = t (surface of the ground) to time t = 0 (surface of the reflector) in reverse

direction. There are three different wave equation migration techniques, namely, Fourier transform wave equation migration, finite difference approach and Kirchhoff migration. The Fourier transform technique does not allow any lateral variation of velocity along the entire section, since it is a non recursive technique. The non recursive techniques cannot be used with the lateral velocity variations. But the vertical velocity variations can be handled by recursive application of the Fourier transform technique [Stolt (1978)., Robinson (1980)].

The finite difference approach is commonly used in seismic migration. It is a recursive technique. The downward extrapolation result at depth level $z_i = i\,\Delta z$ is computed from the previous extrapolation result at $z_{i-1} = (i-1)\,\Delta z$. This technique can be used with lateral velocity variations since it is recursive. The error involved is the major problem in this technique. The error increases with depth. The errors are frequency dependent for a fixed extrapolation step Δz_i. This leads to an undesirable effect called dispersion. By selecting a floating time reference the errors can be made small for small steps [Claerbout (1976)., Berkhout (1980)]. This technique is most suitable for spatially bandlimited recursive migration. In selecting a migration, one can use one's own choice depending on the complexity of the structure. It is not possible to rely on one particular migration technique. Expensive recursive methods should not be used for simple subsurfaces. Simple nonrecursive methods cannot be used for complicated structural situations. Out of all migration techniques one has to select the most suitable technique depending on the particular seismic situation.

parameters of the medium from the reflection data.

Further, a linear velocity profile model for dipping reflectors is considered. The same problem was considered by Michaels 1977. However, in our analysis, the problem is considered in a different way. A model which relates the moving shot/receiver distance and travel time to the parameters of the medium is derived, using normal ray analysis. An explicit formula is then derived for obtaining the true reflector point. Finally, the above model is used to obtain the resultant error due to the constant velocity assumption if the medium has a linear velocity profile. The average velocity of the data generating system is used as the constant velocity of the medium.

Since this study is mainly dealing with raypath analysis, it begins with the raypath approach to the solution of the wave equation and uses this solution for the raypath analysis in constant and linear velocity profile media, before proceeding to the main study.

1.2 OBJECTIVES OF THE THESIS

In seismics, a knowledge of the acoustic velocities is important. Acoustic velocities are characterized by the properties of the media. The velocity of a medium is required for estimating its reflector geometry. The acoustic propagation velocity and depth estimates are indicators of the medium composition, lithology and strategraphy. These factors are also necessary in seismic response interpretation.

The reflection strength plays a major role in seismic analysis. In the case of the non-normal incidences the reflection strength depends on the velocity contrast and the incidence angle. The reflection strength is a function of the velocity contrast only for the normal incidences. The acoustic velocities are used to obtain the density and the elastic properties of the medium.

The velocity of the medium can be approximated by a polynomial function of depth. The simplest approximation to the velocity profile is the constant velocity profile. The segmentwise constant velocity profile is more appropriate than the constant velocity assumption. Since the velocity in a medium is generally increasing with depth it is more appropriate to consider the velocity as a linear function of depth. The normal moveout relation for a linear velocity profile medium was discussed by Slotnick (1959). That relationship is not in a form suitable to estimate the parameters of the medium. Therefore, a different equation structure is developed to the normal moveout relationship for a single zero-dipping reflector using the linear velocity profile assumption. This enables the estimation of the

CHAPTER II

ACOUSTIC PROPAGATION AND ITS RELATIONSHIP TO THE PARAMETERS OF THE MEDIUM

2.1 GENERAL

Sound propagation is governed by a linear second order partial differential equation known as the wave equation. The general three dimensional wave equation* can be written as [Officer (1958)],

$$\nabla^2 \psi = \frac{1}{V^2} \frac{\partial^2}{\partial t^2} \psi \qquad (2.1)$$

where ∇^2 is the scalar operator

$$\nabla^2 \triangleq \frac{\partial^2}{\partial x^2} + \frac{\partial^2}{\partial y^2} + \frac{\partial^2}{\partial z^2} \quad \text{and}$$

V is the acoustic velocity of the medium

2.1.1 RAY THEORETICAL APPROACH TO THE WAVE EQUATION

There are two approaches for obtaining a solution for the above wave equation in terms of ray theory.

i.e., . eikonal equation

. Fermat's principle

The eikonal equation is based on wave surfaces and ray theory. The wave surfaces are the loci of points which undergo the same motion in a one-to-one correspondence at a given instant of time. The rays are normal to the wave surfaces and they give the direction of propagation of energy through the medium. The Fermat's principle postulates ray paths between two points in a medium as the paths of minimum travel

*ψ may represent a pressure, a displacement, or velocity potential, or some other appropriate variable.

time. By solving the above ray equations between two points for a given earth model, it is possible to know the travel time and ray paths between the source and receiver. These ray theory approaches are particularly useful in solving the inverse problem in reflection seismics and earthquake seismology. In the next section, each one of the approaches is considered.

2.1.1.1 EIKONAL EQUATION

The wave equation can be transformed to a first order partial differential equation known as the eikonal equation [Officer (1958), Lee et al (1981)]. The solution can be interpreted in terms of wavefronts and rays. In general, the three-dimensional wave equation 2.1 has an associated characteristic equation given by,

$$\left(\frac{\partial\psi}{\partial x}\right)^2 + \left(\frac{\partial\psi}{\partial y}\right)^2 + \left(\frac{\partial\psi}{\partial z}\right)^2 = \frac{1}{V^2}\left(\frac{\partial\psi}{\partial t}\right)^2 \qquad (2.2)$$

where,

V is the acoustic velocity.

In cases where V is not a constant, equation 2.2 does not represent the associated characteristic equation of the wave equation 2.1. The eikonal equation will be a good approximation to the wave equation if the fractional change in the velocity over a wavelength is small.

It can be shown that a more general solution for equation 2.1 or 2.2 takes the form.

$$\psi = \psi[w(x,y,z) - V_o t] \qquad (2.3)$$

w = function representing the wavefront surface

V_o = constant reference velocity.

By substituting equation 2.3, in equation 2.2, we obtain an equation known as the eikonal equation which is given below,

$$\left(\frac{\partial w}{\partial x}\right)^2 + \left(\frac{\partial w}{\partial y}\right)^2 + \left(\frac{\partial w}{\partial z}\right)^2 = \left(\frac{V_o}{V}\right)^2 = n^2 \qquad (2.4)$$

where n is the index of refraction and $n = \frac{V_o}{V}$

The eikonal equation leads directly to the concept of rays. It is particularly useful in solving problems in a heterogeneous medium where the velocity is a function of the spatial co-ordinates. The eikonal equation is a first order partial differential equation. It's solution, for a specified time t, is given by

$$w(x,y,z) = \text{constant} \qquad (2.5)$$

This represents a surface in three-dimensional space. For a given value of w and at a given instant of time t, any variable at the surface will be in phase, but not necessarily of the same amplitude. This surface is called 'wavefront' since it preserves a one to one correspondance of motion along the surface. The propagation can be described by the time progression of the wavefront. The normal to the wavefront at any spatial coordinate defines the direction of propagation,

and the loci traced out by these normal directions are referred to as rays.

The normals to the wavefront evolve in accordance with the incremental path length relationship

$$ds = \frac{dx}{(\partial w/\partial x)} = \frac{dy}{(\partial w/\partial y)} = \frac{dz}{(\partial w/\partial z)} \qquad (2.6)$$

where the denominator factors are the direction numbers of the normal. The direction cosines are proportional to the direction numbers, so that

$$\frac{dx}{ds} = k.\frac{\partial w}{\partial x}$$

$$\frac{dy}{ds} = k.\frac{\partial w}{\partial y} \qquad (2.7)$$

$$\frac{dz}{ds} = k.\frac{\partial w}{\partial z}$$

where k is a constant and ds is an incremental element of the ray path.

Since an incremental segment 'ds' of a curve in three-dimensional space satisfies

$$\left(\frac{dx}{ds}\right)^2 + \left(\frac{dy}{ds}\right)^2 + \left(\frac{dz}{ds}\right)^2 = 1, \qquad (2.8)$$

we obtain the following from equations 2.4, 2.7 and 2.8:

$$1 = k^2 \left[\left(\frac{\partial w}{\partial x}\right)^2 + \left(\frac{\partial w}{\partial y}\right)^2 + \left(\frac{\partial w}{\partial z}\right)^2\right] = k^2 n^2. \qquad (2.9)$$

From equation 2.9,

$$k = \frac{1}{n}.$$

It is also possible to rewrite equation 2.7 as given below:

$$n \frac{dx}{ds} = \frac{\partial w}{\partial x} \qquad (2.10.1)$$

$$n \frac{dy}{ds} = \frac{\partial w}{\partial y} \qquad (2.10.2)$$

$$n \frac{dz}{ds} = \frac{\partial w}{\partial z} \qquad (2.10.3)$$

By considering the derivative $\frac{d}{ds}$ of the equation 2.10.1, along the raypath we get,

$$\frac{d}{ds}\left(n \frac{dx}{ds}\right) = \frac{d}{ds}\left(\frac{\partial w}{\partial x}\right)$$

$$\frac{d}{ds}\left(n \frac{dx}{ds}\right) = \frac{\partial}{\partial x}\left(\frac{\partial w}{\partial x} \cdot \frac{dx}{ds} + \frac{\partial w}{\partial y} \cdot \frac{dy}{ds} + \frac{\partial w}{\partial z} \cdot \frac{dz}{ds}\right) \qquad (2.11)$$

From equations 2.10.1 and 2.11 we obtain,

$$\frac{d}{ds}\left(n \frac{dx}{ds}\right) = \frac{\partial n}{\partial x} \qquad (2.12.1)$$

Similarly, it is possible to get the following by considering 2.10.2 and 2.10.3.

$$\frac{d}{ds}\left(n\frac{dy}{ds}\right) = \frac{\partial n}{\partial y} \qquad (2.12.2)$$

$$\frac{d}{ds}\left(n\frac{dz}{ds}\right) = \frac{\partial n}{\partial z} \qquad (2.12.3)$$

The above relations indicate that the refraction index n governs the ray evolution and wavefront geometry.

2.1.1.2 FERMAT'S PRINCIPLE

The ray equation can be derived from Fermat's principle [Officer (1958), Caruthers (1977), Aki et al (1980)]. This is specifically appealing in cases when the ray path and travel time between two end points is to be investigated.

This deviation is based on the assumptions that the velocity is only a function of spatial coordinates and that the velocity is continuous and has continuous first partial derivatives. The Fermat's principle states that the path which a ray will trace between two points is such that the travel time is an extremum. It actually means that the time for a ray to travel between two points must be stationary with respect to small variations of the path [Pilant (1979)].

We have to find the stationary value of the integral I given as

$$I = V_o \int_A^B dt$$

Substituting for dt, we have

$$I = V_o \int_A^B \frac{ds}{V}$$

$$= \int_A^B n \; ds, \text{ since } \frac{V_o}{V} = n \qquad (2.13.1)$$

where A and B are the two end points of the travel path. If the length ds is represented as a dummy variable $d\sigma$, one obtains,

$$ds = [(\frac{\partial x}{\partial \sigma})^2 + (\frac{\partial y}{\partial \sigma})^2 + (\frac{\partial z}{\partial \sigma})^2]^{\frac{1}{2}} \, d\sigma \qquad (2.13.2)$$

Equation 2.13.1 with 2.13.2 gives

$$I = \int_A^B n(x,y,z) \cdot [(\frac{\partial x}{\partial \sigma})^2 + (\frac{\partial y}{\partial \sigma})^2 + (\frac{\partial z}{\partial \sigma})^2]^{\frac{1}{2}} \, d\sigma$$

$$\triangleq \int_A^B F(x,y,z, \frac{\partial x}{\partial \sigma}, \frac{\partial y}{\partial \sigma}, \frac{\partial z}{\partial \sigma}) \, d\sigma \qquad (2.14)$$

For a stationary value of I, Euler's equations must be satisfied, namely,

$$\frac{\partial F}{\partial x_i} - \frac{d}{d\sigma} \left[\frac{\partial F}{\partial (\frac{\partial x_i}{\partial \sigma})} \right] = 0, \; i = 1,2,3 \qquad (2.15)$$

which leads equation 2.14 to the following explicit form:*

$$[(\frac{\partial x}{\partial \sigma})^2 + (\frac{\partial y}{\partial \sigma})^2 + (\frac{\partial z}{\partial \sigma})^2]^{\frac{1}{2}} \nabla n - \frac{d}{d\sigma} \left(\frac{n \, (\partial \underline{x}/\partial \sigma)}{[(\frac{\partial x}{\partial \sigma})^2 + (\frac{\partial y}{\partial \sigma})^2 + (\frac{\partial z}{\partial \sigma})^2]^{\frac{1}{2}}} \right) = 0$$

---

* $\underline{x} \triangleq (x,y,z)$ and $\nabla \triangleq i \frac{\partial}{\partial x} + j \frac{\partial}{\partial y} + k \frac{\partial}{\partial z}$

It can be further simplified to the following by virtue of the equatios 2.15 and 2.13.2.

$$\frac{d}{ds}\left(n\,\frac{dx}{ds}\right) = \nabla n \qquad (2.16)$$

The equation 2.16 is identical to equation 2.12, which had been obtained through the eikonal equation. Hence Fermat's principle indicates that the stationary time path is the ray path given by the eikonal equation.

2.2. RAYS IN A VERTICALLY INHOMOGENEOUS MEDIUM

Proceeding further, the vertically inhomogeneous medium is defined as the one in which the medium parameters vary as a function of depth only. One can compute the time necessary for a disturbance to propagate from a point A to point B along a ray path given by T(AB) [Pilant (1979)],

$$T(AB) = \int_A^B \frac{ds}{V} = \int_A^B \frac{[(dz)^2 + (dx)^2]^{\frac{1}{2}}}{V}$$

$$= \int_A^B \frac{[1 + (dz/dx)^2]^{\frac{1}{2}}}{V}\,dx$$

if $z' = \frac{dz}{dx}$, then

$$\frac{1}{V}[1 + (\frac{dz}{dx})^2]^{\frac{1}{2}} = F(z,z')$$

In this case, for travel time to be stationary, an extremum necessitates that,

$$\frac{d}{dx}\left(\frac{\partial F}{\partial z'}\right) - \frac{\partial F}{\partial z} = 0$$

But $\frac{d}{dx}\left[F(z,z') - z'\frac{\partial F}{\partial z}\right] = z'\left[\frac{\partial F}{\partial z} - z'\frac{d}{dx}\left(\frac{\partial F}{\partial z'}\right)\right] = 0$. (2.17)

Using the stationary condition one obtains.

$$z'\frac{\partial F}{\partial z'} = \frac{1}{V}(z')^2\left[1 + (z')^2\right]^{-\frac{1}{2}} \qquad (2.18)$$

By combining 2.17 and 2.18 one obtains,

$$F(z, z') - z'\frac{\partial F}{\partial z'} = \frac{1}{V}\left[1 + (z')^2\right]^{-\frac{1}{2}} = P$$

where P is a constant which is known as the ray parameter. If we designate the incident angle at depth z as θ, then $\frac{dz}{dx} = z' = \cot\theta$ and

$$\frac{\sin\theta(z)}{V(z)} = P \qquad (2.19)$$

This is the generalized form of Snell's Law.

The ray parameter P can be related to two physically observable quantities at the surface, namely incidence angle (θ_s) and acoustic velocity (V_s). The relationship is,

$$P = \frac{\sin\theta_s}{V_s} = \frac{1}{V_{\substack{\text{apparent}\\ \text{horizontal}\\ \text{velocity}}}} = \frac{dT}{dx}$$

where T is the travel-time to depth coordinate z encountered at a range coordinate x. At the maximum depth of penetration of the ray, $\theta = 90°$ and

$$P = \frac{1}{V_{max}}$$

Hence,

$$\frac{dT}{dx} = \frac{1}{V_{max}}$$

Based on the above, the apparent horizontal surface velocity is equal to the medium velocity at the depth of greatest penetration.

By differentiating equation 2.19 with respect to arc length ds along the ray, one obtains,

$$- V^{-2} \sin\theta \frac{dV}{ds} + V^{-1} \cos\theta \frac{d\theta}{ds} = 0 \qquad (2.20)$$

But $$\frac{dV}{ds} = \frac{dV}{dz} \cdot \frac{dz}{ds} = \frac{dV}{dz} \cos\theta$$

By substituting in 2.20

$$\frac{d\theta}{ds} = P \frac{dV}{dz} \qquad (2.21)$$

This indicates that the curvature of a ray in a vertically inhomogeneous medium is directly proportional to the velocity gradient.

From equation 2.19 and 2.21, one obtains,

$$\frac{d\theta}{ds} = \frac{\sin\theta}{V} \cdot \frac{dV}{dz} \qquad (2.22.1)$$

By geometrical relationship, we know that

$$\frac{ds}{dz} = \frac{1}{\cos\theta}$$

It is also possible to write 2.19 or 2.21 in the form

$$\cos\theta \cdot \frac{d\theta}{dV} = \frac{\sin\theta}{V} = P \qquad (2.22.2)$$

The relationships given by equations 2.19, 2.21 and 2.22 will be used to analyse the behaviour of the raypaths in media having different velocity profiles, especially constant velocity profile and linear velocity profile.

2.2.1 RAYPATHS IN A CONSTANT VELOCITY MEDIUM

In a constant velocity medium $V(z) = V_o$ = constant, hence $\frac{dV}{dz} = 0$ and therefore by the equation 2.21, $\frac{d\theta}{ds} = 0$. Accordingly $\theta(z) = \theta_o$ = constant. A constant velocity medium does not alter the ray direction. The ray conserves its initial incident angle. The minimum time path between any two points A and B along the raypath is a straight line.

If $A = (x_A, y_A, z_A)$, and

$B = (x_B, y_B, z_B)$

then the path length between A and B is given by

$$S = [(x_B - x_A)^2 + (y_B - y_A)^2 + (z_B - z_A)^2]^{\frac{1}{2}} ;$$

the travel time t is given by

$t = S/V$; and

the direction cosines for the ray AB are given by

$$\frac{(x_B-x_A)}{S}, \quad \frac{(y_B-y_A)}{S}, \quad \frac{(z_B-z_A)}{S}$$

Hence, the angle of ray departure at the source, θ is given by

$$\theta = \cos^{-1}[(z_B - z_A)/S] .$$

So far we have been concerned with the raypaths in a constant velocity model which is the simplest model. In the next section we will consider raypaths in a linear velocity profile medium.

2.2.2 RAYPATHS IN ONE-DIMENSIONALLY CONTINUOUS LINEAR VELOCITY PROFILE MEDIA

The seismic velocity generally increases with depth in the earth's crust. It is very common to consider velocity to be a continuous function of depth rather than to use the constant velocity assumption [Vetter (1981)., Greenhalgh et al (1981)., Telford et al (1978)., Hubral et al (1980)., Slotnick (1959)]. The next simplest velocity profile to a constant velocity profile is one where the velocity is a linear function of depth. In the situations where the constant velocity gradient assumption is invalid, the medium can be considered to consist of a number of depth intervals. In each of these depth intervals, the velocity profile might be approximated by a constant gradient profile.

The constant gradient velocity profile is given by

$$V(z) = v_0 + g\,z, \qquad (2.23)$$

where V_o and g are constants, the values of which depend upon the particular situation. By taking the derivative with respect to z of the above equation, we get,

$$\frac{d}{dz}\,[V(z)] = g.$$

We are already aware that the following relationships are applicable for an incremental element of a raypath ds,

$$dx = ds \cdot \sin\theta(z) \qquad (2.24.1)$$

$$dz = ds \cdot \cos\theta(z) \qquad (2.24.2)$$

$$ds = V(z) \cdot dt \qquad (2.24.3)$$

Where $\theta(z)$ is the ray angle of incidence at depth z. The travel time t in between two points A and B along the raypath can be represented by,

$$t = \int_A^B dt$$

$$= \int_A^B \frac{ds}{V(z)}$$

$$= \int_A^B \frac{dz}{V(z) \cdot \cos\theta(z)}$$

$$= \int_A^B \frac{d[V(z)]}{g \cdot V(z) \cdot \cos\theta(z)}$$

$$= \frac{1}{g} \int_{\theta_o}^{\theta(z)} \frac{d[\theta(z)]}{\sin\theta(z)}$$

By integrating, we can obtain the raytime relationship

$$t(\theta,\theta_o) = \frac{1}{g} \ln \left[\frac{\tan(\theta/2)}{\tan(\theta_o/2)}\right] \quad . \qquad (2.25)$$

Similarly, $x(\theta)$ and $z(\theta)$ can be found from equation 2.22.1 and 2.24, whence

$$z(\theta,\theta_o) = \frac{1}{Pg} \int_{\theta_o}^{\theta} \cos\theta \, . \, d\theta = \frac{1}{Pg} [\sin\theta - \sin\theta_o] \qquad (2.26)$$

$$x(\theta,\theta_o) = \frac{1}{Pg} \int_{\theta_o}^{\theta} \sin\theta \, . \, d\theta = \frac{1}{Pg} [\cos\theta_o - \cos\theta] \quad . \qquad (2.27)$$

By eliminating the angle θ from equations 2.26 and 2.27, the raypath is obtained as a function of x and z, as given below,

$$\left(x - \frac{\cos\theta_o}{Pg}\right)^2 + \left(z + \frac{\sin\theta_o}{Pg}\right)^2 = \left(\frac{1}{Pg}\right)^2 \quad . \qquad (2.28)$$

By suitably substituting from equation 2.19, we get

$$\left(x - \frac{V_o}{g \tan\theta_o}\right)^2 + \left(z + \frac{V_o}{g}\right)^2 = \left(\frac{V_o}{g \sin\theta_o}\right)^2 \qquad (2.29)$$

where, θ_o = ray departure angle at the datum surface.

It will be seen from equation 2.29, that the raypath is circular, having radius $\frac{V_o}{g \sin\theta_o}$ and center $\left(\frac{V_o}{g \tan\theta_o}, \frac{-V_o}{g}\right)$

$\frac{dV}{dz}$ is positive for a region where the velocity is increasihg with depth, so that from equation 2.21, $\frac{d\theta}{ds}$ is positive. Hence the ray will curve upwards.

Similarly, we can conclude that for a region where the velocity is decreasing with depth, a ray will curve downwards, towards a region of minimum velocity. The same result is also to be expected from a qualitative consideration of the motion of the wavefronts. The portion of the wavefront which is in a region of higher velocity will travel faster than that in a lower velocity region and the wavefront will be bent toward the region of lower velocity.

In petroleum exploration we are usually dealing with more-or-less flat-lying bedding. As a result of slow changes in density and elastic properties of the beds the changes in seismic velocity as we move horizontally are small. The horizontal variations are generally much less rapid than the variations in the vertical direction. This may be due to lithological changes and the increasing pressure with depth. Since the horizontal changes are gradual we can take it into account by dividing the survey area into smaller areas in such a way that horizontal variations can be ignored. Then the same vertical velocity distribution can be used with different parameters.

2.3 REFLECTION - INTRODUCTION

The seismic methods exploit the elastic properties of the material. In seismic prospecting for oil and gas one must consider the frequency content of the probing signal. It is observed that the higher the frequency, the higher is the resolution, but at the same time penetration depth is lower due to larger attenuation caused by absorption

and dispersion. Also, the converse is true i.e. the lower the frequency the larger the penetration but the weaker the resolution. Therefore there is a tradeoff between resolution and penetration. Low frequencies ranging from 0.5 Hz - 60 Hz are of practical interest for the penetration depth of up to 10,000 meters in deep seismic exploration studies. In shallow seismics and geotechnical seismics up to 10 KHz or even 100 KHz is used with penetration of 10m to 100 meters.

Seismic velocities are very much dependent upon the media, in contrast to radio waves. Hence the velocity information plays an important role for extracting the properties of the media. In the case of normal incidence, the mode conversion such as compressional waves to compressional and shear waves does not take place. But for non-normal incidence, the reflected energy appears partly in the form of compressional waves and partly in the form of shear waves. The compressional and shear waves velocities are governed by the properties of the media. For further extraction of medium properties one has to consider non-normal incidences.

In exploration seismics we analyse the reflected signals which carry information about the earth's subsurface. The reflections of seismic waves occur at interfaces with significant change of acoustic impedance. The reflection coefficient is highly dependent on the incidence angle which is the angle between a raypath and the normal to the surface at the incident point. Hence the reflected energy depends on the incident angle in the case of non-normal incidences.

Now, we will attempt to derive the applicable relationships for the case of acoustic media where we study the reflection at an interface in the subsequent paragraph [Temkin (1981)., Caruthers (1977)., Kinsler et al (1962)]. The corresponding relationships for elastic media are considerably more complex and virtually intractable for analytical insight. The phenomena have been extensively studied by Knott (1899) and Zoeppritz (1919), Cerveny and Revindra (1971), Aki and Richards (1980) and many others.

The parametric dependencies for these situations are more conveniently studied on computer generated plots for reflection coefficients as a function of incident angle [Young and Braile (1976)., Telford et al (1976)., Aki and Richards (1980)].

2.3.1 REFLECTION AT AN INTERFACE

Consider the reflection and transmission of a plane acoustic wave at a plane boundary between two media having different densities and sound speeds. Referring to Figure 2, (x,y,z) is a coordinate system such that the boundary is the z = 0 plane. The x-axis is parallel to lines of intersection of the wavefronts and z = 0 plane. We shall consider two coordinates y and z. We consider a single sinusoidal component P_i from the integral sum of the Fourier series representation of the plane wave.

$$P_i = A \exp [j (\underline{k}_i \cdot \underline{r} - \omega_i t)] \qquad (2.30)$$

P_i is an incident upon the z = 0 plane with an incident angle θ_i. This incident wave generates reflected and transmitted waves P_r and P_2,

which are given respectively by [Caruthers (1977)., Temkin (1981)],

$$P_r = B \exp [j (\underline{k}_r \cdot \underline{r} - \omega_r \cdot t)] \quad (2.31)$$

$$P_2 = C \exp [j (\underline{k}_2 \cdot \underline{r} - \omega_2 t)] \quad (2.32)$$

B anc C may be complex to account for phase shifts. The $\underline{k}$'s are the propagation vectors for the respective waves. The $\underline{k} \cdot \underline{r}$'s can be written as,

$$\underline{k}_i \cdot \underline{r} = \frac{\omega_i}{V_1} (y \sin \theta_i + z \cos \theta_i) \quad (2.33.1)$$

$$\underline{k}_r \cdot \underline{r} = \frac{\omega_r}{V_1} (y \sin \theta_r - z \cos \theta_r) \quad (2.33.2)$$

$$\underline{k}_2 \cdot \underline{r} = \frac{\omega_2}{V_2} (y \sin \theta_2 + z \cos \theta_2) \quad (2.33.3)$$

The P_1 and P_2 are the solutions of the wave equation 2.1,

where $P_1 = P_i + P_r$ (2.34)

The boundary conditions become

$$P_1 (y,0) = P_2 (y,0) \quad (2.35)$$

$$\frac{1}{\rho_1} \frac{\partial P_1}{\partial z} \bigg|_{z = 0} = \frac{1}{\rho_2} \frac{\partial P_2}{\partial z} \bigg|_{z = 0} \quad (2.36)$$

At the interface the boundary conditions are independent of time. This is possible only if the frequencies of the transmitted and reflected waves are the same as those of the incident wave,

i.e. $\omega_i = \omega_r = \omega_2 = \omega$

The equation 2.36 shows that the normal particle velocities in the two media be the same at the boundary, i.e. $\theta_i = \theta_r$

$$\text{Let } \theta_i = \theta_r = \theta_1 \tag{2.37}$$

The equation 2.35 gives the Snell's law relation

$$\frac{\sin \theta_i}{V_1} = \frac{\sin \theta_r}{V_1} = \frac{\sin \theta_2}{V_2} \tag{2.38}$$

Equation 2.38 together with 2.37 gives the law of refraction,

$$\frac{\sin \theta_1}{V_1} = \frac{\sin \theta_2}{V_2}$$

The acoustic waves may be expressed by

$$P_i = A \exp\left[j\omega \left(\frac{y \sin \theta_1}{V_1} + \frac{z \cos \theta_1}{V_1} - t\right)\right]$$

$$P_r = B \exp\left[j\omega \left(\frac{y \sin \theta_1}{V_1} - \frac{z \cos \theta_1}{V_1} - t\right)\right] \tag{2.39}$$

$$P_2 = C \exp\left[j\omega \left(\frac{y \sin \theta_1}{V_1} + \frac{z \cos \theta_2}{V_2} - t\right)\right]$$

Applying the boundary conditions at z = 0 one obtains

$$P_i + P_r = P_2 \tag{2.40}$$

$$\frac{\cos\theta_1}{\rho_1 V_1}(P_i - P_r) = \frac{\cos\theta_2}{\rho_2 V_2} \cdot P_2 \qquad (2.41)$$

We define the "reflection coefficient" R by

$$R \triangleq \frac{P_r}{P_i} \qquad (2.42)$$

and the "transmission coefficient" T by

$$T \triangleq \frac{P_2}{P_i} \qquad (2.43)$$

It can be easily shown that

$$T = R + 1 \qquad (2.44)$$

and

$$\frac{\cos\theta_1}{\rho_1 V_1}(1 - R) = \frac{\cos\theta_2}{\rho_2 V_2} \cdot T \qquad (2.45)$$

In general R and T are complex.

By solving the above equations for R and T one obtains,

$$R = \frac{\dfrac{\cos\theta_1}{\rho_1 V_1} - \dfrac{\cos\theta_2}{\rho_2 V_2}}{\dfrac{\cos\theta_1}{\rho_1 V_1} + \dfrac{\cos\theta_2}{\rho_2 V_2}} = \frac{\rho_2 V_2 \cos\theta_1 - \rho_1 V_1 \cos\theta_2}{\rho_2 V_2 \cos\theta_1 + \rho_1 V_1 \cos\theta_2}$$

$$T = \frac{2 \cdot \frac{\cos \theta_1}{\rho_1 V_1}}{\frac{\cos \theta_1}{\rho_1 V_1} + \frac{\cos \theta_2}{\rho_2 V_2}} = \frac{2 \rho_2 V_2 \cos \theta_1}{\rho_2 V_2 \cos \theta_1 + \rho_1 V_1 \cos \theta_2}$$

Using Snell's law relation it can be derived that

$$R = \frac{\rho_2 V_2 \cos \theta_1 - \rho_1 [V_1^2 - V_2^2 \sin^2 \theta_1]^{\frac{1}{2}}}{\rho_2 V_2 \cos \theta_1 + \rho_1 [V_1^2 - V_2^2 \sin^2 \theta_1]^{\frac{1}{2}}} \qquad (2.46)$$

$$T = \frac{2 \rho_1 V_2 \cos \theta_1}{\rho_2 V_2 \cos \theta_1 + \rho_1 V_1 [1 - (\frac{V_2}{V_1})^2 \sin^2 \theta_1]^{\frac{1}{2}}} \qquad (2.47)$$

At normal incidence $\theta_1 = 0$, which reduces 2:46 to

$$R = \frac{\rho_2 V_2 - \rho_1 V_1}{\rho_2 V_2 + \rho_1 V_1} \qquad (2.48)$$

The product of density and acoustic velocity is defined as "acoustic impedance" of the medium, i.e. $Z = \rho V \equiv$ acoustic impedance

By substituting in 2.48

$$R = \frac{Z_2 - Z_1}{Z_2 + Z_1} .$$

If $\rho_2 V_2 = \rho_1 V_1$ the reflection coefficient for normal incidence becomes zero, whereas for oblique incidence the reflection coefficient is not equal to zero. For oblique incidence, the reflection coefficient vanishes and one obtains total transmission for an angle of incidence θ_1^*, which is known as the angle of intromission. The value of θ_1^* is obtained from the relation

$$\rho_2 \tan \theta_2 = \rho_1 \tan \theta_1^*$$

$$\tan^2 \theta_1^* = \frac{\rho_2^2 V_2^2 \sin^2 \theta_1^*}{\rho_1^2 (V_1^2 - V_2^2 \sin^2 \theta_1^*)}$$

$$\tan^2 \theta_1^* = \frac{(\rho_2 V_2)^2 - (\rho_1 V_1)^2}{\rho_1^2 (V_1^2 - V_2^2)} \qquad (2.49)$$

Many inferences can be drawn from the above equation considering the comparative values of velocities and densities of the media as given below:

Intromission is only possible if either:

$$\rho_2 V_2 > \rho_1 V_1 \quad \text{and} \quad V_1 > V_2$$

or

$$\rho_2 V_2 < \rho_1 V_1 \quad \text{and} \quad V_1 < V_2$$

The parameter combinations for an air-water or a water-air interface are such that there is no angle of incidence for which one can offer total transmission.

If $V_2 > V_1$ at an interface, then there exists an angle $\theta_i = \theta_{crit}$, such that the refracted ray has an angle of $\pi/2$ radians, i.e. it is

coincident with the medium boundary. From Snell's Law, this critical angle θ_c is governed by

$$\sin \theta_c = \frac{V_1}{V_2}$$

At critical incidence the refracted wave does not penetrate into the second medium, so that T = 0 and R = 1, i.e. total reflection occurs.

Again, if $V_2 > V_1$, there can be angles of incidence θ_i greater than the critical angle. In the ray-theoretic model the transmission coefficient T takes purely imaginary values. This leads to the interpretation of a lossless interface, wave propagating in the second medium along the boundary with a rapidly decaying penetration depth.

So far we have considered in detail the reflections at interfaces. This study will be followed by raypath analysis, which will form the fundamental basis for our forthcoming discussion on the estimation of acoustic velocities from the surface measurements proposed in the next chapter.

CHAPTER - III

ESTIMATION OF ACOUSTIC MEDIUM VELOCITIES FROM SURFACE MEASUREMENTS

III - A.

MULTILAYERED MEDIUM WITH SEGMENTWISE CONSTANT VELOCITY PROFILES

3.1 COMMON DEPTH POINT STACKING (CDP)

This method is associated with a common mid point between source and receiver. The gather is composited to get common source receiver mid-point. In the horizontal parallel layer case this midpoint is also a common reflection point (CRP). This summing becomes successful since primary CRP reflections are in phase and add constructively, whereas ambient noise and other seismic signals which are not in phase tend to cancel. If we consider the number of traces in a gather is N, this method increases the signal-to-noise ratio (SNR) by a factor of $\sqrt{N}$. Before stacking, CDP traces must be corrected for the travel-time difference caused by varying raypath distances. This correction is referred to as normal-move out (NMO). This NMO depends on depth to the reflecting horizon. It is also called as dynamic correction. The improved signal-to-noise ratio (SNR) and attenuation of multiples utilizing the CRP can be attained only by applying the proper NMO time corrections.

The CRP method can be used to obtain the velocity spectra. The velocity spectra provide the basis for identifying primary reflections and to determine stacking velocities which can be used to determine interval velocities. They are also useful to predict information relevant to lithology. Further estimation of the datum velocity (i.e. the velocity at Z_{ref}) can also be obtained using velocity spectra.

Before we get into the details of the velocity spectra, it is necessary to obtain travel time and source receiver distance relationships for the parallel layers case.

3.0 GENERAL

In this section we discuss the segmentwise horizontally parallel multi-layered medium. The methods and relationships for estimating depths, layer intervals and interval velocities through the concepts of normal moveout (and stacking velocity), Dix's formula, velocity spectra etc., are presented. The results for the simulation data have been given.

3.2 TRAVEL TIME AND SOURCE-RECEIVER DISTANCE RELATIONSHIP FOR HORIZONTALLY LAYERED EARTH

We shall select the x axis as horizontal and z axis as vertically downward. The source is at point (0,0) and reciver is at (x,0). We will assume n-layers of earth [Taner et al (1969)., Dix (1955)] having layerwise constant propagation velocities. Using the method of ray-paths, we can compute the time for a ray starting from the origin in its travel through n-horizontal layers and after reflection from the n-interfaces, returning to the surface at (x,0). The solution can be obtained by use of Fermat's principle.

Let the thickness of the n-layers of earth be d_1, d_2, $d_3 \ldots \ldots d_n$ and the compressional velocities V_1, V_2, $V_3 \ldots\ldots\ldots V_n$. It is assumed that the length of downward travelling ray within the K^{th} layer is λ_k having horizontal component x_k and angle θ_k to the vertical.

The total down-up travel time T_x is then given by

$$T_x = 2 \sum_{k=1}^{n} \frac{\lambda_k}{V_k} \tag{3.1}$$

which should be a minimum under the conditions given by geometrical relations,

$$\lambda_k^2 = d_k^2 + x_k^2 \tag{3.2}$$

$$2(x_1 + x_2 + \ldots\ldots\ldots + x_n) = x \text{ (sensor offset)} \tag{3.3}$$

The condition for a minimum value for equation 3.1, under the constraints 3.2 and 3.3 is given by,

$$\frac{\delta T_x}{\delta x_k} = \frac{2x_k}{\lambda_k V_k} = 2P, \quad k = 1, 2 \ldots\ldots n \tag{3.4}$$

where P is the Lagrange multiplier and it is given by,

$$P = \frac{x_k}{\lambda_k V_k} = \frac{\sin \theta_k}{V_k}, \quad k = 1, 2, 3 \ldots\ldots n$$

This is the Snell's Law relationship, and P can be identified as the ray parameter for any particular ray. Equations 3.4 and 3.2 give the relation

$$x_k^2 = \frac{P^2 V_k^2 d_k^2}{1 - P^2 V_k^2} \tag{3.5}$$

From equations 3.1 and 3.3 together with 3.5, one obtains,

$$x = 2P \sum_{k=1}^{n} \frac{V_k d_k}{\sqrt{1 - P^2 V_k^2}} \tag{3.6}$$

$$T_x = 2 \sum_{k=1}^{n} \frac{d_k / V_k}{\sqrt{1 - P^2 V_k^2}} \tag{3.7}$$

Now, considering the constant velocity medium we have $V_1 = V_2 = \ldots\ldots = V_n$. Let the constant compressional velocity be equal to V. By using this condition in above equations 3.6 and 3.7, one obtains,

$$x = \frac{2P\ Vd}{\sqrt{1 - P^2 V^2}}$$

$$T_x = \frac{2d/V}{\sqrt{1 - P^2 V^2}}$$

where, $d = d_1 + d_2 + \ldots\ldots + d_n$.

Eliminating P from these x and T_x relationships one obtains,

$$T_x^2 = \frac{4d^2}{V^2} + \frac{x^2}{V^2}$$

$$T_x^2 = T_o^2 + \frac{x^2}{V^2} \qquad (3.8)$$

where, $T_o^2 = \frac{4d^2}{V^2}$

From the above equation 3.8, we get the approximated relation for the normal moveout correction ΔT_{NMO} for $x << d$,

$$\Delta T_{NMO} = T_x - T_o \approx \frac{x^2}{2T_o V^2}$$

where T_o is the two-way travel time for zero offset. T_x is the two-way travel time for a trace of offset distance x.

In most of the cases, the velocities of each of the layers having thickness $d_1, d_2, d_3 \ldots\ldots d_n$, are different and they are given by $V_1, V_2, V_3 \ldots\ldots V_n$. In view of the above, the travel time to offset distance x can be represented as an infinite series which is given below.

$$T_x^2 = c_1 + c_2x^2 + c_3x^4 + c_4x^6 \ldots\ldots\ldots$$

The values of the coefficients $c_1, c_2 \ldots\ldots$ will depend on $d_1, d_2, \ldots\ldots d_n$ and $V_1, V_2 \ldots\ldots V_n$. The coefficients can be obtained [Taner et al (1969)] by representing the above series as a power series of P^2 and equating the coefficients.

For the first two coefficients accordingly, we get

$$c_1 = \left(2 \sum_{k=1}^{n} \frac{d_k}{V_k}\right)^2$$

$$c_2 = \frac{\sum_{k=1}^{n} d_k/V_k}{\sum_{k=1}^{n} V_k d_k}$$

Let $t_k = \frac{d_k}{V_k}$, which is the one-way travel time for a vertical ray to cross the k^{th} layer.

$$\frac{1}{c_2} = \bar{V}^2 = \frac{\sum_{k=1}^{n} V_k d_k}{\sum_{k=1}^{n} \frac{d_k}{V_k}} = \frac{\sum_{k=1}^{n} t_k V_k^2}{\sum_{k=1}^{n} t_k}$$

The $1/c_2$ is the weighted average of the squares of the interval velocities. The weights are vertical travel time in the respective layers.

Since the effect of higher order coefficients are small, a second order approximation is normally used. The approximated formula is given by

$$T_x^2 = \left(2 \sum_{k=1}^{n} \frac{d_k}{V_k}\right)^2 + \frac{x^2}{\bar{V}^2} \qquad (3.9)$$

This is the same formula given by Dix 1955.

Having obtained the above relationship, we will use it as the basis in our ensuing discussion on velocity spectra.

3.3 VELOCITY SPECTRA

In seismology the distances to subsurface reflectors are calculated using travel times and the estimated velocities. Therefore the velocity becomes a most important factor in seismic prospecting. Knowledge of the velocities are so important since it is related to the properties of the medium. As it is observed from equation 3.8, hyperbolic characteristics of reflection time-distance curves provide a means to establish necessary velocity-time relationships. The velocity-time display is called a velocity spectrum. This can be obtained by scanning CDP ensembles along hyperbolic trajectories qualified by assumed $\overline{V}$ - rms velocity values for signal coherence. The determination of velocities becomes a matter of scanning various hyperbolic trajectories for maximum reflection coherency. The spectra can be generated as shown in figure 3.3.1 by incrementing normal incidence travel time T_o and keeping them constant while incrementing $\overline{V}$ at regular intervals between some minimum and maximum value. Each (T_o, $\overline{V}$) pair defines a hyperbola. The coherency of data contained in a time gate about this curve is measured and plotted in a three dimensional space (time, velocity, coherency). From the set of trial $\overline{V}$ values for a particular T_o, one assigns that $\overline{V}$ value which gives rise to the maximum coherency. If it is plotted in a two dimensional space the coherency can be displayed as contour lines. It is shown in figure 3.3.2.

In addition to the primary reflections, multiple reflections may align along the hyperbolic trajectories and therefore careful interpretation of velocity spectra is required. The above interpretation can be made by locating the peak on the coherency surface which corresponds to

primary reflections. The peaks can be joined carefully to obtain a profile of the velocities. The estimates of the datum velocity V_0 can be obtained by extending this profile (figure 3.3.2).

3.3.1 COHERENCY MEASUREMENTS

Cross-correlation and semblance are commonly used for coherence measurements. The coherency function S evaluated at zero lag is normally used since it is not sensitive to the rms signal amplitude variation between channels.

S is given by [Robinson et al 1980],

$$S = \frac{2}{M(M-1)} \sum_{i=1}^{M} \sum_{i>i'} \frac{R_{ii'}(0)}{\sqrt{R_{ii}(0)\, R_{i'i'}(0)}}$$

where, M = number of folds (traces in the gather),

$R_{ii}(0)$ = zero lag value of the autocorrelation function of the i^{th} trace

$R_{i'i'}(0)$ = zero lag value of the autocorrelation function of the i'^{th} trace,

$R_{ii'}(0)$ = zero lag value of the crosscorrelation function of the i^{th} and the i' traces.

$$-1 \leq S \leq +1$$

S = 1 corresponds to perfect coherency.

The other useful coherency measure is semblance. The semblance coefficient - S_c is sensitive to channel amplitude differences.

$$0 \leq S_c \leq 1$$

The value of S_c is given by,

$$S_c = \frac{\sum_{i=1}^{M} \sum_{i'=1}^{M} R_{ii'}(0)}{M \sum_{i=1}^{M} R_{ii}(0)}$$

3.4 USES OF THE VELOCITY SPECTRA

Uses of the velocity spectra can be summarized as follows.

- velocity spectra determines the velocity function for optimum stacking.
- It helps to determine the effects of multiple interference. In many cases it can be used to determine the timing, order, apparent velocity and relative power of multiples. By comparing this with primary reflections we can get the amount of multiple content in the stacked section.
- We can obtain the interval velocities between major reflections using the relationship

$$V_n^2 = \frac{\bar{V}_n^2 \, T_{o,n} - \bar{V}_{n-1}^2 \, T_{o,n-1}}{T_{o,n} - T_{o,n-1}}$$

The interval velocities can be used in calculating the reflection depth, layer thickness, dip and other parameters for migration. The interval velocities are also the parameters used for lithological correlation (geology).

- It can be used to estimate stratigraphic and structural information. Changes of character of primaries on velocity spectra indicate the changes in stratigraphy. Figure 3.2 shows that primaries appear

up to 1.2 sec. In the region of 1.2 sec. to 2.4 sec. primaries dissappear and only the multiples are present. From 2.4 sec. onwards primaries appear again. This disappearance of primaries between 1.2 sec. to 2.4 sec. shows the stratigraphic change.

In order to obtain the acoustic velocities of the media using the constant velocity gradient model one must obtain the value of the datum velocity and the velocity gradient - g of the medium. It can be seen from the figure 3.3.2 that the

$$\lim_{t \to o} V \simeq \text{datum velocity} = V_o .$$

III - B

LINEAR VELOCITY PROFILE

MEDIUM

3.5.0 GENERAL

In the previous section, the segmentwise constant acoustic velocity profile model has been considered. It is more appropriate to consider the linear velocity profile assumption since the acoustic velocities are increasing with depth, which is very clear from the figure 3.5.0.

In this section we develop a linear velocity profile model in the form which is suitable for the estimation of the medium parameters from the reflection data. A methodology for obtaining the linear velocity gradient and the reflector geometry has been presented.

3.5 NORMAL MOVEOUT RELATIONSHIP FOR THE LINEAR VELOCITY PROFILE MODEL

This problem has been considered by Vetter 1983. In this section we present a derivation of normal moveout relation for the linear velocity model. Further, a method for obtaining the reflector geometry and the velocity gradient is discussed with a simulation example.

We shall consider zero dipping reflector for our proposed analysis. Figure 3.5.2 shows a raypath for the normal moveout in a linear velocity profile medium.

Now referring to Figure 3.5.2, we have,

$$\theta_o = \phi - \alpha$$
$$\theta = \phi + \alpha \qquad (3.5.1)$$

where ϕ is the angle of the chord between source and the reflection point on the reflector measured from the vertical.

Using the Snell's Law relation (equation 2.19), one obtains,

$$\frac{V_o}{\sin(\phi - \alpha)} = \frac{V_r}{\sin(\phi + \alpha)} \qquad (3.5.2)$$

where

V_o = datum velocity

V_r = velocity at the reflector

Equation 3.5.1 and 3.5.2 gives the relation,

$$\tan\alpha = \left[\frac{V_r - V_o}{V_r + V_o}\right] \tan\phi \qquad (3.5.3)$$

Since, $V_r = V_o + gz$ for the linear velocity profile model, one obtains

$$\tan \alpha = \frac{gz}{2V_a} \tan \phi \qquad (3.5.4)$$

where, $V_a = (V_o + V_r)/2$

$$= V_o + \frac{gz}{2} \text{ (profile average velocity)} \qquad (3.5.5)$$

From figure 3.5.2 it can be seen that

$$x = z \tan \phi \, . \qquad (3.5.6)$$

Therefore, equation 3.5.4 can be rewritten as,

$$\tan \alpha = \frac{gx}{2V_a} \, . \qquad (3.5.7)$$

Using equations 3.5.1 and 2.25, one can obtain the relationship [Vetter (1983)]

$$\exp (gt) = \frac{\sin \phi + \sin \alpha}{\sin \phi - \sin \alpha} \qquad (3.5.8)$$

Equation 3.5.8 can be rearranged to the form

$$\sin \alpha = \left[\frac{\exp (gt) - 1}{\exp (gt) + 1}\right] \sin \phi \qquad (3.5.9)$$

Equation 3.5.3 and 3.5.9 can be then combined to give the relationship,

$$(x^2 + z^2)^{\frac{1}{2}} \cos \alpha = \left[\frac{\exp (gt) - 1}{\exp (gt) + 1}\right] \frac{2V_a}{g}$$

Simplifying further, we have

$$x^2 \left[1 - \left(\frac{\exp (gt) - 1}{\exp (gt) + 1}\right)^2\right] + z^2 = \left(\frac{\exp (gt) - 1}{\exp (gt) + 1}\right)^2 \left(\frac{2V_a}{g}\right)^2 \qquad (3.5.10)$$

From equation 3.5.8 together with 3.5.4 one can obtain the one way travel time,

$$t = \frac{1}{g} \ln \frac{[1 + (\frac{x}{z})^2 (\frac{gz}{2V_a})^2]^{\frac{1}{2}} + \frac{gz}{2V_a} [1 + (\frac{x}{z})^2]^{\frac{1}{2}}}{[1 + (\frac{x}{z})^2 (\frac{gz}{2V_a})^2]^{\frac{1}{2}} - \frac{gz}{2V_a} [1 + (\frac{x}{z})^2]^{\frac{1}{2}}} \quad . \tag{3.5.11}$$

For a given medium with vertical linear velocity profile (V_o, g) and reflector depth z, $\frac{gz}{2V_a}$ becomes a parameter, which we designate as Q,

$$Q \triangleq \frac{gz}{2V_a} \quad . \tag{3.5.12}$$

It can also be written in the form,

$$Q = \frac{V_r - V_o}{V_r + V_o} = \frac{(V_r/V_o) - 1}{(V_r/V_o) + 1} \tag{3.5.13}$$

Q can also be considered as the velocity contrast of the medium.

Since $0 \leq \frac{V_r}{V_o} < \infty$

the value of Q lies in the range,

$$-1 \leq Q < 1 \quad .$$

By rearranging the equation 3.5.13 we get

$$\frac{V_r}{V_o} = \frac{1 + Q}{1 - Q} \quad \text{and}$$

$$\frac{gz}{V_o} = \frac{2Q}{1 - Q} \quad . \tag{3.5.14}$$

For normal incidence it can be shown that the oneway travel time t_N is given by (Appendix 3.5)

$$t_N = \frac{1}{g} \ln \frac{V_r}{V_o} \qquad (3.5.15)$$

i.e. $$\frac{z}{V_o} = \left[\frac{(V_r/V_o) - 1}{\ln (V_r/V_o)}\right] t_N \qquad (3.5.16)$$

It can also be shown that,

$$\frac{z}{V_o} = \frac{1}{g} \left[\frac{V_r}{V_o} - 1\right] . \qquad (3.5.17)$$

The graphs representing the equations 3.5.16 and 3.5.17 are shown in Figure 3.5.3. The same two equations can be represented in a different manner using the parameter Q and the profile average velocity V_a.

$$\frac{z}{V_a} = t_N \left[\frac{2Q}{\ln \left(\frac{1+Q}{1-Q}\right)}\right] \qquad (3.5.18)$$

$$\frac{z}{V_a} = \frac{2}{g} \cdot Q \qquad (3.5.19)$$

The graphs which represent the equations 3.5.18 and 3.5.19 are shown in Figure 3.5.4. It can be seen that the effect of Q on travel time is small for small value of Q, whereas it is considerable for large Q.

Using the parameter Q the travel time relation (equation 3.5.11) can be rewritten as follows

$$t = \frac{1}{g} \ln \frac{[1 + (\frac{Qx}{z})^2]^{\frac{1}{2}} + Q[1 + (\frac{x}{z})^2]^{\frac{1}{2}}}{[1 + (Q\frac{x}{z})^2]^{\frac{1}{2}} - Q[1 + (\frac{x}{z})^2]^{\frac{1}{2}}} \quad (3.5.20)$$

The travel time for normal incidence t_N, given by equation 3.5.15, can be rewritten in the form

$$t_N = \frac{1}{g} \ln [\frac{1 + Q}{1 - Q}] \quad (3.5.21)$$

The relationship for a normalized travel time t/t_N is then

$$\frac{t}{t_N} = \frac{\ln \frac{[1 + (Q\frac{x}{z})^2]^{\frac{1}{2}} + Q[1 + (\frac{x}{z})^2]^{\frac{1}{2}}}{[1 + (Q\frac{x}{z})^2]^{\frac{1}{2}} - Q[1 + (\frac{x}{z})^2]^{\frac{1}{2}}}}{\ln [\frac{1 + Q}{1 - Q}]} \quad (3.5.22)$$

which displays the parametric dependence on the single parameter Q as a function of the ray chord tangent $\frac{x}{z} = \tan \phi$.

The graphical representation of equation 3.5.22 is shown in Figure 3.5.5. It is seen that the effect of Q becomes considerable only for the large offsets.

The apparent velocity can be defined as

$$V_{ap}(x, z, t) \triangleq \frac{d(x,z)}{t(x,z)} = \frac{[x^2+z^2]^{\frac{1}{2}}}{t(x,z)} \quad (3.5.23)$$

where $d = (x^2 + z^2)^{\frac{1}{2}}$.

The deviation of the apparent velocity from the average velocity of the medium is a measure of constant velocity gradient effect.

A normalized apparent velocity with respect to average velocity V_a is then given by

$$V_{apn} \triangleq \left(\frac{d}{t}\right)/V_a$$

$$= \frac{2Q\left[1 + \left(\frac{x}{z}\right)^2\right]^{\frac{1}{2}}}{\ln \frac{\left[1 + \left(Q\frac{x}{z}\right)^2\right]^{\frac{1}{2}} + Q\left[1 + \left(\frac{x}{z}\right)^2\right]^{\frac{1}{2}}}{\left[1 + \left(Q\frac{x}{z}\right)^2\right]^{\frac{1}{2}} - Q\left[1 + \left(\frac{x}{z}\right)^2\right]^{\frac{1}{2}}}} \qquad (3.5.24)$$

The graphical representation of equation 3.5.24 is shown in Figure 3.5.6.

If the apparent velocity $V_{ap}(x,z,t)$ is normalized with respect to the apparent velocity for the normal incidence $V_{ap}(x = 0, z, t)$, we obtain

$$\frac{V_{ap}(x,z,t)}{V_{ap}(x=0,z,t)} = \left(\frac{d}{t}\right)/\left(\frac{z}{t_N}\right)$$

$$= \left(\frac{d}{z}\right)/\left(\frac{t}{t_N}\right),$$

$$= \frac{\left[1 + \left(Q \cdot \frac{x}{z}\right)^2\right]^{\frac{1}{2}} \ln\left[\frac{1+Q}{1-Q}\right]}{\ln \frac{\left[1 + \left(Q \cdot \frac{x}{z}\right)^2\right]^{\frac{1}{2}} + Q\left[1 + \left(\frac{x}{z}\right)^2\right]^{\frac{1}{2}}}{\left[1 + \left(Q \cdot \frac{x}{z}\right)^2\right]^{\frac{1}{2}} - Q\left[1 + \left(\frac{x}{z}\right)^2\right]^{\frac{1}{2}}}} \qquad (3.5.25)$$

The graphical representation of the equation 3.5.25 is shown in Figure 3.5.7. The above relationships can be used as the basis for estimating the reflector depth z and the parameter Q.

3.5.1 ESTIMATION OF THE PARAMETERS OF THE MEDIUM FROM SURFACE MEASUREMENTS USING NORMAL MOVEOUT RELATION

Let us consider the equations 3.5.21 and 3.5.10,

$$gt_N = \ln \left[\frac{1 + Q}{1 - Q}\right] \qquad (3.5.21)$$

$$x^2 \left[1 - \left(\frac{\exp(gt) - 1}{\exp(gt) + 1}\right)^2\right] + z^2 = \left(\frac{\exp(gt) - 1}{\exp(gt) + 1}\right)^2 \left(\frac{2V_a}{g}\right)^2 \qquad (3.5.10)$$

Using the parameter Q, equation 3.5.10 can be rewritten,

$$x^2 \left[1 - \left(\frac{\exp(gt) - 1}{\exp(gt) + 1}\right)^2\right] = z^2 \left[\frac{1}{Q^2} \left(\frac{\exp(gt) - 1}{\exp(gt) + 1}\right)^2 - 1\right] \qquad (3.5.26)$$

By multiplying the equation 3.5.21 by t and rearranging, one obtains,

$$\exp(gt) = \left(\frac{1 + Q}{1 - Q}\right) t/t_N \qquad (3.5.27)$$

If we define A as

$$A \triangleq \left(\frac{1 + Q}{1 - Q}\right) t/t_N = A\,(t/t_N, Q). \qquad (3.5.28)$$

Substitution of the equation 3.5.28 in the equation 3.5.26 gives

$$x^2 \left[1 - \left(\frac{A - 1}{A + 1}\right)^2\right] = z^2 \left[\frac{1}{Q^2} \left(\frac{A - 1}{A + 1}\right)^2 - 1\right] \qquad (3.5.29)$$

Equation 3.5.29 can be further rearranged to the form shown below:

$$(A + \frac{1}{A}) = \left(\frac{4Q^2}{1 + Q^2}\right) \frac{x^2}{z^2} + 2\left(\frac{1 + Q^2}{1 - Q^2}\right) \qquad (3.5.30)$$

$$z = \left[\frac{4Q^2}{(1 - Q^2)\left[(A + \frac{1}{A}) - 2\left(\frac{1 + Q^2}{1 - Q^2}\right)\right]}\right]^{\frac{1}{2}} x \qquad (3.5.31)$$

The equation 3.5.31 is suitable for estimating the reflector depth z from x - t moveout data for a reflection event for sequentially altered trial Q values. The above relationship has been used to estimate the Q value using simulated t Vs x data for a chosen system having Q = 0.5 and z - 500 meters. The graphical representation of equation 3.5.31 for different trial Q values are shown in Figure 3.5.8. The curve representing the smallest variability of depth z against the offset x corresponds to the best estimate of parameters for the x - t data-generating medium. However, the above graph does not represent an observable deviation against small Q variations. Fairly good discrimination can be obtained using the graphs shown in Figure 3.5.9 and 3.5.10. Figure 3.5.9 shows the error of the estimates for different Q values, whereas Figure 3.5.10 gives the estimated depth against different Q values. It can be observed that all the graphs intersect together at the point which corresponds to the data-generating medium. The Figure 3.5.10 is a very sensitive indicator of depth estimate and estimate of Q value.

A fairly accurate estimate of Q can be obtained, if the data generating system Q value is fairly large as we have seen from the figure 3.5.4.

Once the Q values and the reflector depth z are obtained, and also the datum velocity V_o is obtainable from the velocity spectra, the constant velocity gradient g can be obtained from the relation,

$$Q = \frac{gz}{2V_a}$$

i.e.
$$g = \frac{2V_o}{z} \frac{Q}{1 - Q}$$

If the t_N is known presumably, estimates of the velocity gradient g and the average acoustic velocity V_a can be obtained without the knowledge of V_o from the relations,

$$g = \frac{1}{t_N} \ln \left(\frac{1 + Q}{1 - Q}\right)$$

$$V_a = \frac{gz}{2Q}$$

Therefore the linear velocity profile of the medium can be obtained. This knowledge of the velocity profile will be used in the next chapter for identification of a dipping reflector and also for the error analysis in the latter chapter.

APPENDIX 3.5

THE ONEWAY TRAVEL TIME FOR NORMAL INCIDENCE

The oneway travel time for normal incidence can be obtained from the relation,

$$t_N = \int_{t(z=0)}^{t(z)} dt$$

$$= \int_{z=0}^{z} \frac{1}{V(z)}\, dz = \int_{z=0}^{z} \frac{1}{(V_o + gz)}\, dz$$

$$= \frac{1}{g} \int_{z=0}^{z} \frac{d\,(V_o + gz)}{(V_o + gz)}$$

$$= \frac{1}{g} \ln \frac{V_o + gz}{V_o}$$

$$= \frac{1}{g} \ln \frac{V(z)}{V_o}$$

where $V(z) = V_o + gz$

V_o = datum velocity

g = linear velocity gradient (1 - D)

$V(z)$ = velocity at depth z

CHAPTER IV

LINEAR VELOCITY PROFILE MODEL FOR DIPPING REFLECTORS

4.0 GENERAL

The equations which have been developed for horizontal reflectors do not apply to the sloping reflectors. We derive now the applicable relationships for raypath and travel time of the normal rays in a constant velocity gradient model for this situation. These relationships can then be used for estimating reflector geometry and velocity profile parameters from surface observed two-way normal ray travel time as a function of progressive shot/receiver locations along a survey line.

The analysis to be detailed extends introductory work by Vetter (1981) and some related work by Michaels (1977).

4.1 NORMAL RAY ANALYSIS ON A DIPPING REFLECTOR USING LINEAR VELOCITY PROFILE MODEL

We assume that any geophysical reflector surface can be divided into a number of small linearized dipping segments. The parameters of each and every segment is then obtained from the reflection data. In this particular method of analysis, transmitter and receiver have to be located at the same point. If the medium has linear velocity profile, ray will follow a circular path described by equation 2.29. The receiver can accept reflected signal if a ray meets a reflector at an angle of 90 degrees. The reflection path will be the same as the forward path. These rays are called normal rays. The sloping reflector and raypaths for this particular analysis are shown in Figure 4.1.1.

Referring to the Figure 4.1.1,

LM = linearized segment of the reflector surface

O = shot/receiver location

$\tan \delta$ = the slope of the linearized reflector portion, which is assumed to be constant within a small segment of a reflector.

R = the centre of the circle which describes the raypath for linear velocity profile medium. ($g \neq 0$)

If $g = 0$, the normal ray takes the direct path OP, i.e. the direct path perpendicular to the surface of the reflector. A linearized reflector portion can be represented by the equation,

$$z = z_0 - x \tan \delta \qquad (4.1)$$

where,

z = depth measured downward from the datum surface.

z_0 = the vertical depth measured from the datum surface to the point of interception, S, between the vertical line through the shot/-receiver location O and the extrapolated linearized reflector ML.

The extrapolated linearized reflector segment - LM must pass through the centre of the circle - R, that describes the raypath in the linear velocity profile media, since the raypath 'ON' is perpendicular to the reflector segment at the point N.

Let us assume that the centre of the circle R = (x_r, z_r).

The value of (x_r, z_r) is given by

$$x_r = \frac{V_o}{g \tan \theta_o}$$

and,

$$z_r = \frac{-V_o}{g}$$

where θ_o = ray departure angle

V_o = datum velocity

The centre point of the circle satisfies equation 4.1, since the centre lies on the line described by equation 4.1. Therefore, from equation 4.1, we obtain

$$\frac{-V_o}{g} = z_o - \tan\delta \cdot \frac{V_o}{g \tan\theta_o},$$

where $\tan\delta$ is the slope of the linearized reflector portion.

By rearranging the above equation, we obtain

$$\tan\theta_o = \frac{\tan\delta}{[1 + \frac{g z_o}{V_o}]} \qquad (4.2)$$

$$\sin\theta_o = \frac{\tan\delta}{[\tan^2\delta + (1 + \frac{g z_o}{V_o})^2]^{\frac{1}{2}}} \qquad (4.3)$$

By using the triangular geometry relationship

$$\tan\theta_o = \frac{2\tan\theta_o/2}{1 - \tan^2\theta_o/2}$$

equation 4.2 can be written as

$$\frac{2\tan\theta_o/2}{(1 - \tan^2\theta_o/2)} = \frac{\tan\delta}{[1 + gz_o/V_o]} \qquad (4.4)$$

Referring to equation 2.25, the travel time at any point on the raypath

is given by

$$t(\theta,\theta_o) = \frac{1}{g} \ln \left[\frac{\tan \theta/2}{\tan \theta_o/2}\right] . \qquad (4.5)$$

Considering the diagram shown in Figure 4.1.1, we have the ray incident angle at the reflector as $\theta = \delta$.

Let $t_N = t(\delta,\theta_o)$, where t_N = the one way normal ray travel time from O to N.

Then, equation 4.5 can be written as

$$t_N = \frac{1}{g} \ln \left[\frac{\tan \delta/2}{\tan \theta_o/2}\right] . \qquad (4.6)$$

Combining equation 4.6, with 4.2 we get,

$$t_N = \frac{1}{g} \ln \left[\frac{\tan \delta/2}{\tan \left[\frac{1}{2} \left(\tan^{-1} \left[\frac{\tan \delta}{1 + \frac{g z_o}{V_o}}\right]\right)\right]}\right] . \qquad (4.7)$$

This is the equation describing the one way travel time relationship in terms of the parameters of the medium and reflector geometry parameters.

Equation 4.6 can be rewritten in the form,

$$\tan \theta_o/2 = \tan \delta/2 \cdot \exp(-gt_N) . \qquad (4.8)$$

Equation 4.4, together with equation 4.8 gives,

$$\frac{2 \tan(\delta/2) \cdot \exp(-gt_N)}{1 - [\tan(\delta/2) \cdot \exp(-gt_N)]^2} = \frac{\tan\delta}{[1 + \frac{g z_o}{V_o}]}$$

The above equation can be restructured as,

$$\exp(gt_N) - \tan^2(\delta/2) \cdot \exp(-gt_N) = (1 + \frac{gz_o}{V_o})(1 - \tan^2 \delta/2). \quad (4.9)$$

To enable us to obtain the estimates of parameters from the reflection data, let us consider moving shot/reveiver location $0_1, 0_2 \ldots\ldots 0_n$, having coordinates $x_1, x_2, x_3 \ldots\ldots x_n$ with respect to shot/receiver point - 0. We assume that the short/receiver at all the above locations interacts with a particular linearized dipping segment of the geophysical structure.

Then z_o can be replaced by $z_o - x_i \tan\delta$ for the i^{th} shot/receiver location where,

x_i = distance to the i^{th} shot/receiver location from the point-0.

Any of the points on the reflector can be uniquely described by its x, z coordinates together with travel time from the corresponding shot/-receiver point on the z = o.line.

i.e. $N_i = (x_{N_i}, z_{N_i}, t_{N_i})$.

In the case of moving shot/receiver locations, equation 4.9 becomes

$$\exp(gt_{N_i}) - \tan^2(\delta/2) \cdot \exp(-gt_{N_i})$$

$$= \left(1 + \frac{g}{V_o}(z_o - x_i \tan\delta)\right)\left(1 - \tan^2 \delta/2\right) \qquad (4.10)$$

where, t_{N_i} is the travel time corresponding to the i^{th} shot/receiver location. This equation relates the medium parameters to the travel time and distance characteristics.

The exact relationship given in equation 4.10 can be simplified to obtain an approximate relationship given below for the case when $\tan^2 \delta/2$ is small. This approximation would be possible even up to 20° of δ values without much error.

$$\exp(gt_{N_i}) = 1 + \frac{g}{V_o}(z_o - x_i \tan\delta)$$

By rearranging we get,

$$\frac{V_o}{g}\left[\exp(gt_{N_i}) - 1\right] = z_o - x_i \tan\delta \qquad (4.11)$$

This time-distance relationship can be used to obtain the z_o and tan δ from travel time and distance data with the knowledge of V_o and g. The above relationship is used in the comparative analysis considered in the next chapter.

In order to derive a model for the condition where $gt_{N_i} < 1$, equation 4.10 can be simplified further using Taylor's series expansion,

$$1 + gt_{N_i} + \frac{(gt_{N_i})^2}{2!} + \frac{(gt_{N_i})^3}{3!} + \cdots\cdots$$

$$- \tan^2 \delta/2 \left[1 - gt_{N_i} + \frac{(gt_{N_i})^2}{2!} - \frac{(gt_{N_i})^3}{3!} + \cdots\cdots\right]$$

$$= (1 - \tan^2 \delta/2) + \frac{g z_o}{V_o} (1 - \tan^2 \delta/2)$$

$$- \frac{g}{V_o} x_i \tan \delta \cdot (1 - \tan^2 \delta/2) \qquad (4.12)$$

Equation 4.12 can be compacked to

$$\sinh gt_{N_i} \cdot (1 + \tan^2 \frac{\delta}{2}) + (\cosh gt_{N_i} - 1)(1 - \tan^2 \frac{\delta}{2})$$

$$= \frac{g}{V_o} (z_o - x_i \tan \delta)(1 - \tan^2 \frac{\delta}{2})$$

or

$$\sinh gt_{N_i} + (\cosh gt_{N_i} - 1) \cos \delta = \frac{g}{V_o} (z_o - x_i \tan \delta) \cos \delta.$$

The constant velocity gradient of media is usually small, especially for most of the deep seismic media where it is typically less than 1, i.e. $g < 1$. For small values of t_{N_i}, the above series can be approximated upto the second order terms. Then the equation 4.12 becomes,

$$gt_{N_i} + \frac{(gt_{N_i})^2}{2!} + gt_{N_i} \cdot \tan^2 \delta/2 - \frac{(gt_{N_i})^2}{2!} \tan^2 \delta/2$$

$$= \frac{g z_o}{V_o} (1 - \tan^2 \delta/2) - \frac{g}{V_o} x_i \tan \delta \cdot (1 - \tan^2 \delta/2)$$

$$\text{i.e. } (1 + \tan^2 \delta/2)\, gt_{N_i} + (1 - \tan^2 \delta/2) \cdot \frac{(gt_{N_i})^2}{2!}$$

$$= \frac{g z_o}{V_o} (1 - \tan^2 \delta/2) - \frac{g x_i}{V_o} \tan \delta \cdot (1 - \tan^2 \delta/2)$$

$$gt_{N_i} = \left[\frac{g z_o}{V_o} - \frac{g x_i}{V_o} \tan \delta - \frac{(gt_{N_i})^2}{2!}\right] \left[\frac{1 - \tan^2 \delta/2}{1 + \tan^2 \delta/2}\right]$$

$$\text{Since, } \cos \delta = \frac{1 - \tan^2 \delta/2}{1 + \tan^2 \delta/2}$$

$$gt_{N_i} = \left[\frac{g z_o}{V_o} - \frac{g x_i}{V_o} \tan \delta - \frac{g^2 t^2_{N_i}}{2}\right] \cos \delta$$

$$V_o t_{N_i} = [z_o - x_i \tan \delta - \frac{g V_o}{2} t^2_{N_i}] \cos \delta \qquad (4.13)$$

For the situations where δ is small, $\lim_{\delta \to 0} \cos \delta \to 1$, equation 4.13 becomes:

$$V_o t_{N_i} = z_o - x_i \tan \delta - \frac{g V_o}{2} t^2_{N_i} \qquad (4.14)$$

This represents the approximated model for constant velocity gradient media which relates the travel time and distance to the parameters of the media in cases where $gt_{N_i} < 1$. This analytical model equation 4.14 relates the parameters g, V_o, z_o, tan δ with the observable (t_{N_i}, x_i) data. This is a suitable model for estimating the reflector geometry from the surface observable data set if the velocity profile parameters V_o and g are known.

4.2 NORMAL RAY APPROACH TO THE REFLECTOR IDENTIFICATION

This method of true reflector identification can be used, where there are simple geophysical structures such as slopes. In this method the apparent dip in the reflection seismogram for the normal rays is converted to the true reflector geometry by using least squares technique. A one-dimensional linear velocity profile model is considered. This analysis can be applied equally to the constant velocity media. This analysis can also be used with the lateral velocity variations by dividing the survey area into a number of small areas which have constant lateral velocity.

Consider the linear velocity profile model developed in the previous section, i.e. equation 4.14.,

$$V_o\, t_{N_i} = z_o - x_i \tan\delta - \frac{gV_o}{2}\, t_{N_i}^2 \,, \qquad (4.14)$$

$$V_o\, t_{N_i} + \frac{gV_o}{2}\, t_{N_i}^2 = z_o - x_i \tan\delta \,. \qquad (4.15)$$

If the velocity distribution of the medium is known, least squares technique can be used to estimate z_o and tan δ.

Once z_o and tan δ have been obtained, then the true reflector point (x_N, z_N) can be obtained. The mathematical relations for (x_N, z_N) can be derived as follows:

The true reflector point (x_N, z_N) is the intersection point of the raypath given by equation 2.29 and the segmentized linear reflector portion given by equation 4.1. Hence the solution of these two equations gives the common point (x_N, z_N).

Consider the equations,

$$(x - \frac{V_o}{g \tan \theta_o})^2 + (z + \frac{V_o}{g})^2 = (\frac{V_o}{g \sin \theta_o})^2 \qquad (2.29)$$

$$z = z_o - x \tan \delta \qquad (4.1)$$

Also, from equations 4.2 and 4.3,

$$\tan \theta_o = \frac{\tan \delta}{[1 + \frac{g z_o}{V_o}]} \qquad (4.2)$$

$$\sin \theta_o = \frac{\tan \delta}{[\tan^2 \delta + (1 + \frac{g z_o}{V_o})^2]^{\frac{1}{2}}} \qquad (4.3)$$

Since the point (x_N, z_N) is common to both equation 2.29 and 4.1, we obtain,

$$\left[\frac{z_o - z_N}{\tan\delta} - \frac{V_o\,(1 + gz_o/V_o)}{g\tan\delta}\right]^2 + \left[z_N + \frac{V_o}{g}\right]^2$$

$$= \left[\frac{V_o}{g\tan\delta}\left[\tan^2\delta + (1 + \frac{gz_o}{V_o})^2\right]^{\frac{1}{2}}\right]^2$$

This represents a second order equation in z_N, which has the solution

$$z_N = \frac{-V_o}{g} \pm \left[\left(\frac{V_o}{g}\right)^2 + \frac{z_o\,(z_o + 2V_o/g)}{(1 + \tan^2\delta)}\right]^{\frac{1}{2}} \qquad (4.4)$$

Since the depth must be positive valued, the right hand side of the equation should be the positive square root. Once z_N has been obtained, the equation 4.1 can be used to obtain x_N,

$$x_N = \frac{z_o - z_N}{\tan\delta} \qquad (4.5)$$

For a linear velocity profile medium the above equations, i.e. 4.4. and 4.5 describe the true reflection point.

For a constant velocity medium, z_o and $\tan\delta$ can be obtained using the same model as was used in the linear velocity profile case, i.e. equation 4.14 with $g = 0$. For this case the true reflector identification task reduces to the estimation of (x_p, z_p) as shown in figure 4.1.1.

The true reflector position for the constant velocity medium can be obtained using the simple geometric relationships given below:

$$x_p = \frac{z_o}{2} \sin 2\delta$$

$$z_p = z_o \sin^2 \delta$$

By summarizing this chapter, we can say that we have described a methodology for obtaining estimates of the true sloping reflector under a linear velocity profile medium. As in the case of the horizontally stratified medium, the constant gradient model might represent an approximation for the velocity profile details of a composite of several medium layers above the reflector. The estimation accuracy will then depend on the degree of applicability of the profile model. Since the gradient velocity model has an additional parameter over the constant velocity model, one can expect to have better estimates for the true reflector geometry by use of this model.

CHAPTER V

ANALYSIS OF ERRORS DUE TO CONSTANT VELOCITY ASSUMPTION IF THE MEDIUM HAS A LINEAR VELOCITY PROFILE

5.1 ANALYSIS OF THE EFFECT OF CONSTANT VELOCITY GRADIENT ON TRAVEL TIME

The computer simulation was performed with an assumed reflector geometry given by (Reference Figure 4.1.1)

$$z = z_o - x_i \tan \delta .$$

The travel time distance relation for a sloping reflector can be obtained from the equation 4.7 by substituting $z_o - x_i \tan \delta$ instead of z_o. The effect of g on travel time is observed for given V_o, z_o and δ. The travel time - distance relations for different values of velocity gradients g are obtained and given in Figure 5.1.1 and 5.1.2 for the slopes of 10 and 20 degrees. The specification of the medium parameters are given under respective graphs.

From the above graphs it is evident that the velocity gradient has a considerable influence on the travel time. Also, it is observed that the effect cannot be disregarded even at the depth of 500 meters. The figures indicate that the effect of velocity gradient becomes negligible as the depth decreases.

5.2 ANALYSIS OF THE EFFECT OF CONSTANT VELOCITY GRADIENT ON THE RAYPATH

The constant slope reflector has been used for the above analysis. The specification for the parameters of the medium is given under the respective figures. The equations 2.29, 4.1, 4.2 and 4.3 has been used to observe the effects of g on raypaths for given V_o, z_o and δ. From the figures 5.2.1 to 5.2.6 it is observed that constant velocity gradient has no considerable effect on the raypaths in the most practical range of $0 \leq g \leq 1.0$ at the depth

of 200 meters and slopes of 10 and even 20 degrees.

The influence of slope of the reflector is also observed to be considerable on the raypaths. If the slope is larger, the deviation from the raypaths, under the constant velocity assumption, is also observed to be larger.

This analysis indicates that the constant velocity gradient has a considerable influence on the raypaths in the deep seismic situations. However, the influence in shallow seismics are negligible.

5.3 ANALYSIS OF THE EFFECT OF CONSTANT VELOCITY GRADIENT ON THE DEVIATION COMPARED TO CONSTANT VELOCITY ASSUMPTION

In this analysis the numerical values for (x_p, z_p), (x_N, z_N), $(x_p - z_N)$, $(z_N - z_p)$ and $(z_o - z_N)$ are calculated for different velocity gradients, g, to get an idea about the quantitative values of the deviations. The co-ordinates of the points $N(x_N, z_N)$, $P(x_p, z_p)$ are obtained using the equations 4.4, 4.5, 4.6 and 4.7 for given z_o, V_o and δ. The results for $g = 0.5$ are tabulated in the Table 5.3. The above symbols are used keeping Fig. 4.1.1 as reference. The deviations $(x_p - x_N)$, $(z_N - z_p)$ and $(z_o - z_N)$ with respect to depth are plotted in Figures 5.3.7 to 5.3.12 for the slopes of 10 and 20 degrees. This analysis supports our conclusion in section 5.2, i.e. if the medium is a linear velocity profile one, the deviation of the raypaths under the constant velocity assumption are found to be considerable in deep seismics.

Further, from table 5.3 a horizontal shift of about 100 meters and a vertical shift of 36 meters are observed at the depth of 2000 meters and velocity gradient of 0.5 as a result of the constant velocity assumption.

We consider the resultant error ϵ under the constant velocity assumption is given by

$$\epsilon = [(x_N - x_p)^2 + (z_N - z_p)^2]^{\frac{1}{2}} .$$

Then at the depth of 2000 meters ϵ would be approximately 106 meters for the medium of $g = 0.5$.

Sometimes, this error may be misleading to the interpreter.

5.4 ANALYSIS OF THE EFFECTS OF CONSTANT VELOCITY GRADIENT ON THE ESTIMATION OF THE REFLECTOR GEOMETRY

We use the linear velocity profile model equation 4.15 together with equations 4.4 and 4.5 for this analysis. The least squares technique is used for the true sloping reflector identification with equation 4.15. As in the previous cases, we have considered a constant sloping reflector. We generate the x-t data for a constant velocity gradient model. This data is used to estimate the parameters under the assumption that the medium is one of constant velocity equal to the average velocity of the data generating system. The specification of the medium parameters are given under the respective graphs.

Our interest is to study the effect of g on the error that is generated due to the assumption that the velocity of the medium is constant. The estimated reflectors using the above analysis for depths of 500,

2000 and 5000 meters are shown in figures 5.4.1 to 5.4.3. The error is clearly brought out in these graphs indicating that the error due to the constant velocity assumption is considerable. It is also visible that the error becomes more considerable as we go deeper and deeper. This analysis supports our conclusion in the previous analysis.

The estimated reflector considered in the above figures does not display the corresponding shift of the actual point on the reflector. Therefore, we have developed figures 5.4.4 for the case of 500 meters depth, which is more informative showing the actual shift of the reflector points as a result of the assumption that the velocity is constant. These figures leads us to conclude that the estimated reflector points are at a lower depth compared to the true reflector points on the reflector.

5.5 IMPLICATIONS OF FINDINGS

Based on the above analysis, the following implications can be made for deep seismic and shallow seismic separately.

5.5.1 DEEP SEISMIC EXPLORATION

- The effect of linear velocity profile on raypaths are fairly considerable.
- Deviations from the constant velocity assumption are fairly large.
- Estimation based on constant velocity assumption give rise to a considerable error.
- Due to the considerable error of the estimates the results may be misleading, in the interpretation of geometry, lithology and

during the drilling activities for oil and gas in seismics.

5.5.2 SHALLOW SEISMIC APPLICATIONS

- The effect of linear velocity profile on raypaths are negligible.
- Deviation from the constant velocity approximation are much smaller.
- Estimation of the parameters based on constant velocity assumption give a fairly good match.
- On account of negligible error effects the constant velocity model may be used for physical media with velocity gradients.

CHAPTER VI

CONCLUSION AND FURTHER AREAS OF RESEARCH

CONCLUSION:

In virtually all current seismic data processing, the response data is interpreted in the light of the segmentwise constant propagation velocity hypothesis for medium segments. The linear velocity profile hypothesis constitutes a further degree of freedom, and hence with the potential to effect more accurate estimates about the medium than can be obtained with the constant velocity hypothesis.

In the first part of our study we have given a method for estimating the reflector geometry and the constant velocity gradient from the surface observable data for a zero-dipping reflector. The accuracy of the estimates depends on the accuracy of the travel time - offset data. An accurate estimate can be obtained from the simulated data although difficulties may be encountered due to the inherent noise associated with practical data.

In the second part of our study, we have developed a suitable linear velocity profile model for dipping reflectors using the normal ray analysis. With the help of this model we have observed that the errors due to the linear velocity assumption are small in the case of shallow seismic studies, whereas in the case of deep seismic exploration the linear velocity profile approximation gives rise to a considerable error.

The analysis, and insight from the simulation results improve our understanding of velocity gradient effects in the estimates of the parameters. The analytical results offer refinements for the medium structures and parameters estimation problem, for situations where the linear velocity profile model is appropriate.

FURTHER AREAS OF RESEARCH

The extension of the linear velocity profile model to the multilayered system and the development of the velocity spectra for the linear velocity profile model are some of the directions suggested for further research.

REFERENCES

REFERENCES

Aki, A., P.G. Richards., 1980, Quantitative Seismology Theory and Methods: Volume - 1, Volume - 11, W.H. Freeman and Company, San Francisco.

Bayless, J.W., E.O. Brigham., 1970, Application of the Kalman Filter to Continuous Signal Restoration: Geophysics, V.35, P. 2-23.

Berkhout, A.J., P.R. Zaanen., 1976, A Comparison Between Wiener Filtering, and Deterministic Least Squares Estimation: Geophysical Prospecting, V.24, P. 141-197.

Berkhout, A.J., 1980, Seismic Migration, Imaging of Acoustic Energy By Wave Field Extrapolation: Elsevier Scientific Publishing Company, New York.

Burg, J.P., 1967, Maximum Entropy Spectral Analysis: Paper Presented at the 37th SEG Meeting, Tulsa.

Burg, J.P., 1970, A New Analysis Technique for Time Series Data: Paper Presented at the NATO Meeting.

Burg, J.P., 1972, The Relationship Between Maximum Entropy Spectra and Maximum Likelihood Spectra: Geophysics, V.37, P. 375-376.

Capon, J., 1969, High-Resolution Frequency-Wave Number Spectrum Analysis: Proc. IEEE, V.57, P. 1408-1418.

Caruthers, J.W., 1977, Fundamentals of Marine Acoustics: Elsevier Scientific Publishing Company, New York.

Cerveny, V., R. Ravindra., 1971, Theory of Seismic Head Waves: University of Toronto Press.

Chen, C.H. (editor), 1982, Digital Waveform Processing and Recognition: CRC Press.

Claerbout, J.F., 1976, Fundamentals of Geophysical Data Processing - With Applications to Petroleum Prospecting: McGraw-Hill.

Crump, N.D., 1972, A Kalman Approach to the Deconvolution of Seismic Signals: Geophysics, V.39, P. 1-12.

Dix, H.C., 1955, Seismic Velocities from Surface Measurements: Geophysics, V.XX, P. 68-86.

Findley, D.F. (editor), 1978, Applied Time Series Analysis: Academic Press, New York.

Greenhalgh, S.A., D.W. King., 1981 Curved Ray Path Interpretation of Seismic Refraction Data: Geophysical Prospecting, V.29, P. 853-882.

Hagedoorn, J.G., 1954, A Process of Seismic Reflection Interpretation: Geophysical Prospecting, V.2, P. 85-127.

Hubral, P., 1977, Time Migration - Some Ray Theoretical Aspects: Geophysical Prospecting, V.25, P. 738-745.

Hubral, P., T. Krey., 1980., Interval Velocities from Seismic Reflection Time Measurements: Society of Exploration Geophysicists.

James, M.L., G.M. Smith., J.C. Wolford., 1967, Applied Numerical Methods for Digital Computation with FORTRAN and CSMP: Thomas Y. Crowell, Harper and Row Publishers, New York.

Kinsler, L.E., A.R. Frey., 1962, Fundamentals of Acoustics: John Wiley and Sons, Inc.

Knott, C.G., 1899, Reflection and Refraction of Seismic Waves with Seismological Applications: Phil. Mag. 48, 64-97.

Kormylo, J.J., J.M. Mendel., 1983, Maximum-Likelihood Seismic Deconvolution: IEEE Transaction on Geoscience and Remote Sensing, V.GE-21, No. 1, January, P. 72-82.

Lacoss, R.T., 1971, Data Adaptive Spectral Analysis Methods: Geophysics, V.36, P. 661-675.

Lee, W.H.K., S.W. Stewart., 1981, Principles and Applications of Micro-earthquake Networks: Academic Press, New York.

Ljung, L., 1979, Asymptotic Behavior of the Extended Kalman Filter as a Parameter Estimator for Linear Systems: IEEE Transaction on Automatic Control, February, V.AC-24, No. 1, P. 36-50.

McQuillin, R., M. Bacon., W. Barclay., 1981, An Introduction to Seismic Interpretation: Gulf Publishing Company.

Mendel, J.M., J. Kormylo, 1977, New Fast Optimal White-Noise Estimators for Deconvolution: IEEE Transactions on Geoscience Electronics, V. GE-15, January, P. 32-41.

Mendel, J.M., J. Kormylo., 1978, Single-Channel White-Noise Estimators for Deconvolution: Geophysics, V.43, P.102-124.

Mendel, J.M., 1981, Minimum Variance Deconvolution: IEEE Transactions of Geoscience and Remote Sensing, V. GE-19, July, P. 161-171.

Michaels, P., 1977, Seismic Raypath Migration With the Pocket Calculators: Geophysics, V.42, P. 1056-1063.

Officer, C.B., 1958, Introduction to the Theory of Sound Transmission: McGraw-Hill.

Oppenheim, A.V., R.W. Schafer., 1975, Digital Signal Processing: Prentice-Hall Inc.

Ott, N., H.G. Meder., 1972, The Kalman Filter as a Prediction Error Filter: Geophysical Prospecting, V.20, P. 549-560.

Pilant, W.L., 1979, Elastic Waves in the Earth: Elsevier Scientific Publishing Company, New York.

Robinson, E.A., 1967, Predictive Decomposition of Time Series with Application to Seismic Exploration: Geophysics, V.XXXII, P. 418-484.

Robinson, E.A., S. Treitel., 1980, Geophysical Signal Analysis: Prentice-Hall,

Robinson, E.A., 1982, Migration of Geophysical Data: International Human Resources Development Corporation, Boston.

Silvia, M.T., E.A. Robinson., 1979, Deconvolution of Geophysical Time Series in the Exploration for Oil and Natural Gas: Elsevier Scientific Publishing Company, New York.

Slotnick, M.M., 1959, Lessons in Seismic Computing, A Memorial to the Author: SEG Spec. Publ., Tulsa.

Stolt, R.H., 1978, Migration by Fourier Transform: Geophysics, V.43, P. 23-48.

Telford, W.M., L.P. Geldart., R.E. Sheriff., D.A. Keys., 1978, Applied Geophysics: Cambridge University Press.

Temkin, S., 1981, Elements of Acoustics: John Wiley and Sons, New York.

Tribolet, J.M., 1979, Seismic Applications of Homomorphic Signal Processing: Prentice-Hall Inc.

Taner, T.M., F. Koehler., 1969, Velocity Spectra-Digital Computer Derivation and Applications of Velocity Functions: Geophysics, December.

Ulrych, T.J., 1972, Maximum Entropy Power Spectrum of Truncated Sinusoids: Journal of Geophysical Research, V.77, P. 1396-1401.

Ulrych, T.J., T.N. Bishop., 1975, Maximum Entropy Spectral Analysis and Autoregressive Decomposition: Reviews of Geophysics and Space Physics, V.13, P. 183-200.

Van den Bos, A., 1971, Alternative Interpretation of Maximum Entropy Spectral Analysis: IEEE Transaction on Information Theory, July, V.IT-17, No. 4, P. 493-494.

Vetter, W.J., 1981, On Raypaths in Media with Constant Velocity Gradients: Internal Correspondence to Dr. R.T. Cutler.

Vetter, W.J., 1983, Normal Moveout for the Linear Velocity Profile Model: Personal Correspondence.

BIBLIOGRAPHY

BIBLIOGRAPHY

Anstey, N.A., 1977, Seismic Interpretation - The Physical Aspects: International Human Resources Development Corporation, U.S.A.

Al-Chalabi, M., 1974, An Analysis of Stacking, RMS, Average and Interval Velocities Over a Horizontally Layered Ground: Geophysical Prospecting, V.22, P.458-475.

Baggeroer, A.B., High Resolution Velocity/Depth Spectra Estimation for Seismic Profiling.

Beitzel, J.E., J.M. Daivd., 1974, A Computer Oriented Velocity Analysis Interpretation Technique: Geophysics, October.

Chen, C.H. (editor), 1978, Computer and Seismic Analysis and Discrimination: Elsevier Scientific Publishing Company.

Cressman, K.S., 1968, How Velocity Layering and Steep Dip Affect CDP: Geophysics, June, V.33, No. 3, P. 399-411.

Dampney, C.N.G., R.J. Whiteley., 1980, Velocity Determination and Error Analysis for the Seismic Refraction Method: Geophysical Prospecting, V.28, P.1-17.

Davis, J.M., 1972, Interpretation of Velocity Spectra Through an Adaptive Modeling Strategy: Geophysics, December, V.37, No. 6, P. 953-962.

Everett, J.E., 1974, Obtaining Interval Velocities from Stacking Velocities When Dipping Horizons are Included: Geophysical Prospecting, V.22, P. 122-142.

French, S.W., 1975, Computer Migration of Oblique Seismic Reflection Profiles: Geophysics, V.40, P. 961-980.

Garotta, R., D. Michon., 1967, Continuous Analysis of the Velocity Function and of the Moveout Corrections: Geophysical Prospecting, V.15, P. 584-597.

Gibson, B.S., M.E. Odegard., G.H. Sutton., 1979, Nonlinear Least-Squares Inversion of Travel Time Data for a Linear Velocity-Depth Relationship: Geophysics, V.44, No. 2, P. 185-194.

Goguel, J.M., 1951, Seismic Refraction with Variable Velocity: Geophysics, V.16, P. 81-101.

Hajnal, Z., I.T. Sereda., 1981, Maximum Uncertainty of Interval Velocity Estimates: Geophysics, V.46, P. 1543-1547.

Kaufman, H., 1953, Velocity Functions in Seismic Prospecting: Geophysics, V.18, P. 289-297.

Loewenthal, D.L. Lu., R. Robinson., J. Sherwood., 1976, The Wave Equation Applied to Migration: Geophysical Prospecting, V.24, P. 380-399.

Papoulis, A., 1977, Signal Analysis: McGraw-Hill.

Oppenheim, A.V. (editor)., 1978, Application of Digital Signal Processing: Prentice-Hall. Inc.

Robinson, E.A., M.T. Silvia:, 1978, Digital Signal Processing and Time Series Analysis: Holden-day, Inc., San Francisco.

Robinson, J.C., C.A. Aldrich., 1972, A Novel High-Speed Algorithm for Summational Type Seismic Velocity Analysis: Geophysical Prospecting, December, V. 20, P. 814-827.

Robinson, J.C., 1969, HRVA - A Velocity Analysis Technique Applied to Seismic Data: Geophysics, June, V.34, No.3, P. 330-356.

Shah, P.M., 1973, Use of Wavefront Curvature to Relate Seismic Data with Subsurface Parameters: Geophysics, V.38, P. 812-825.

Sherwood, J.W.C., P.H. Poe., 1972, Continuous Velocity Estimation and Seismic Wavelet Processing: Geophysics, October.

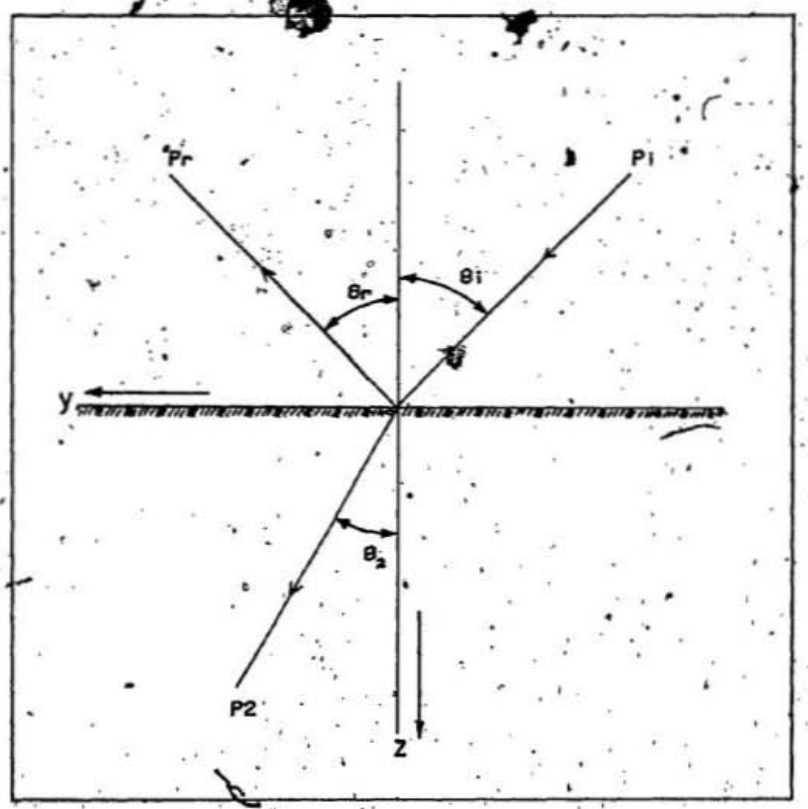

FIGURE 2

OBLIQUE INCIDENCE AT AN INTERFACE

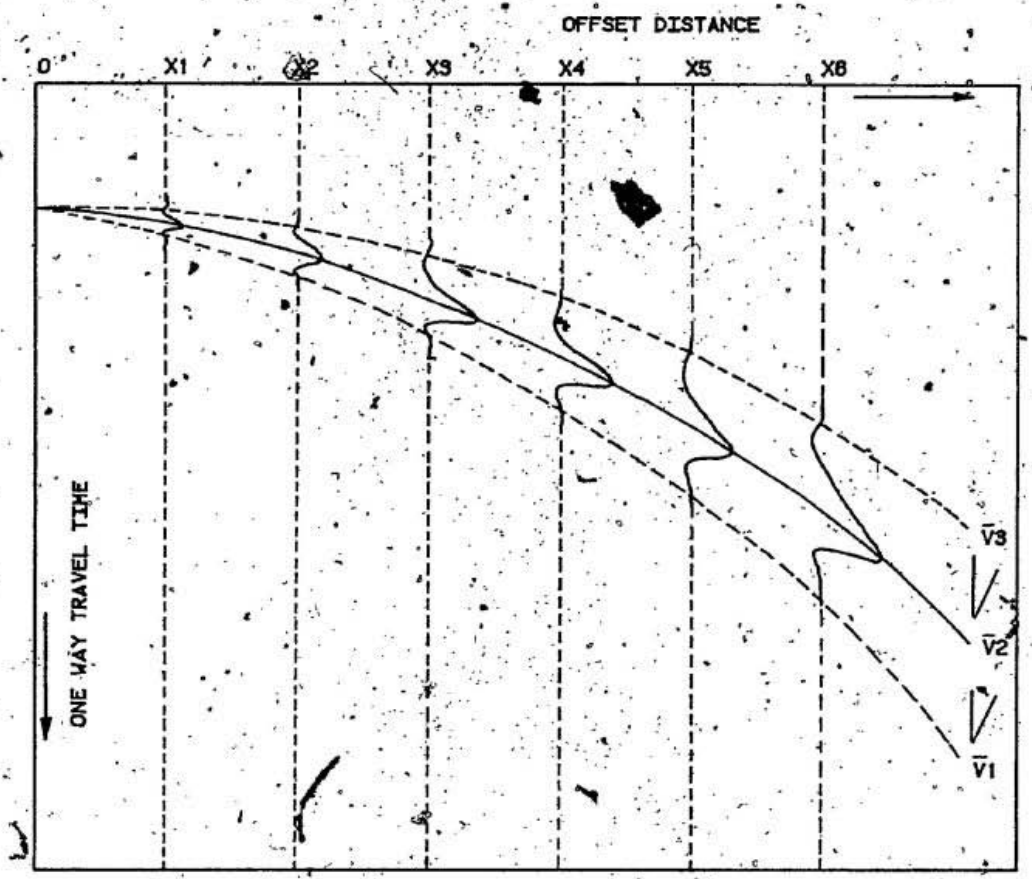

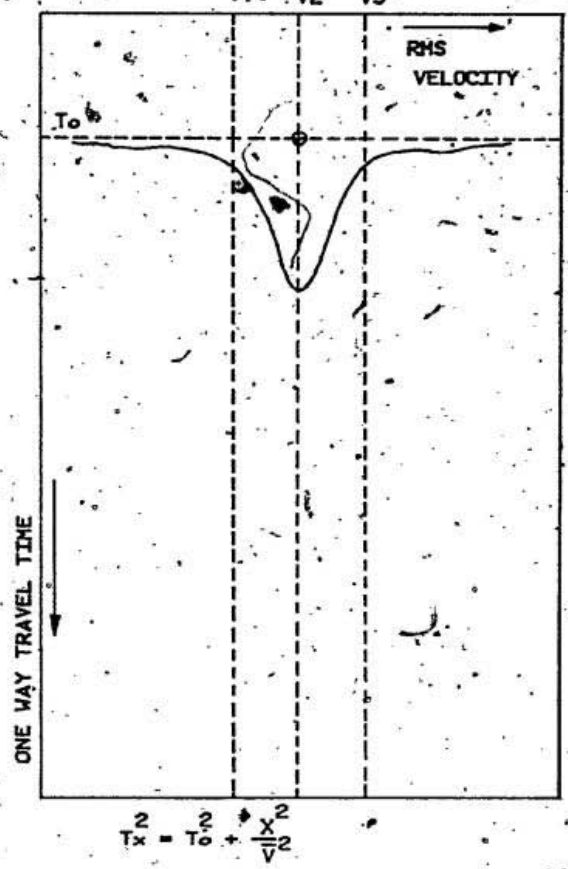

FIGURE : 3.3.1

COHERENCIES FOR VARIOUS TRAJECTORIES

(REFERENCE : TANER , M.T et al.[1969])

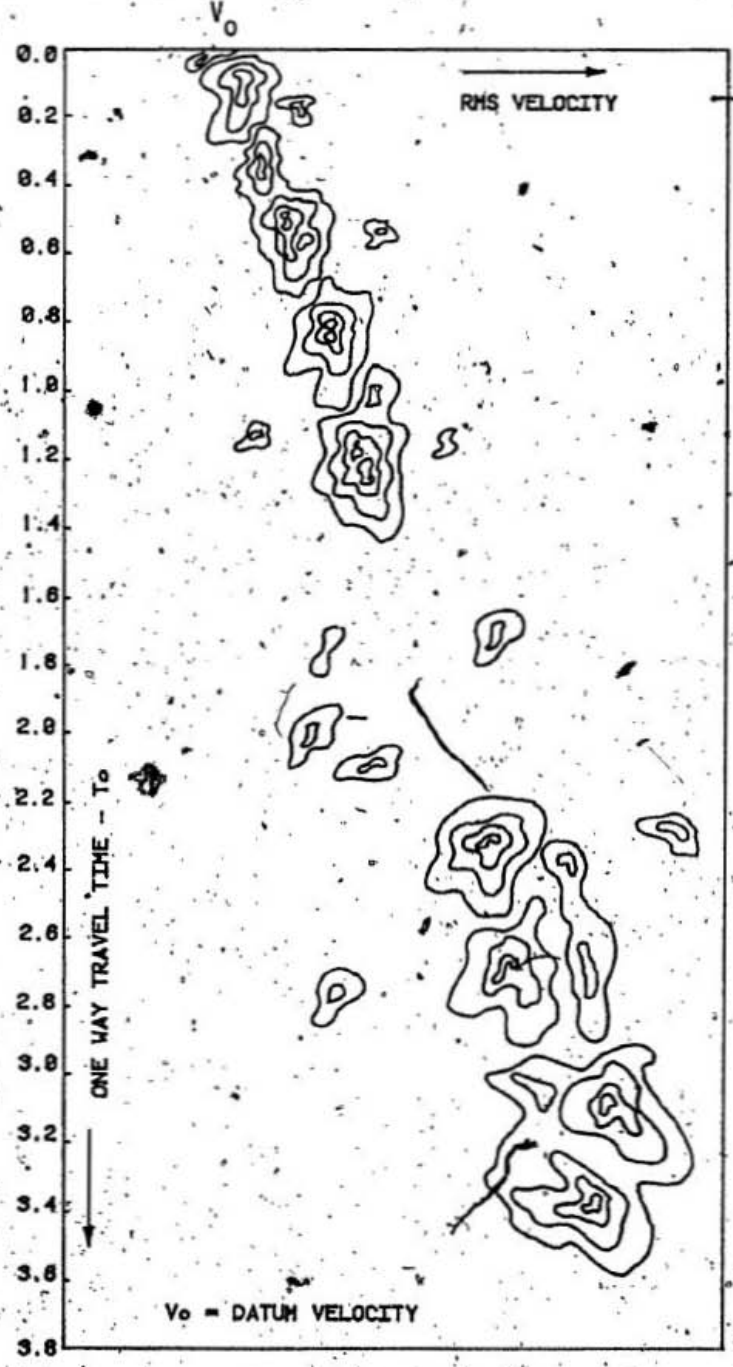

FIGURE : 3.3.2

VELOCITY SPECTRA SHOWING REFLECTION LOSS CAUSED BY SHALE BODY

(REFERENCES : McQILLIN,R et al.[1980]., TANER,M.T et al.[1969])

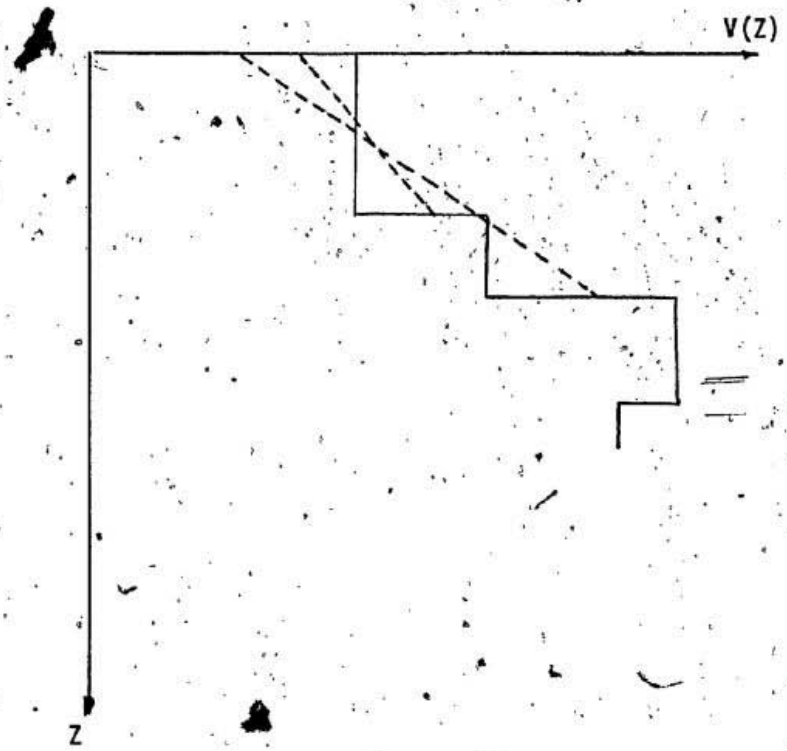

- - - linear to a reflector

____ layerwise constant

Figure : 3.5.0

SEGMENTWISE CONSTANT AND LINEAR VELOCITY PROFILES

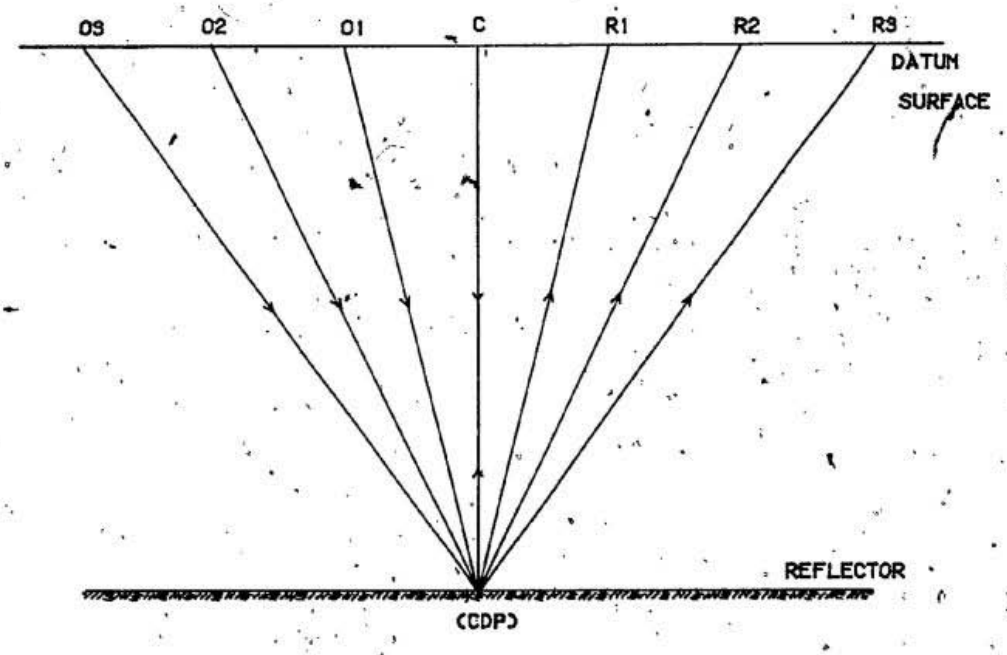

Rn = RECEIVER POINTS
On = SHOT POINTS
C = CENTER POINT

FIGURE : 3.5.1

COMMON DEPTH POINT DATA GATHERING

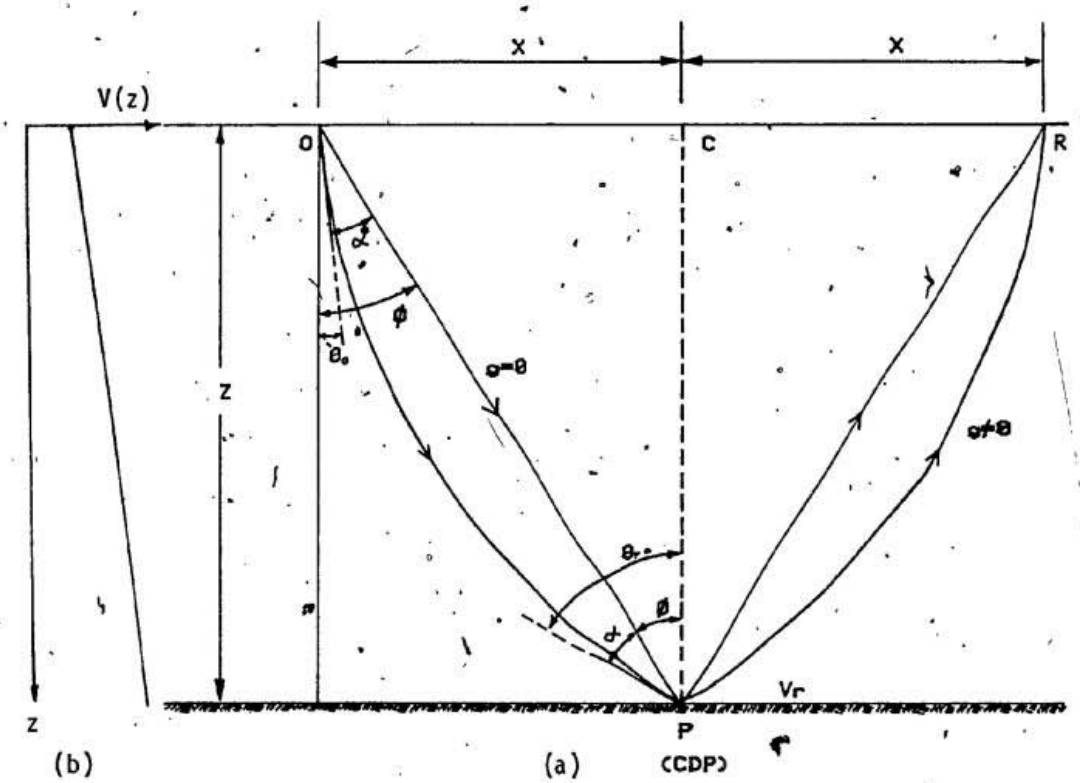

FIGURE : 3.5.2

(a) RAYPATHS IN A LINEAR VELOCITY PROFILE MEDIUM

(b) LINEAR VELOCITY PROFILE

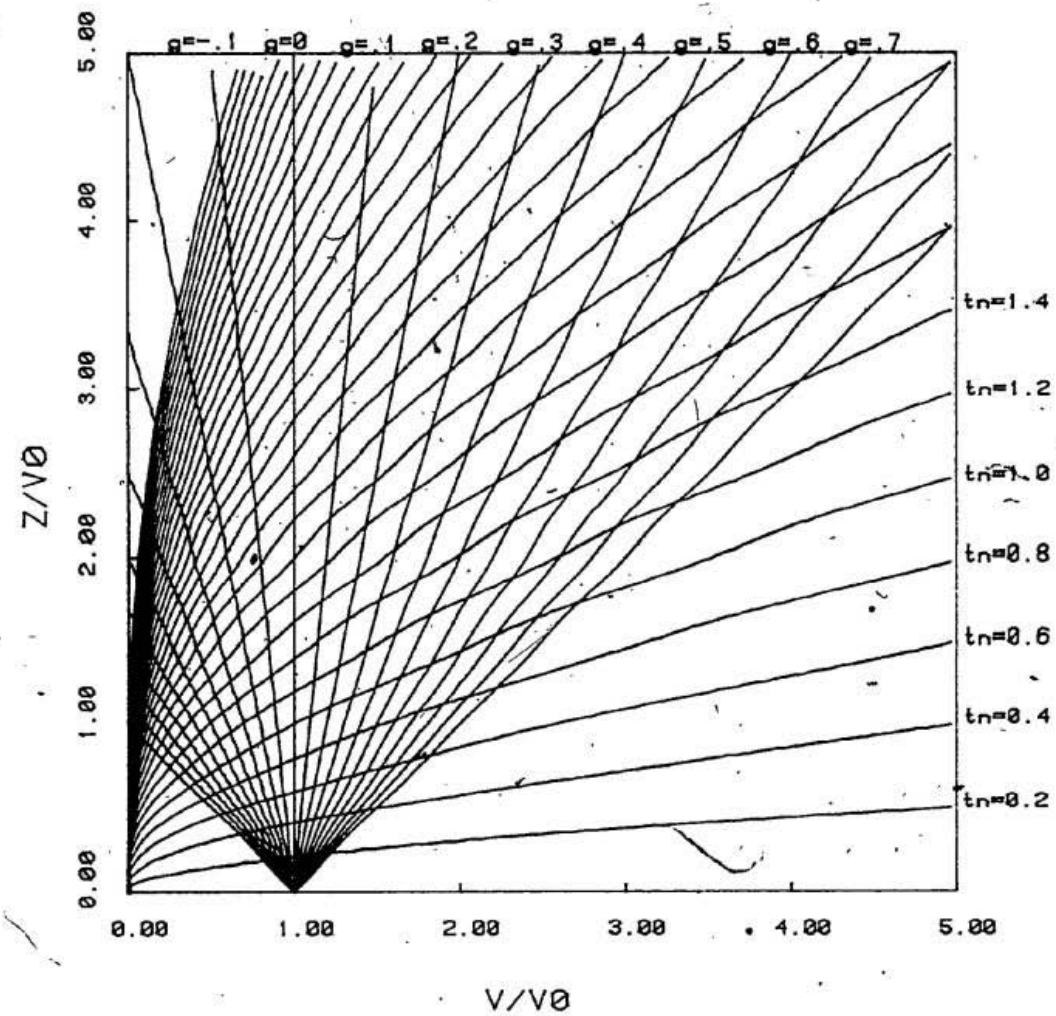

Figure : 3.5.3 z/V0 vs V/V0

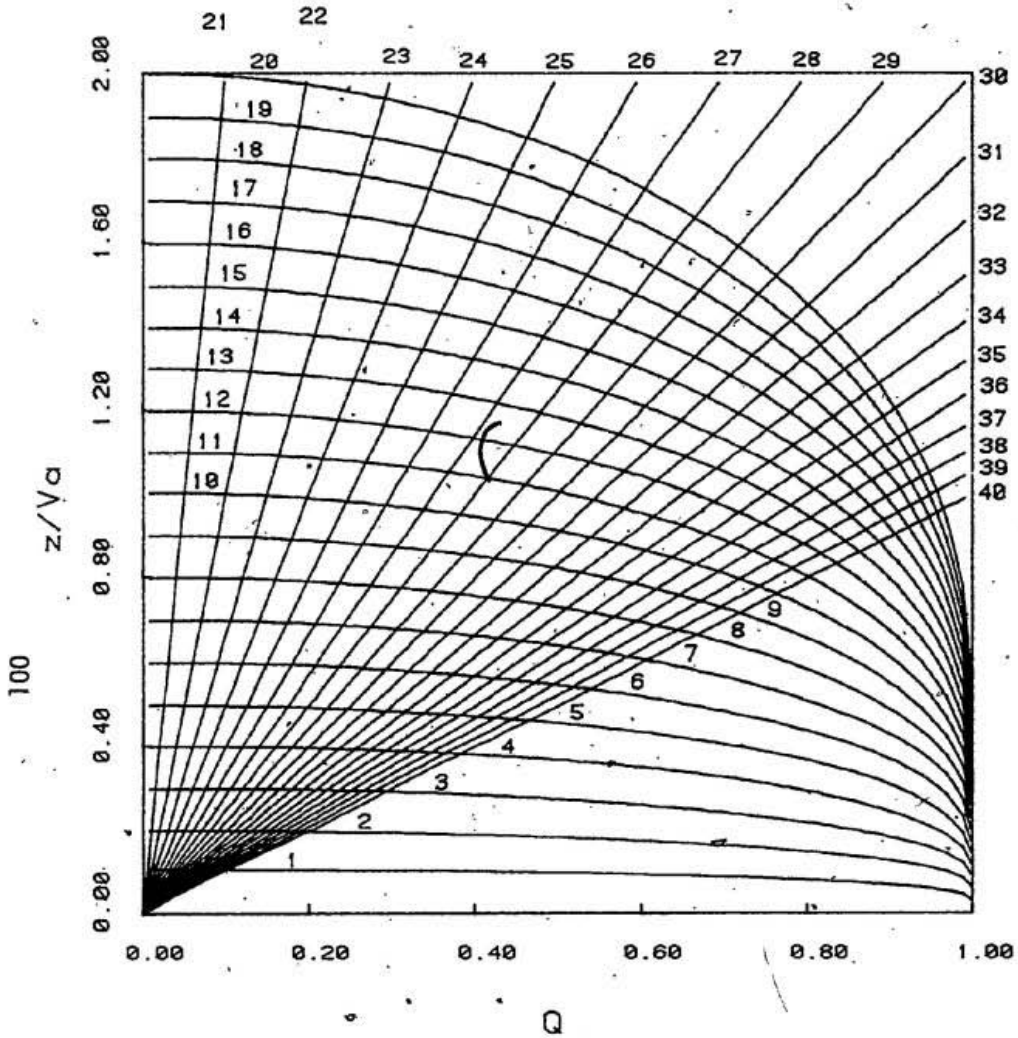

20. tn = 2.0
19. tn = 1.9
18. tn = 1.8
17. tn = 1.7
16. tn = 1.6
15. tn = 1.5
14. tn = 1.4
13. tn = 1.3
12. tn = 1.2
11. tn = 1.1
10. tn = 1.0
9. tn = 0.9
8. tn = 0.8
7. tn = 0.7
6. tn = 0.6
5. tn = 0.5
4. tn = 0.4
3. tn = 0.3
2. tn = 0.2
1. tn = 0.1

21. g = 0.1
22. g = 0.2
23. g = 0.3
24. g = 0.4
25. g = 0.5
26. g = 0.6
27. g = 0.7
28. g = 0.8
29. g = 0.9
30. g = 1.0
31. g = 1.1
32. g = 1.2
33. g = 1.3
34. g = 1.4
35. g = 1.5
36. g = 1.6
37. g = 1.7
38. g = 1.8
39. g = 1.9
40. g = 2.0

Figure : 3.5.4 z/Va vs Q

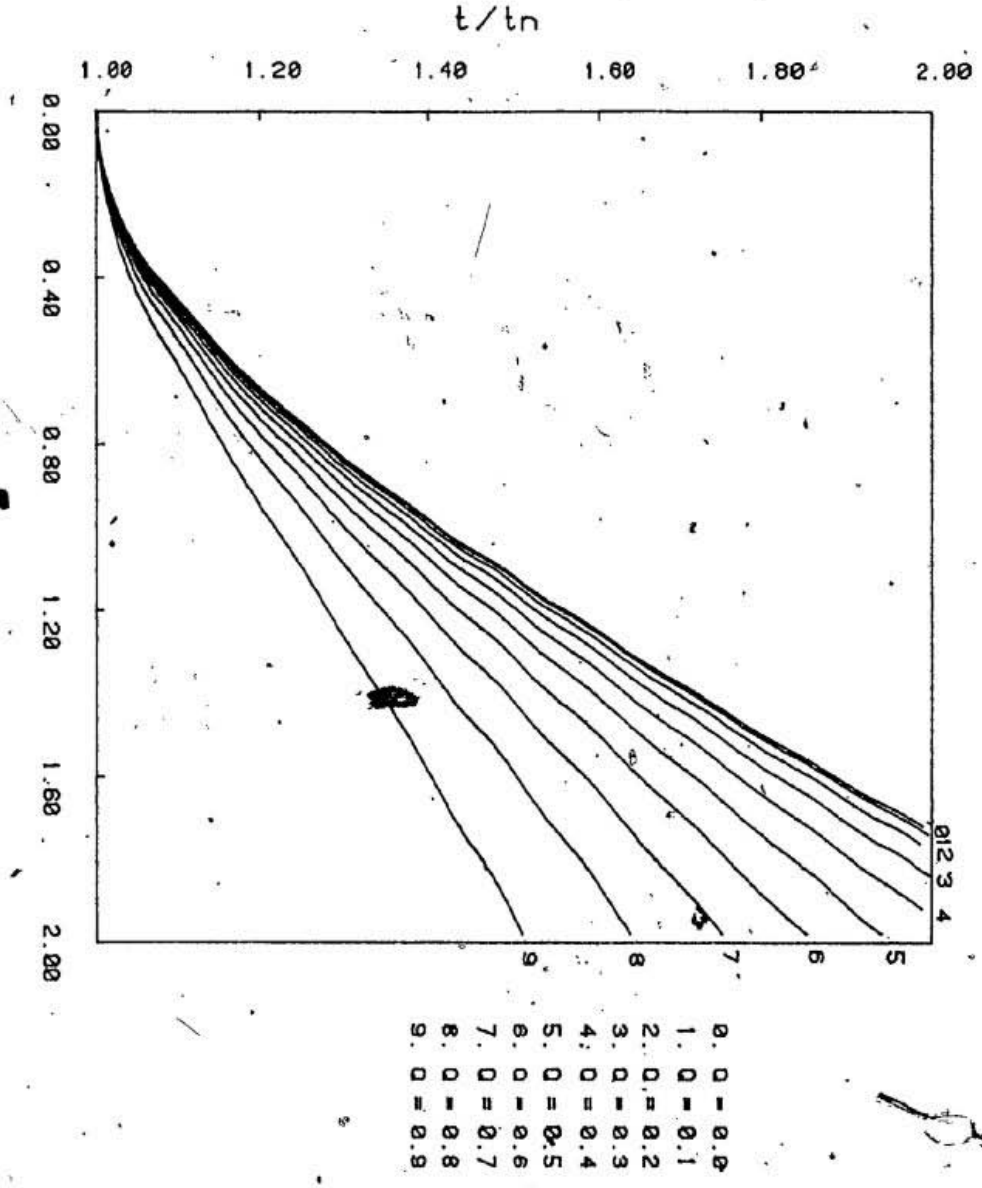

Figure : 3.5.5 t/tn vs x/z

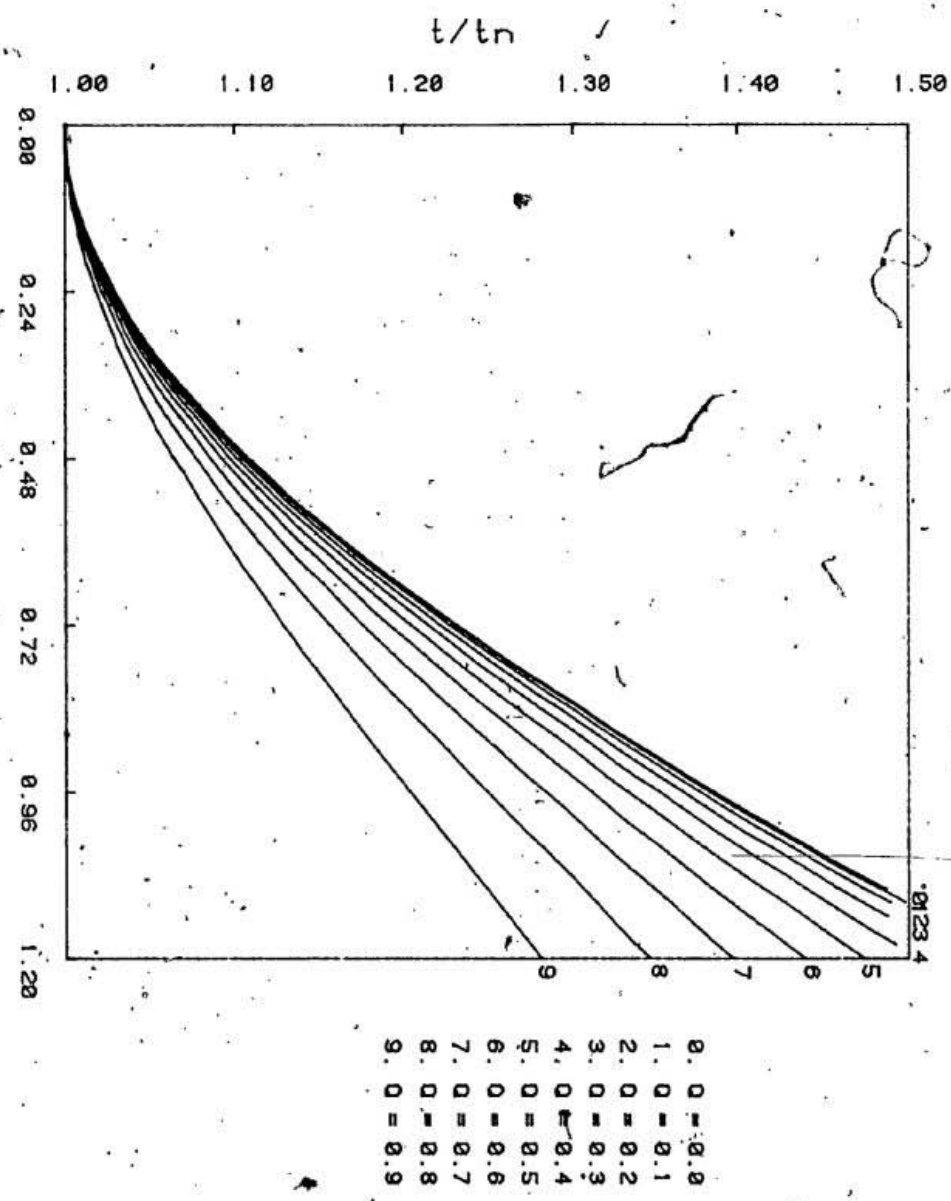

Figure : 3.5.5 t/tn vs x/z

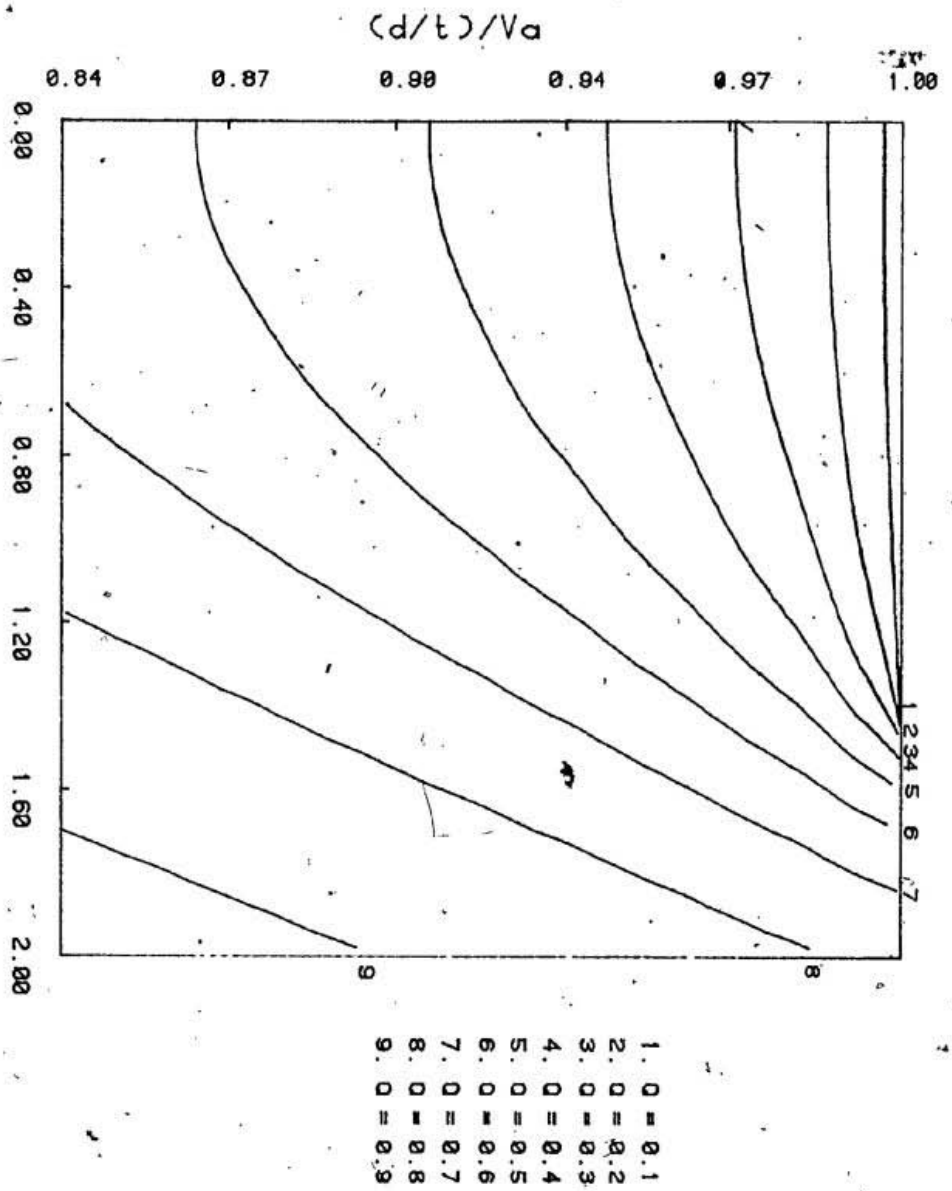

Figure : 3.5.6 (d/t)/Va vs x/z

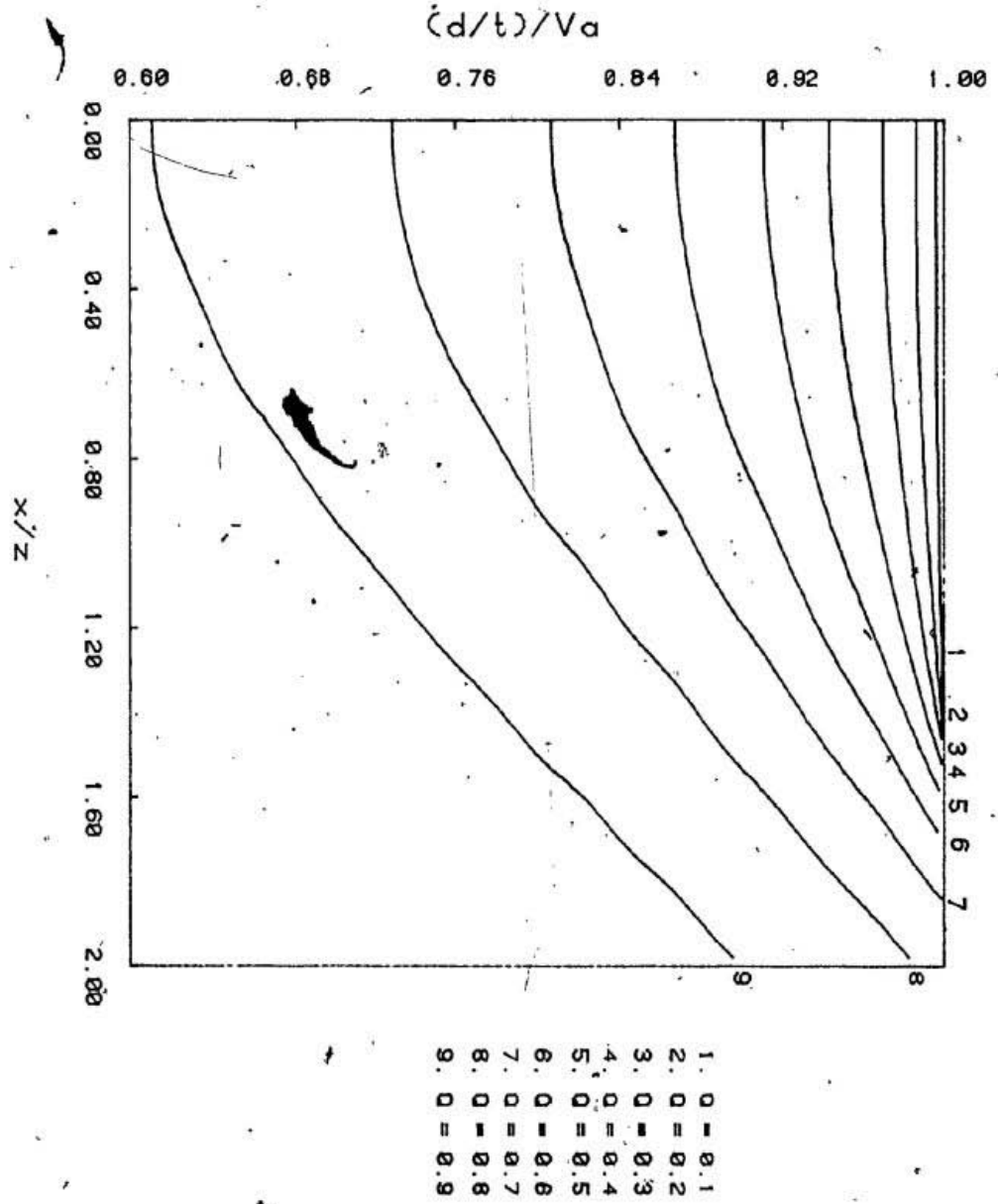

Figure : 3.5.6 (d/t)/Va vs x/z

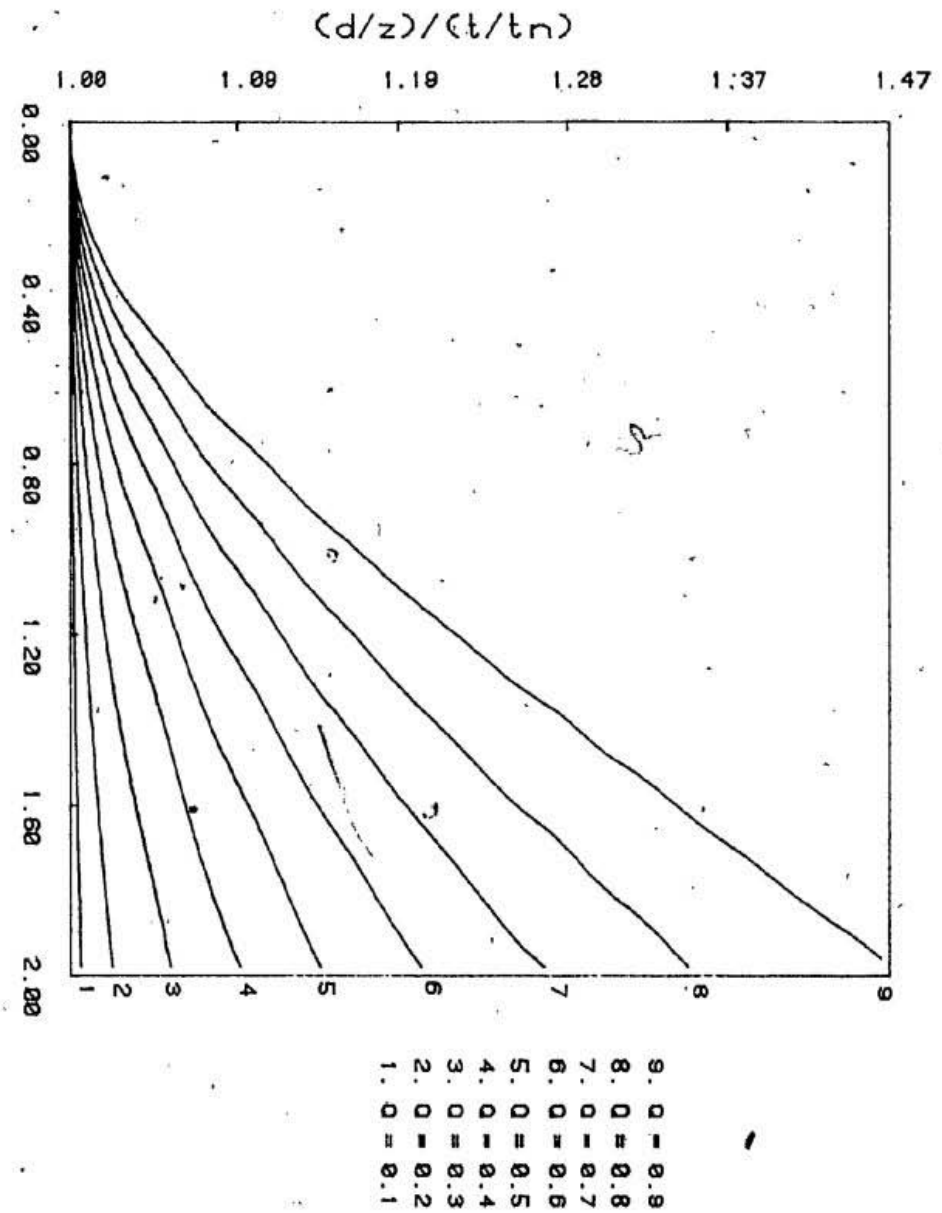

Figure : 3.5.7 (d/z)/(t/tn) vs x/z

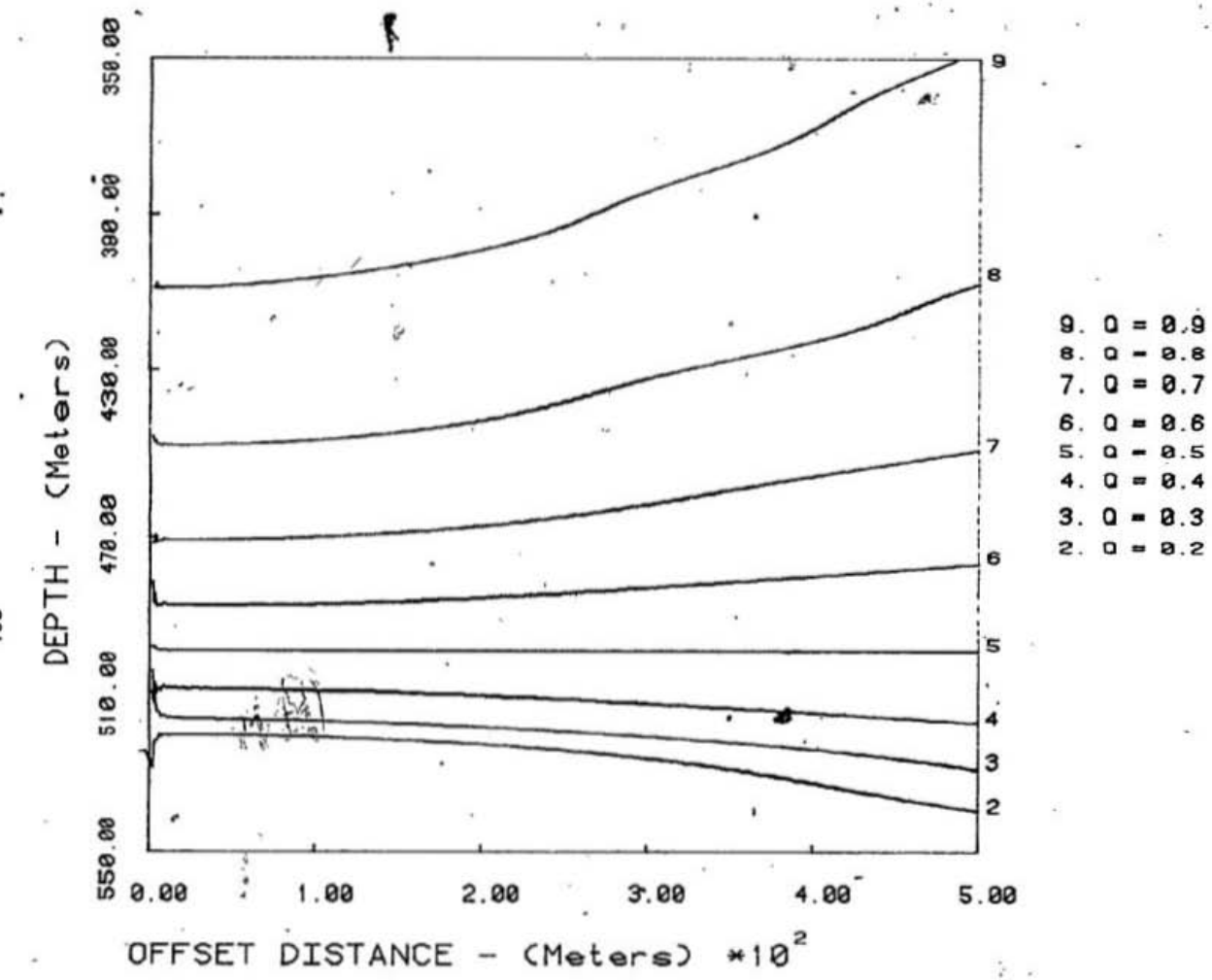

Figure : 3.5.8 Parameter Estimation using Normal Moveout for the Linear Velocity Profile Model.

System Parameters : Q = 0.5 , Z0 = 500 (Meters)

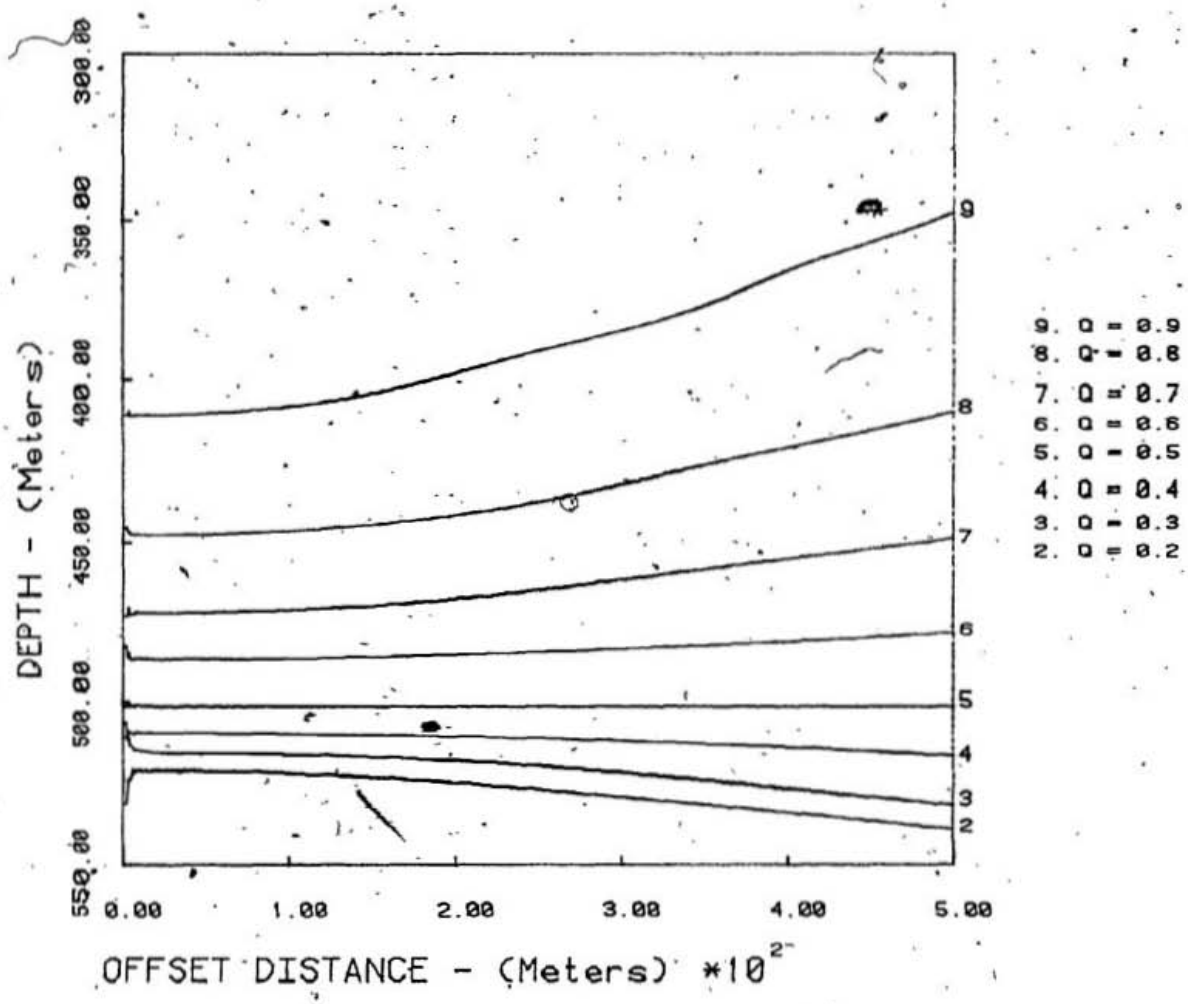

Figure : 3.5.6 Parameter Estimation using Normal Moveout for the Linear Velocity Profile Model.

System Parameters : Q = 0.5 , Z0 = 500 (Meters)

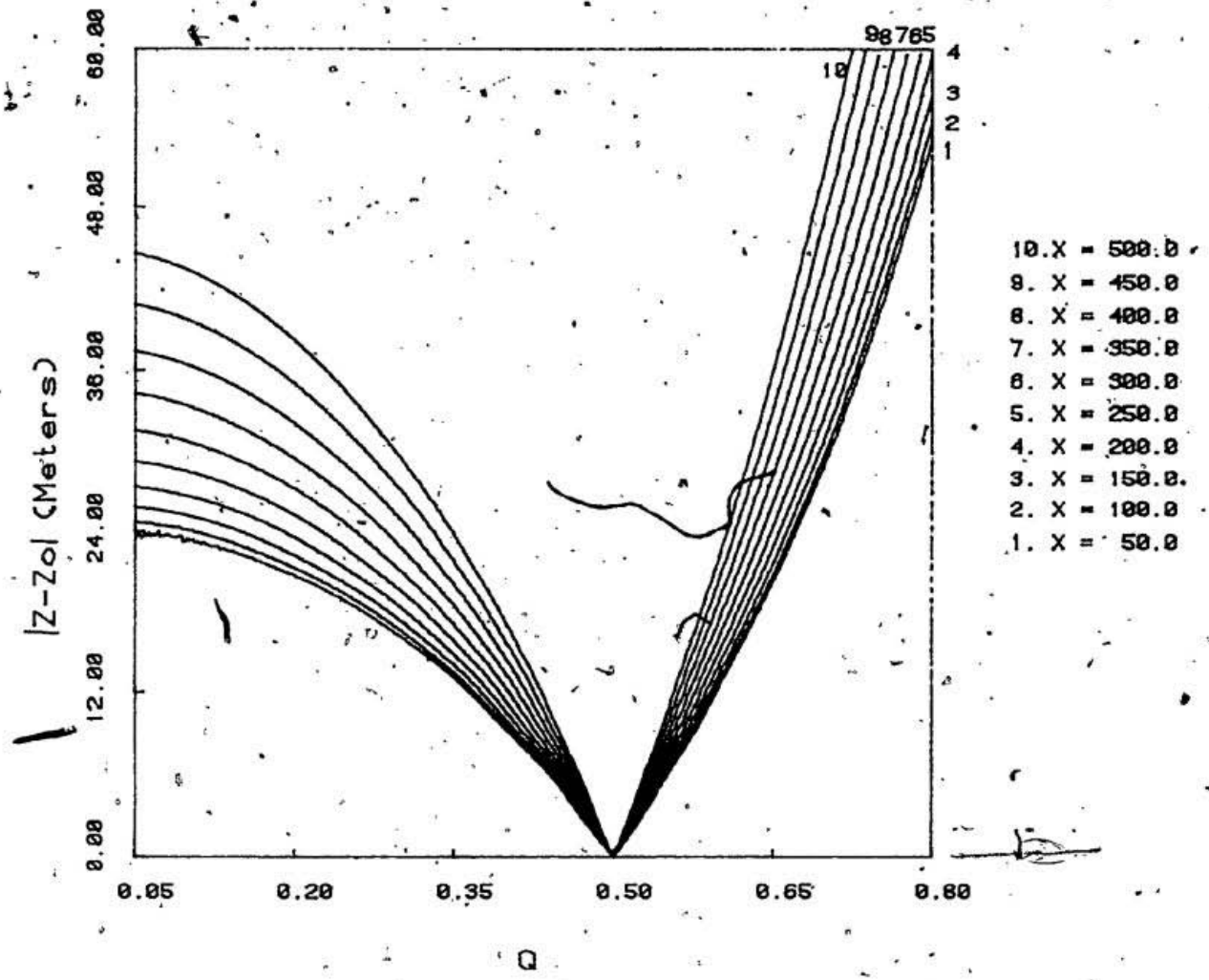

Figure : 3.5.9 Q vs Estimation Error for different offset - X (Meters)

System Parameters : Q = 0.5 , Zo = 500.0 (Meters)

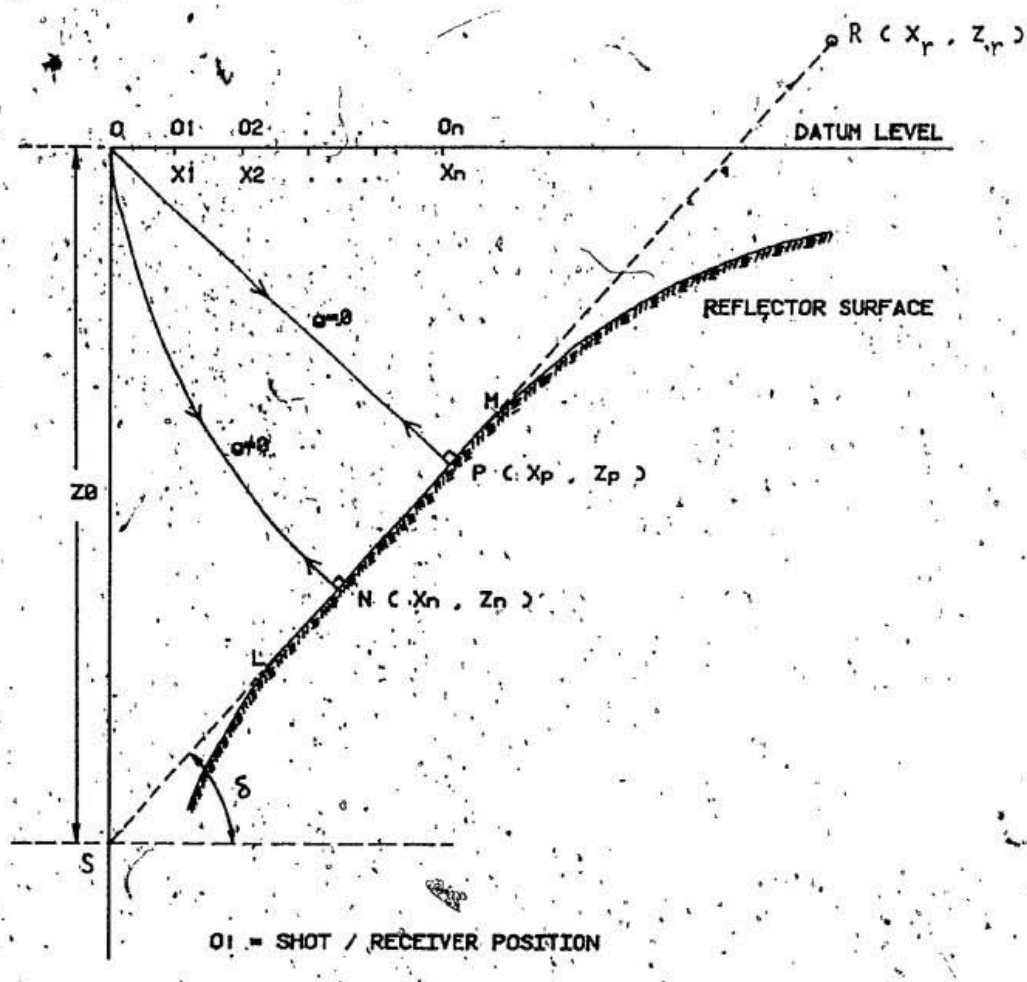

FIGURE : 4.1.1

1 - D. LINEAR VELOCITY PROFILE MODEL.

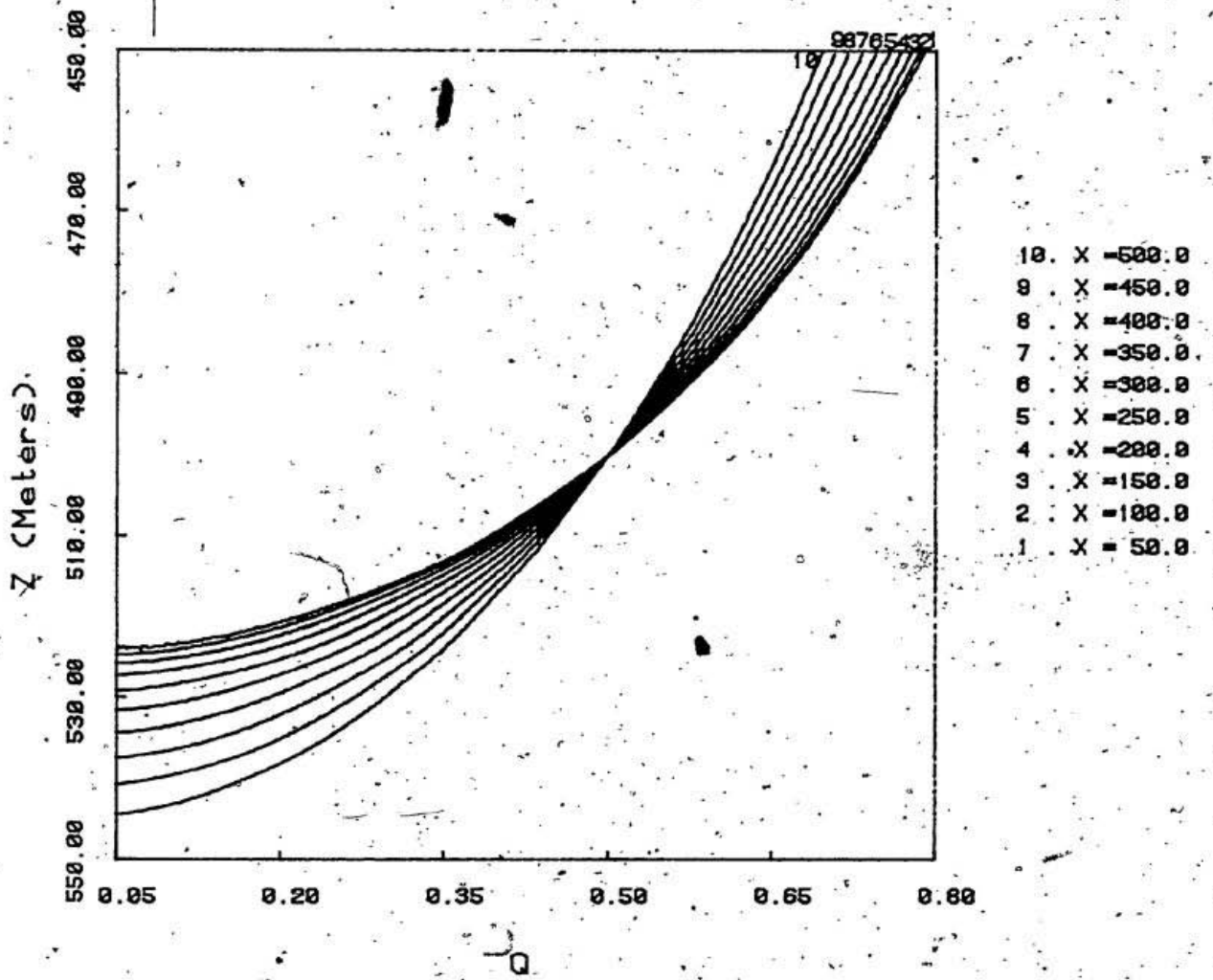

Figure : 3.5.10 Q vs Estimated Depth - Z for different - X (Meters)

System Parameters : Q = 0.5 , Zo = 500.0 (Meters)

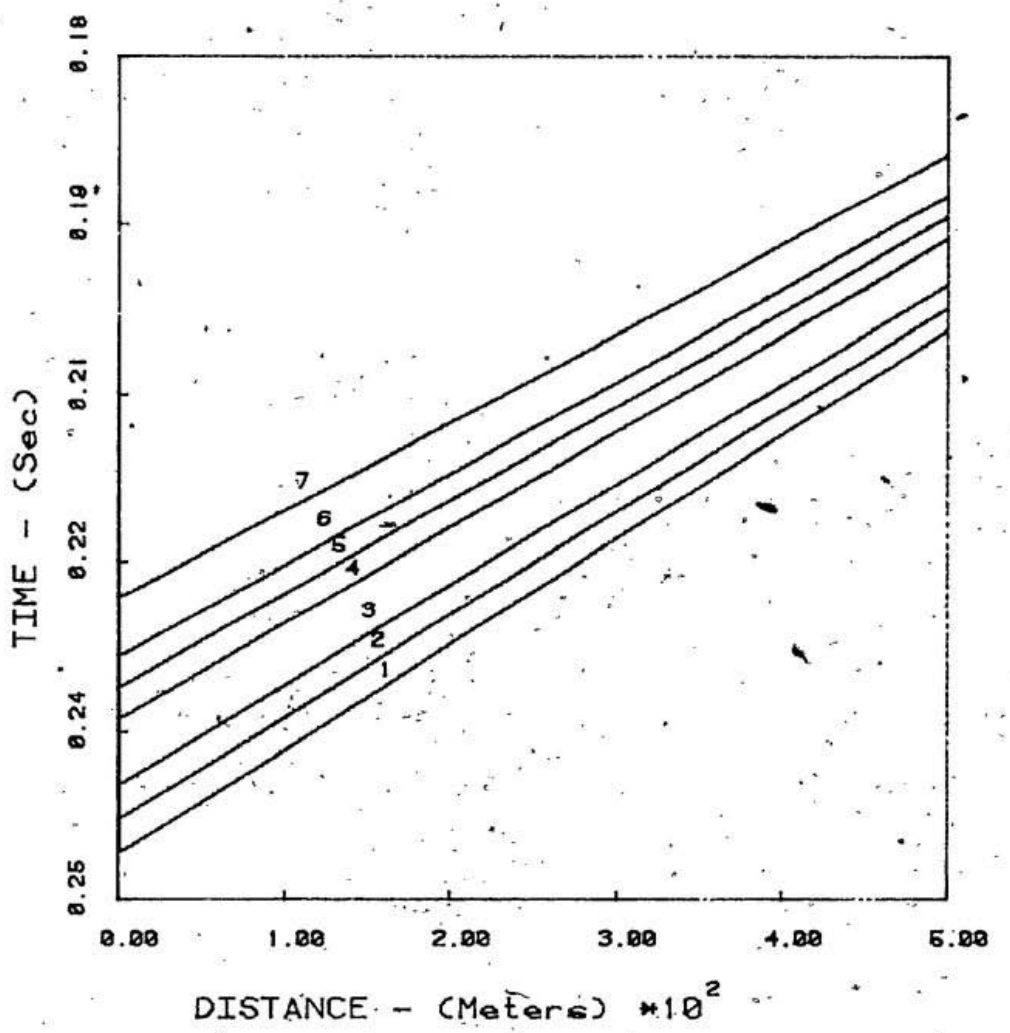

Figure - 5.1.1 Time vs Distance plot for Linear Velocity Profile Model

True Reflector Geometry $Z = Z0 - X * TAN(\delta)$ δ = 10.0 (Degrees)

Z0 = 500.0 (Meters) V0 = 2000.0 (Meters/sec)

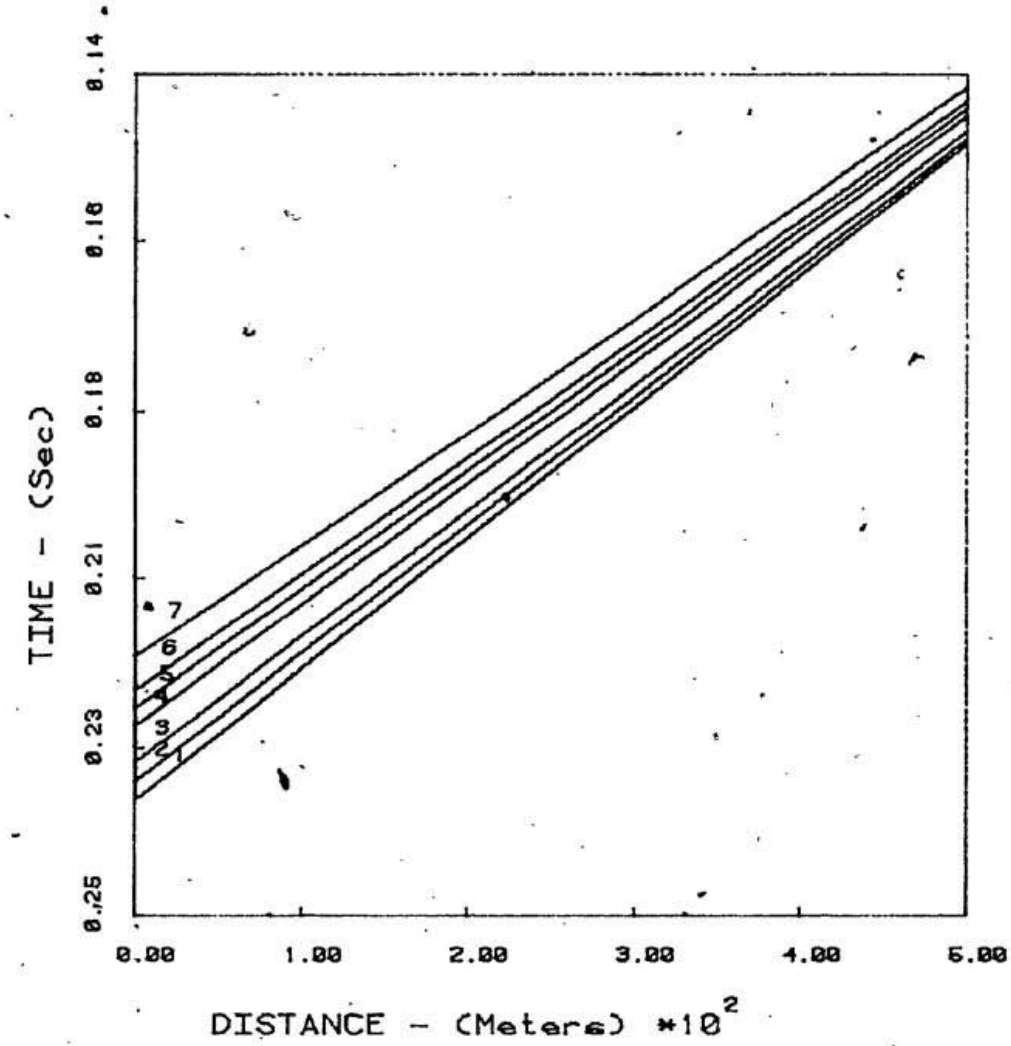

Figure - 5.1.2 Time vs Distance plot for Linear Velocity Profile Model

True Reflector Geometry $Z = Z0 - X * TAN(\delta)$ $\delta = 20.0$ (Degrees)

Z0 = 500.0 (Meters) V0 = 2000.0 (Meters/sec)

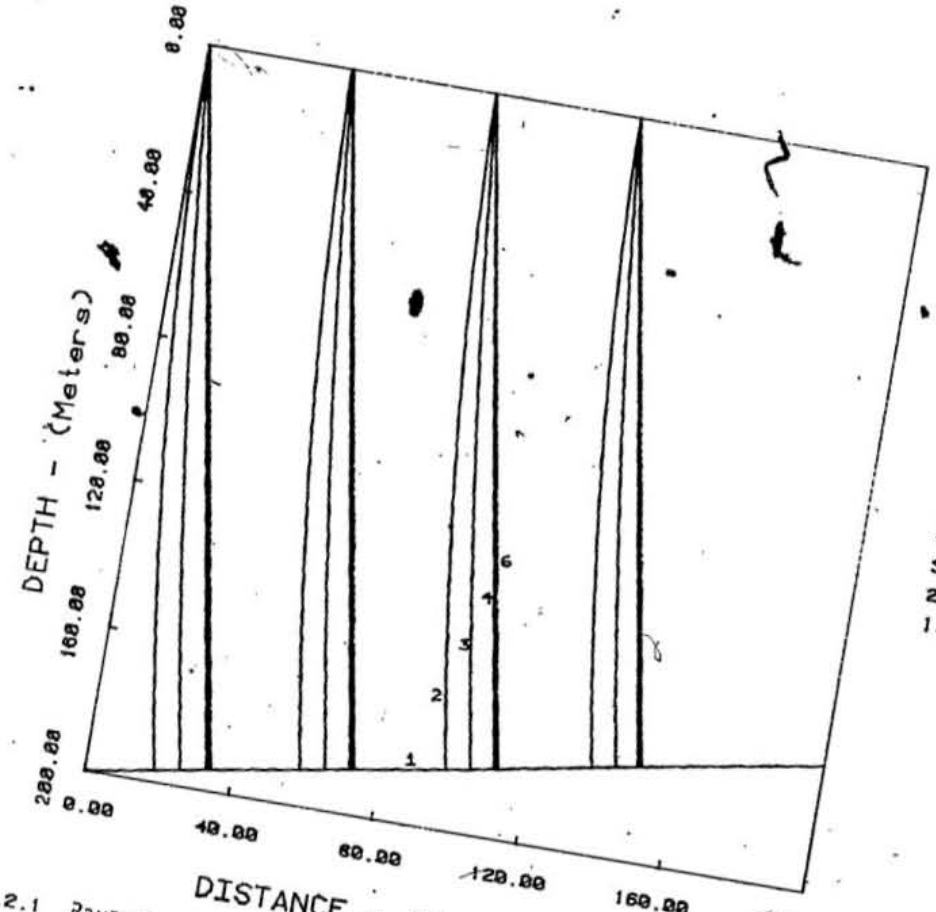

Figure - 5.2.1 Raypaths for Linear Velocity Profile Model
True Reflector Geometry Z = Z0 - X * TAN (δ)
V0 = 2000.0 (Meters/sec) δ = 10 (Degrees)

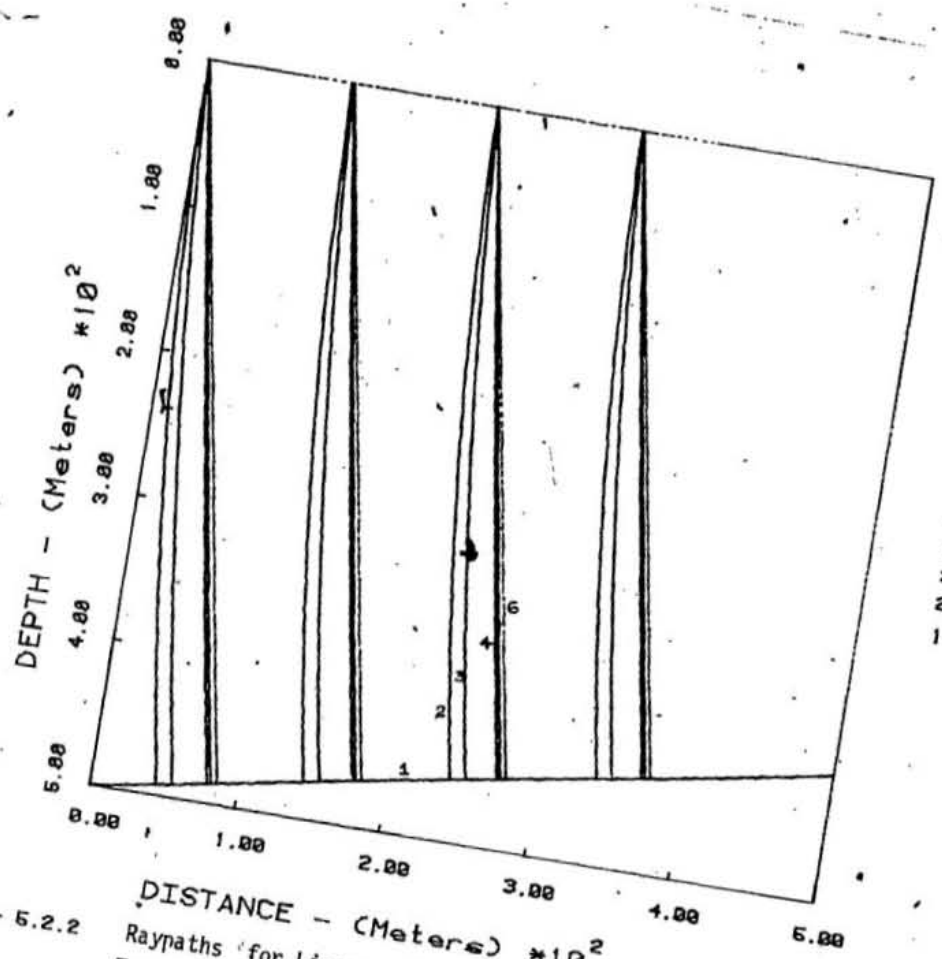

6. σ = 0.0
5. σ = 0.5
4. σ = 0.6
3. σ = 10.0
2. σ = 100.0
1. True Reflector Geometry

Figure - 5.2.2 Raypaths for Linear Velocity Profile Model
True Reflector Geometry $Z = Z0 - X * TAN(\delta)$
V0 = 2000.0 (Meters/sec) δ = 10 (Degrees)

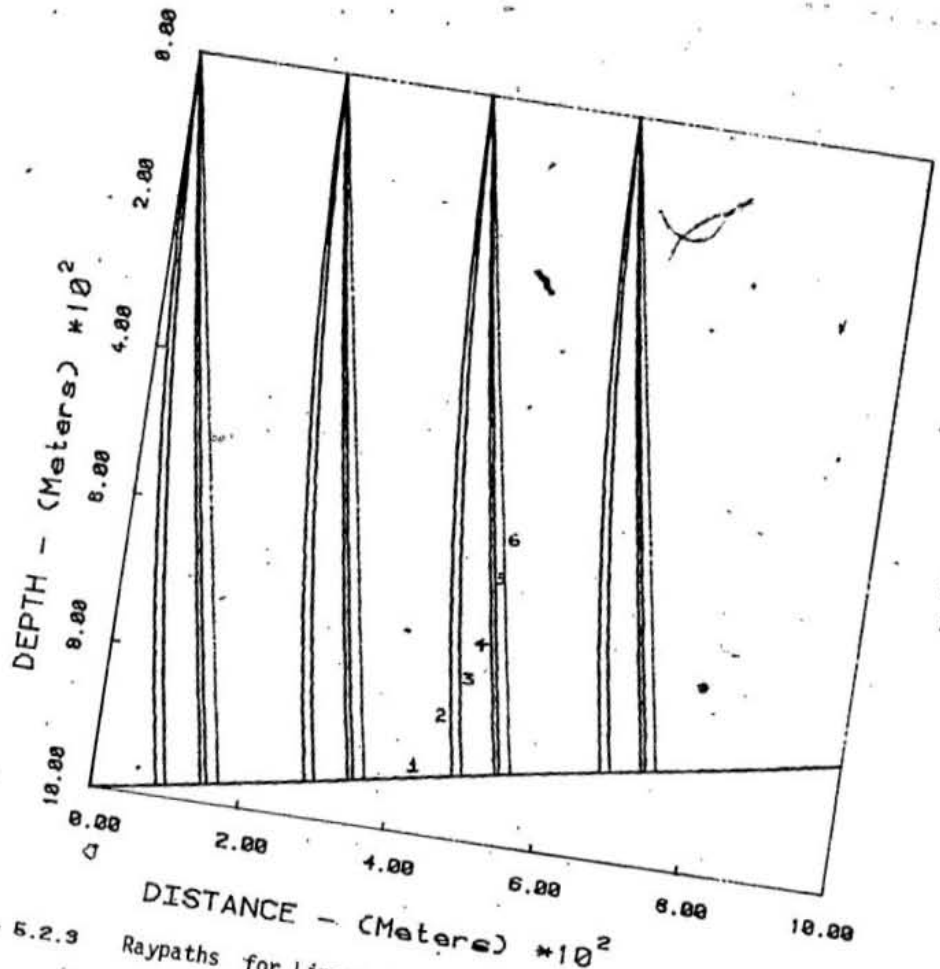

6. θ = 0.0
5. θ = 0.5
4. θ = 0.6
3. θ = 10.0
2. θ = 100.0
1. True Reflector Geometry

Figure - 5.2.3 Raypaths for Linear Velocity Profile Model
True Reflector Geometry Z = Z0 - X * TAN (δ)
V0 = 2000.0 (Meters/sec) δ = 10 (Degrees)

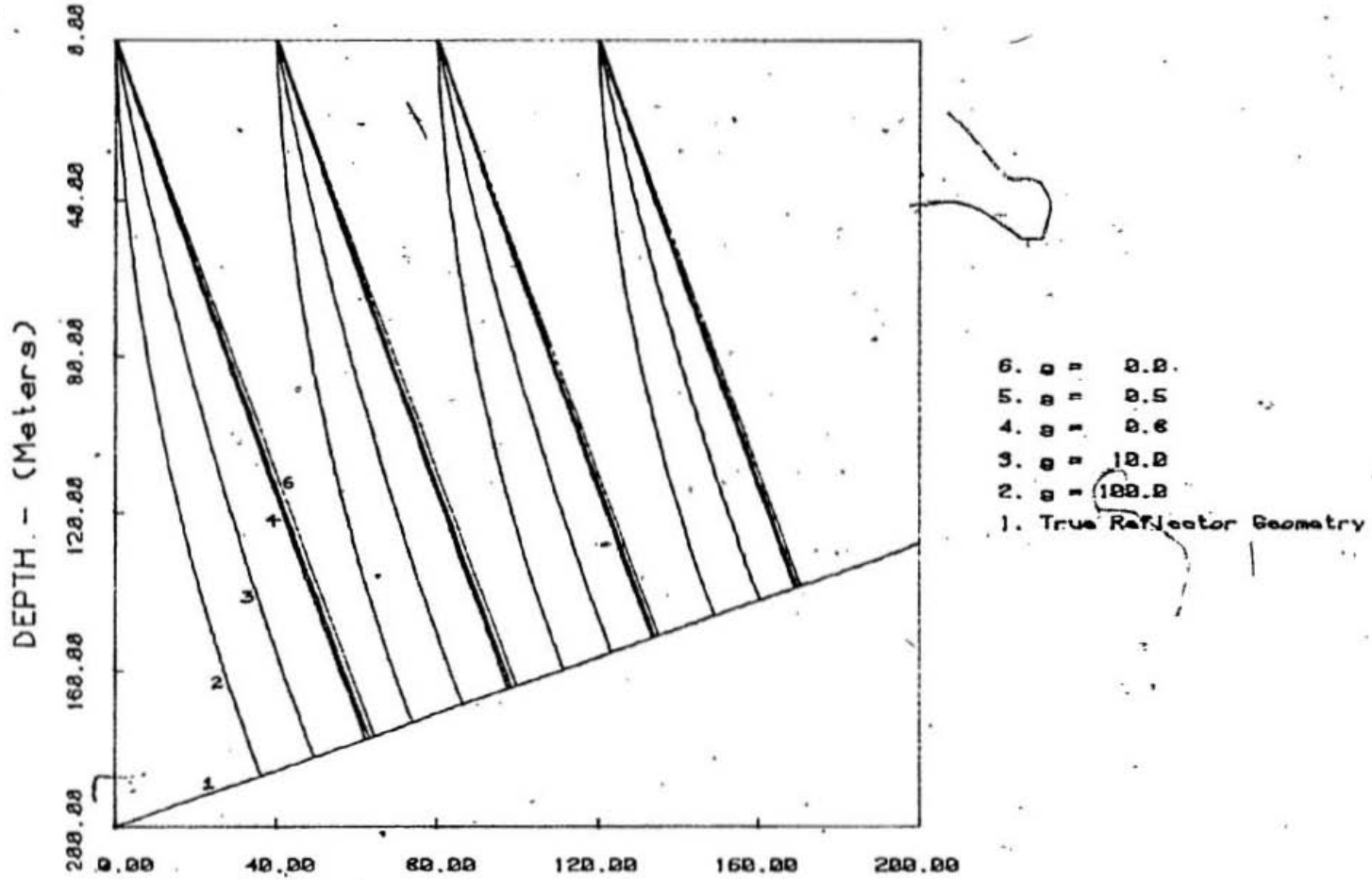

Figure - 5.2.4 Raypaths for Linear Velocity Profile Model
True Reflector Geometry $Z = Z0 - X * TAN(\delta)$
V0 = 2000.0 (Meters/sec) δ = 20.0 (Degrees).

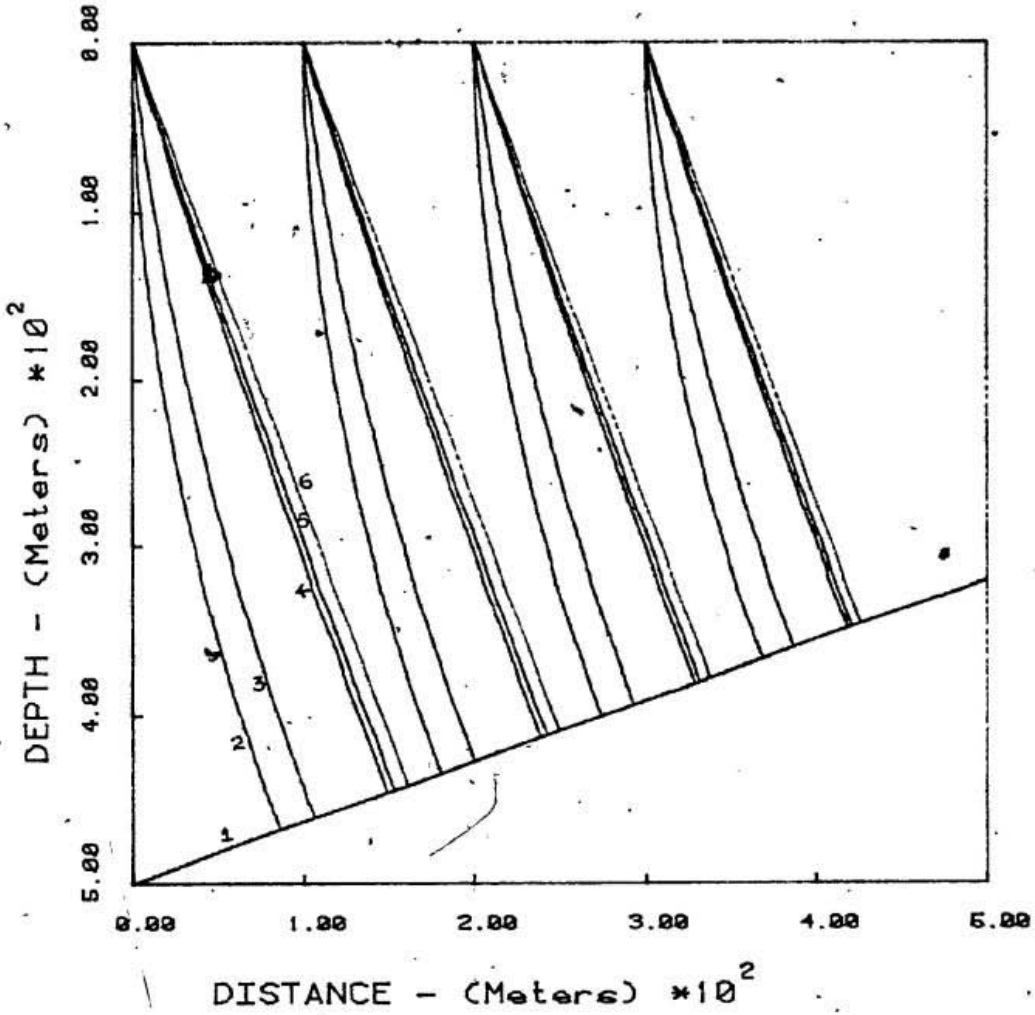

Figure - 5.2.5 Raypaths for Linear Velocity Profile Model
True Reflector Geometry $Z = Z0 - X * TAN\ (\delta)$
V0 = 2000.0 (Meters/sec) , δ = 20.0 (Degrees)

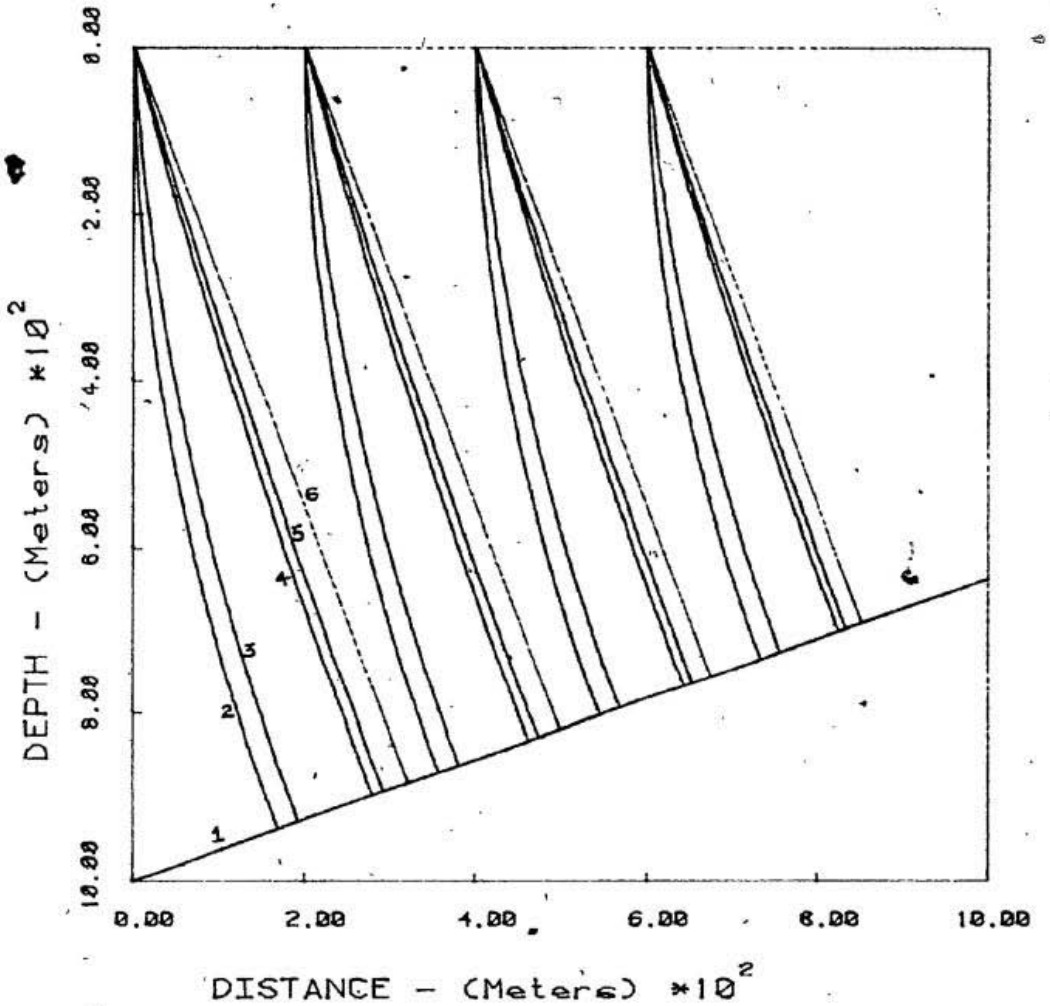

Figure - 5.2.6 Raypaths for Linear Velocity Profile Model

True Reflector Geometry $Z = Z0 - X * TAN(\delta)$

$V0 = 2000.0$ (Meters/sec) $\delta = 20.0$ (Degrees)

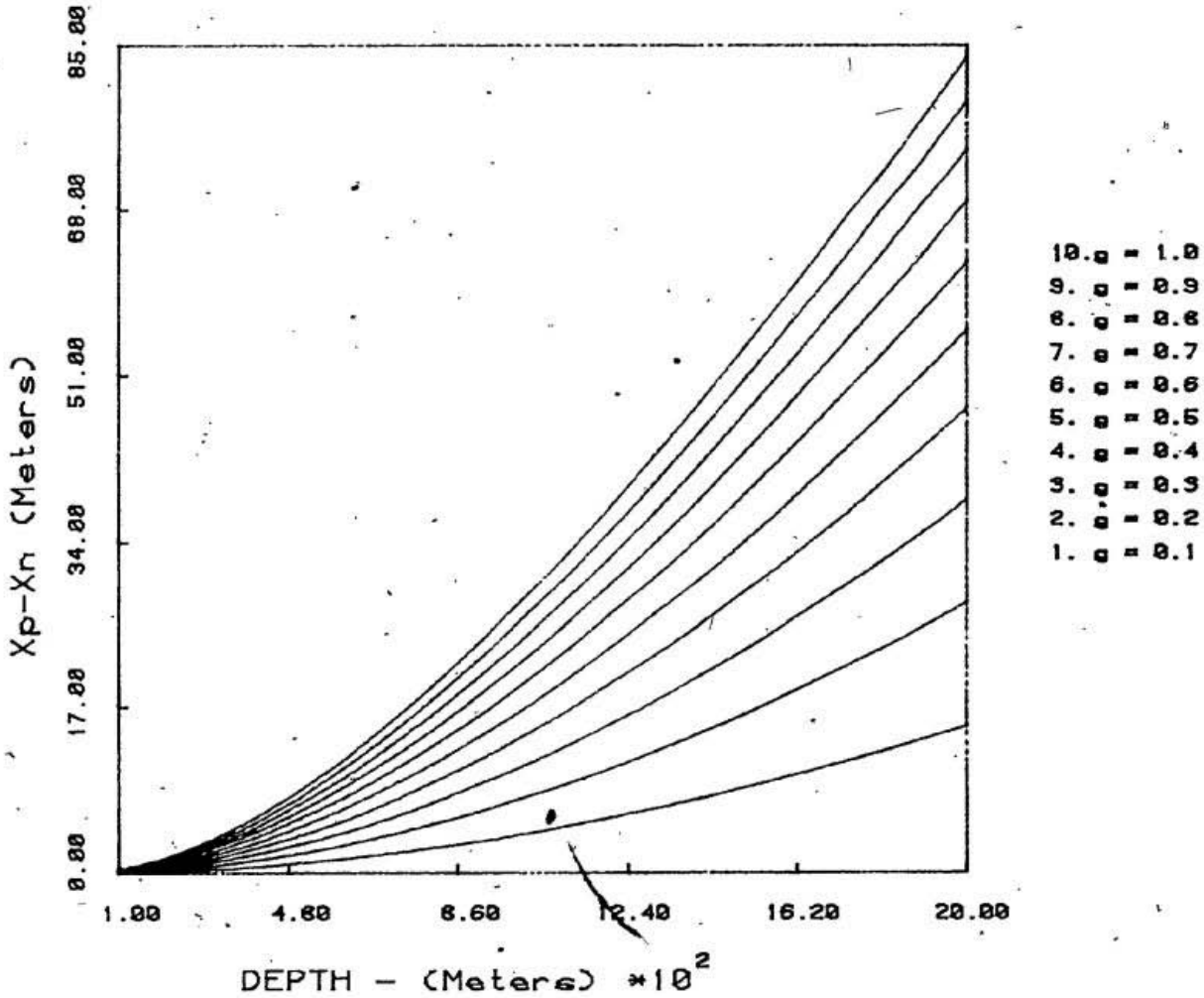

Figure - 5.3.7 - Depth Zo,v= Error due to Constant Velocity Assumption
δ = 10.0 (Degrees) , V0 = 2000.0 (Meters/sec)

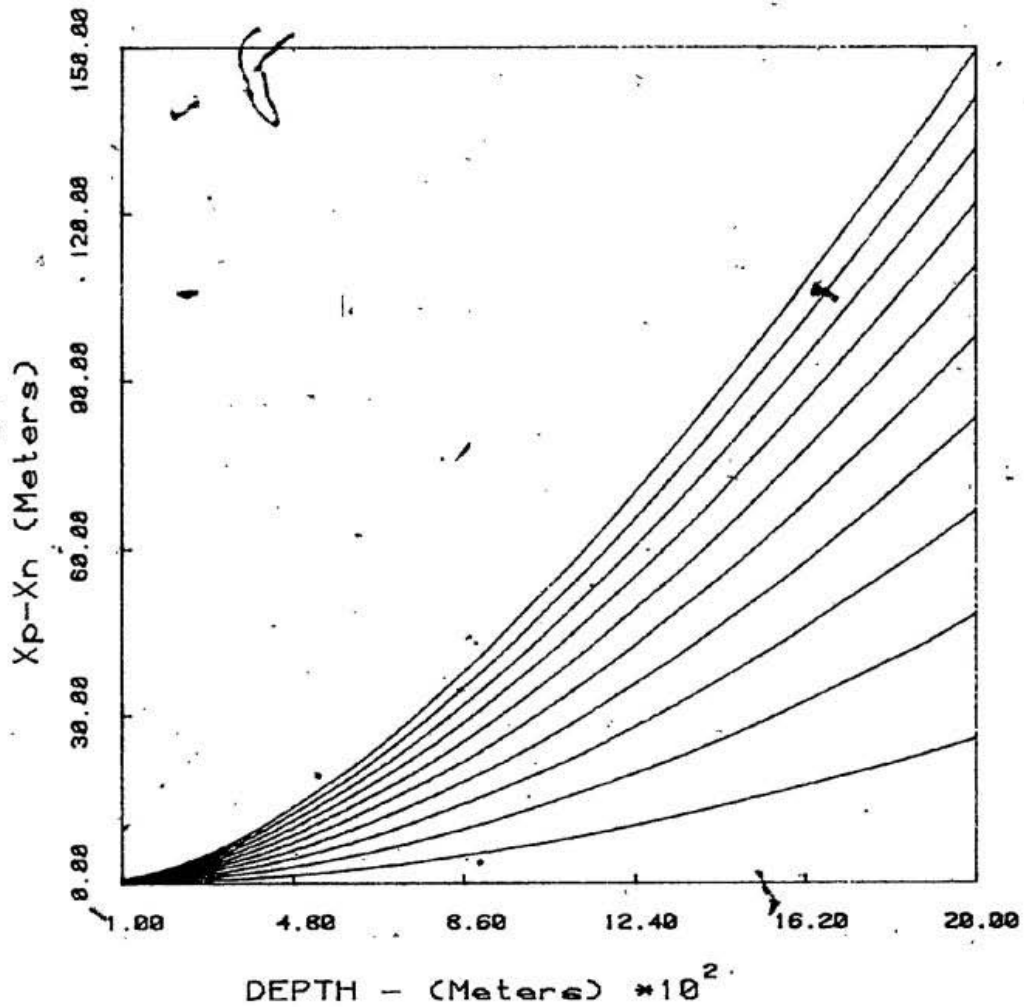

Figure - 5.3.8 Depth Zo v = Error due to Constant Velocity Assumption
δ = 20.0 (Degrees) , V0 = 2000.0 (Meters/sec)

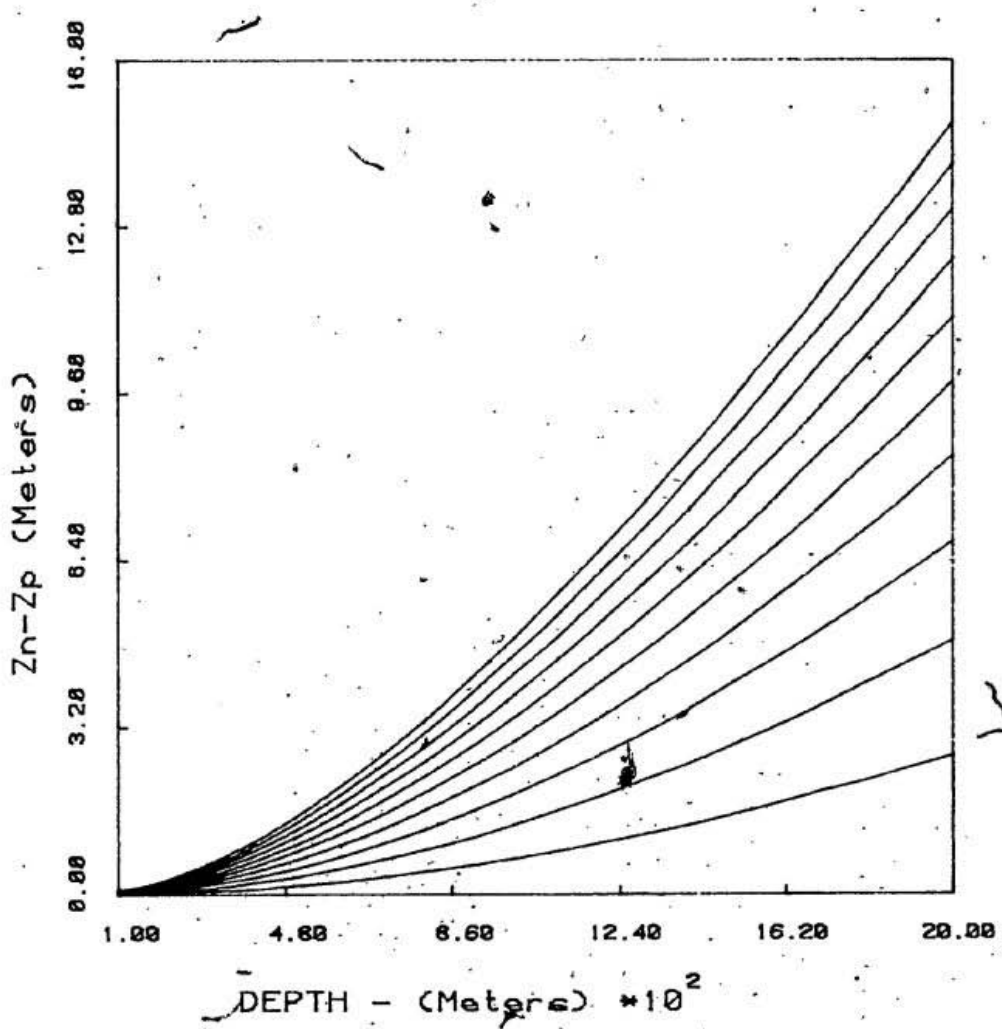

Figure - 5.3.9 - Depth Zo v = Error due to Constant Velocity Assumption
δ = 10.0 (Degrees) V0 = 2000.0 (Meters/sec)

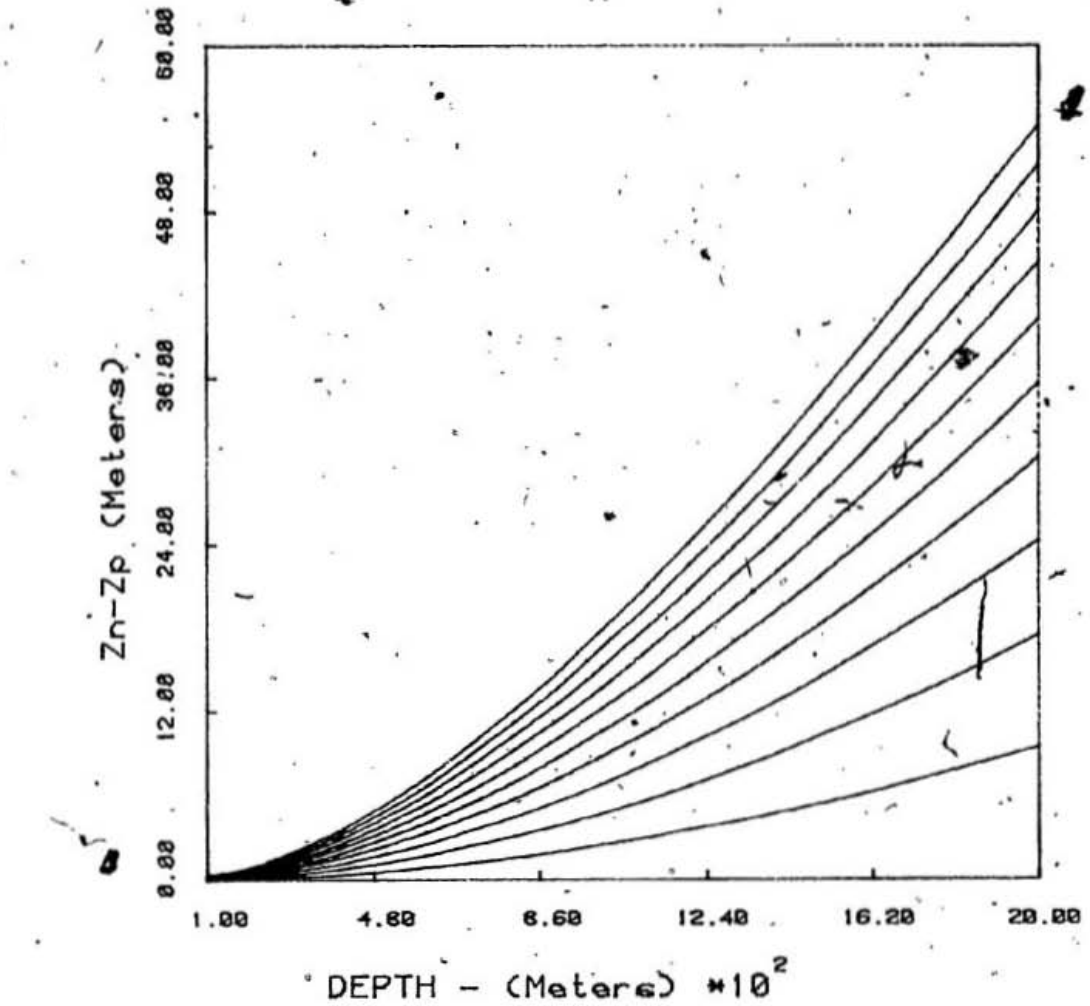

Figure - 5.3.10 Depth Zo v = Error due to Constant Velocity Assumption
δ = 20.0 (Degrees) , V0 = 2000.0 (Meters/sec)

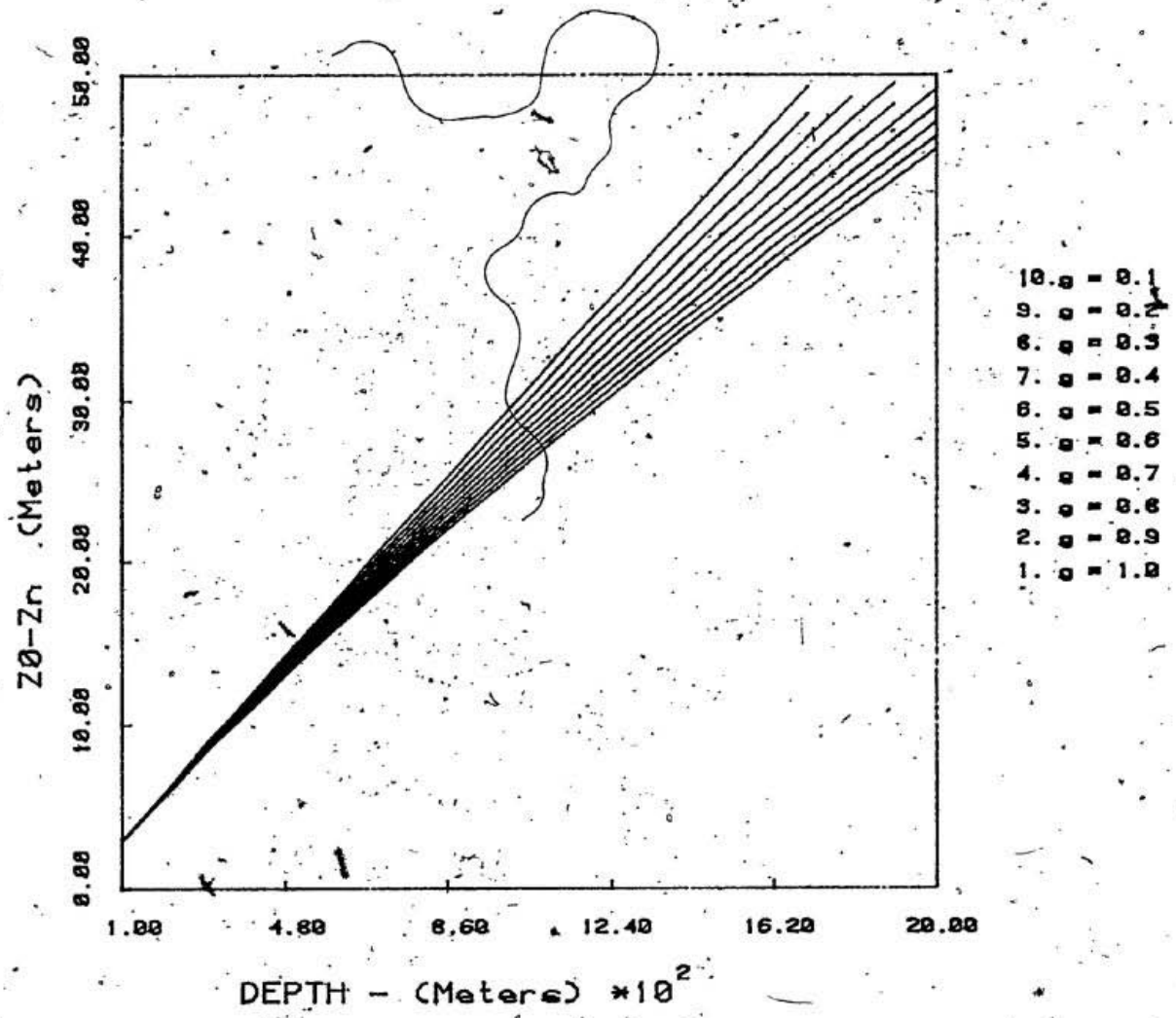

Figure - 5.3. 11 Depth Zo v. = Error for 1-1 correspondence
δ = 10.0 (Degrees) , V0 = 2000.0 (Meters/sec)

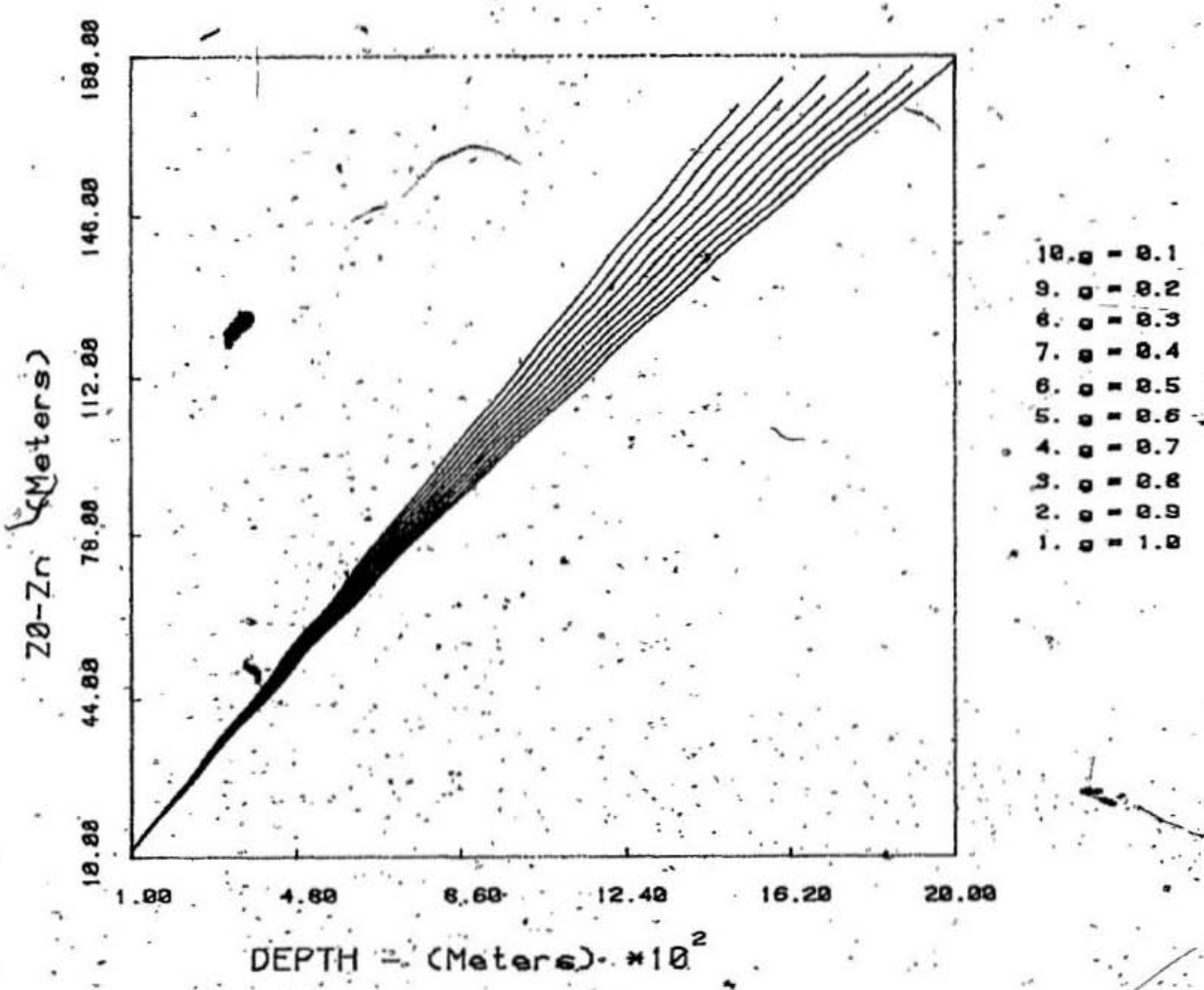

Figure - 6.3.12 Depth Zo v = Error for 1-1 correspondence
δ = 20.0 (Degrees) V0 = 2000.0 (Meters/sec)

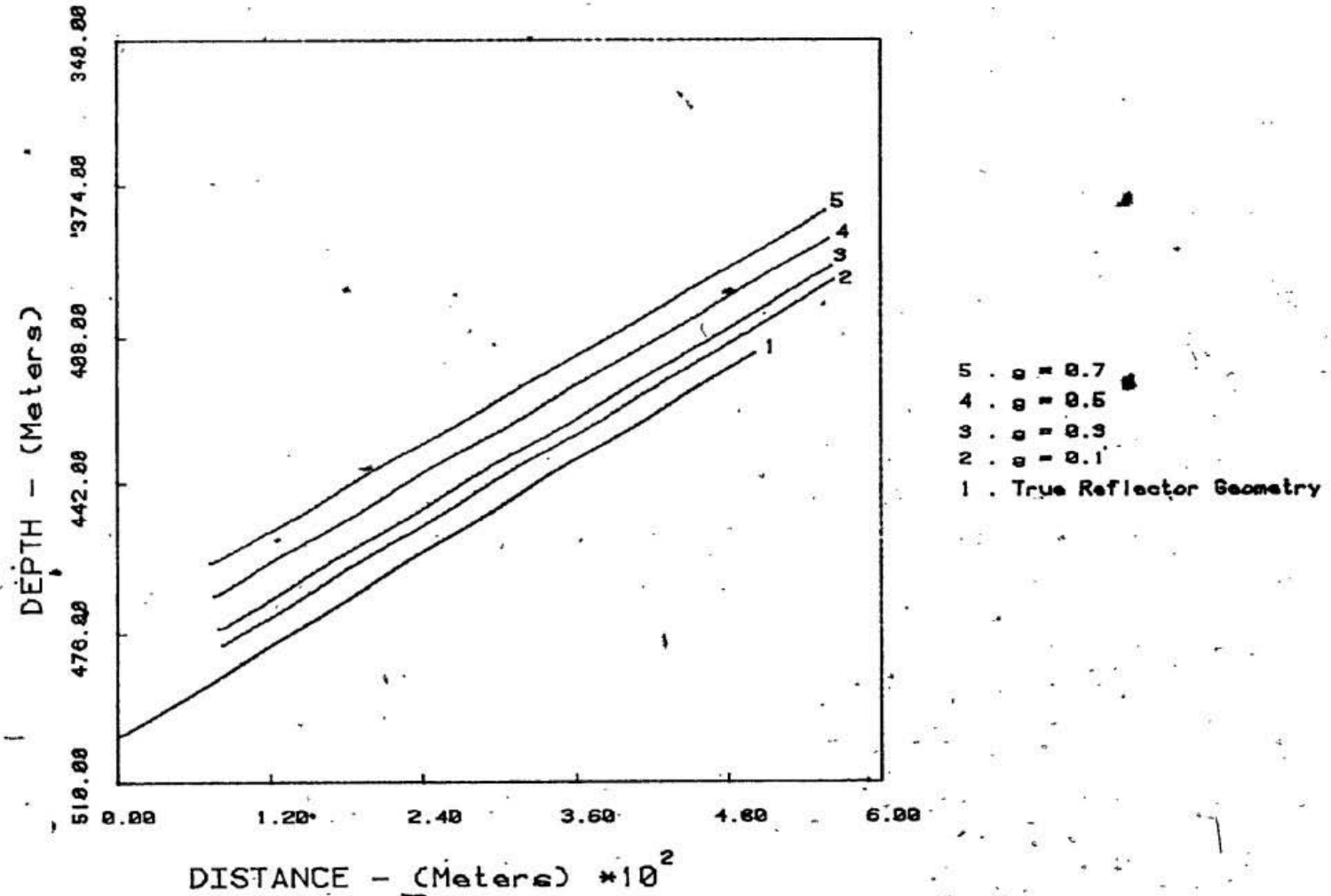

Figure - 5.4.1 Errors due to Constant Velocity Assumption

V_0 = 20000.0 (meters/sec) Z_0 = 500 (Meters) , δ = 10 (Degrees)

True Reflector Geometry $Z = Z_0 - X * TAN(\delta)$

- The different g values are used for different x-t data simulations.
- In the reverse computation the average velocity of the data generating system is used as V_o.

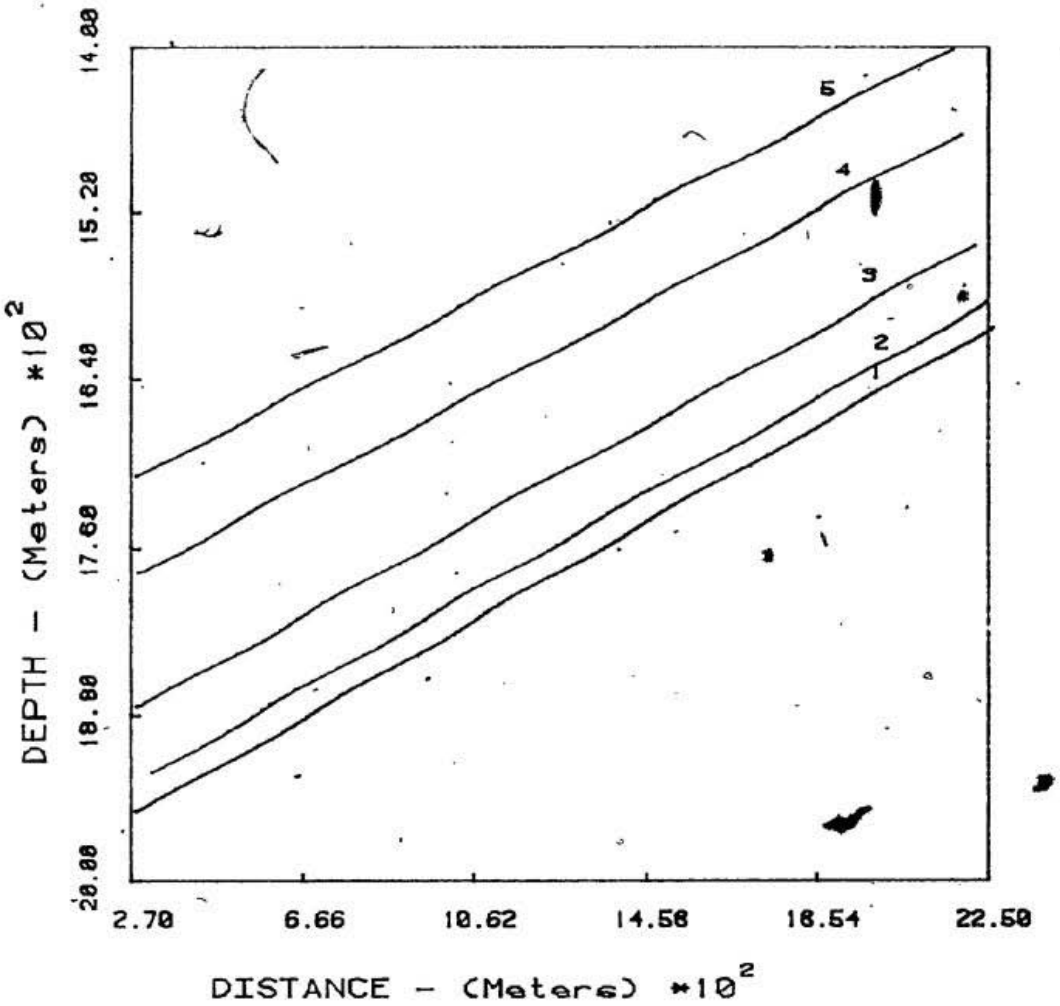

Figure - 5.4.2 Errors due to Constant Velocity Assumption

V0 =2000.0(meters/sec) , Z0 = 2000 (Meters) δ = 10 (Degrees)

True Reflector Geometry Z = Z0 - X * TAN (δ)

.The different g values are used for different x-t data simulations.

. In the reverse computation the average velocity of the data generating system is used as V_0.

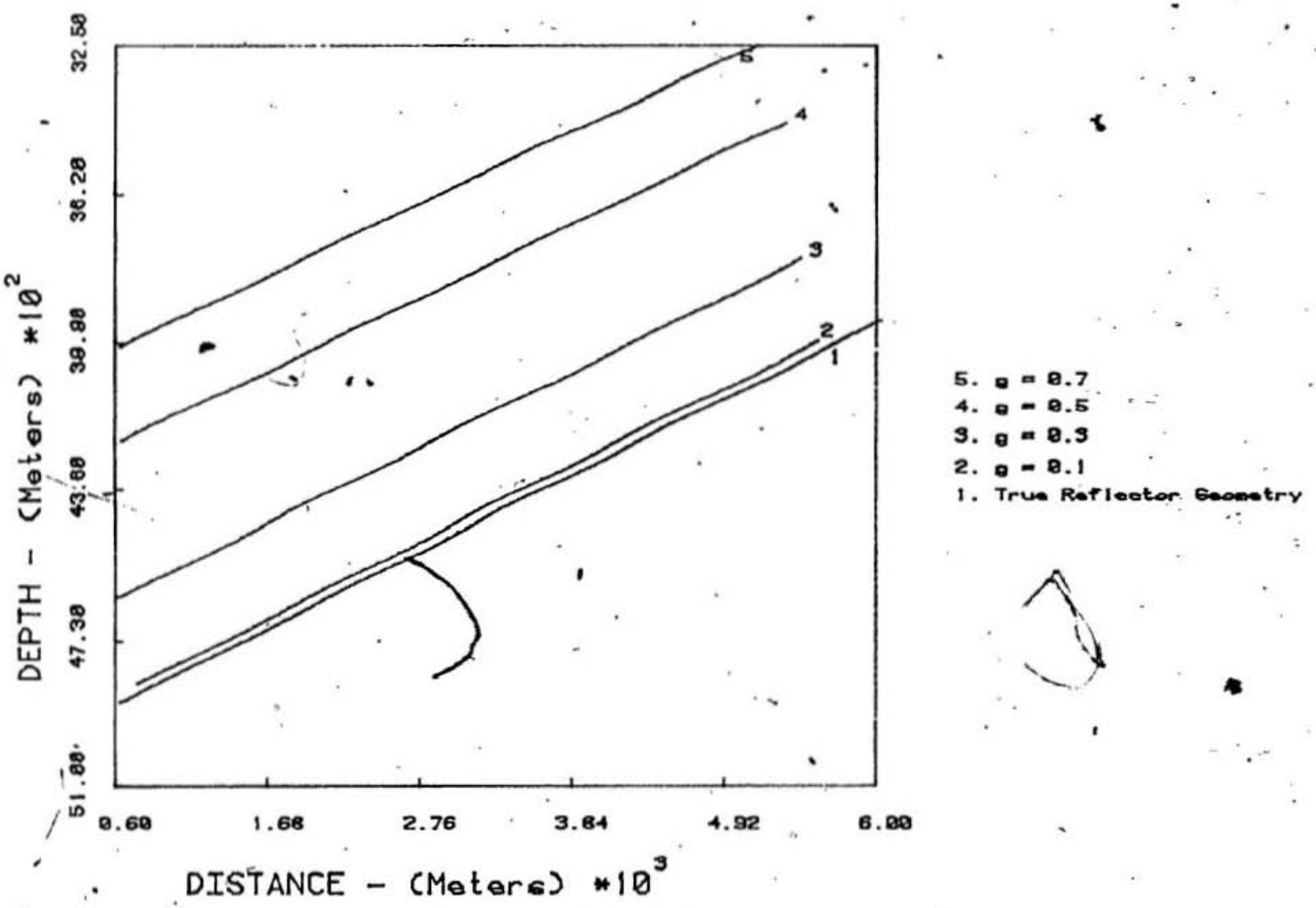

Figure - 5.4.3 Errors due to Constant Velocity Assumption
V0 = 2000.0(meters/sec) , Z0 = 5000 (Meters) , δ = 10 (Degrees)
True Reflector Geometry $Z = Z0 - X * TAN(\delta)$

.The different g values are used for different x-t data simulations.

.In the reverse computation the average velocity of the data generating system is used as V_o.

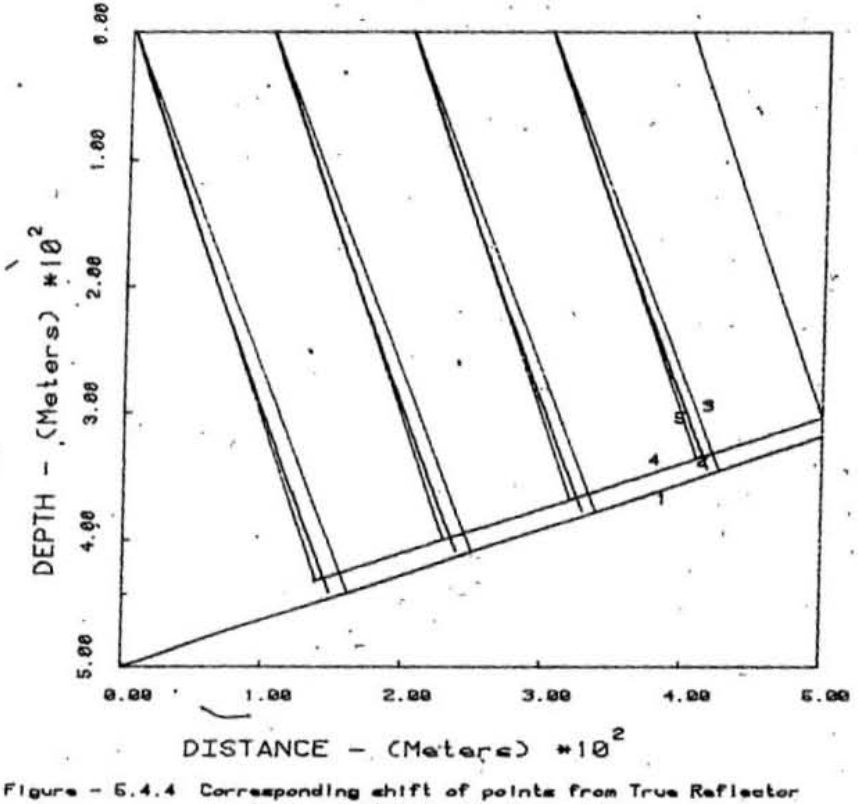

5. ϱ = 0.0
4. Estimated Reflector Geometry
3. ϱ = 0.0
2. ϱ = 0.6
1. True Reflector Geometry

Figure - 6.4.4 Corresponding shift of points from True Reflector due to Constant Velocity Assumption
True Reflector Geometry : $Z = Z0 - X * \tan(\delta)$, δ = 20 (Degrees)
Z0 = 500 (Meters) , V_0 = 2000.0 (meters/sec)

. In the reverse computation the average velocity of the data generating system is used as V_0.

TABLE 5.3

ERRORS DUE TO CONSTANT VELOCITY ASSUMPTION IF THE MEDIUM HAS A LINEAR VELOCITY PROFILE

Slope (Degrees) 20.00000

VELOCITY GRADIENT - g (1/Sec) 0.5000000

Z_o	X_P	Z_P	X_n	Z_n
100.0000	32.13939	88.30222	31.79252	88.42847
200.0000	64.27877	176.6044	62.91964	177.0991
300.0000	96.41815	264.9066	93.42361	265.9966
400.0000	128.5575	353.2089	123.3440	355.1064
500.0000	160.6969	441.5111	152.7130	444.4170
600.0000	192.8363	529.8133	181.5642	533.9160
700.0000	224.9757	618.1155	209.9285	623.5923
800.0000	257.1151	706.4177	237.8338	713.4355
900.0000	289.2545	794.7200	265.3046	803.4370
1000.000	321.3939	883.0222	292.3662	893.5874
1100.000	353.5332	971.3244	319.0387	983.8794
1200.000	385.6726	1059.627	345.3450	1074.305
1300.000	417.8120	1147.929	371.3052	1164.856
1400.000	449.9514	1236.231	396.9340	1255.528
1500.000	482.0908	1324.533	422.2502	1346.313
1600.000	514.2302	1412.835	447.2700	1437.207
1700.000	546.3695	1501.138	472.0066	1528.204
1800.000	578.5089	1589.440	496.4737	1619.298
1900.000	610.6483	1677.742	520.6858	1710.486
2000.000	642.7877	1766.044	544.6538	1801.762

Z_o	X_P-X_n	Z_n-Z_P	Z_o-Z_n
100.0000	0.3468628	0.1262512	11.57153
200.0000	1.359131	0.4946899	22.90088
300.0000	2.994537	1.089935	34.00342
400.0000	5.213531	1.897583	44.89355
500.0000	7.983887	2.905884	55.58301
600.0000	11.27206	4.102722	66.08398
700.0000	15.04724	5.476746	76.40771
800.0000	19.28123	7.017822	86.56445
900.0000	23.94986	8.717041	96.56299
1000.000	29.02768	10.56519	106.4126
1100.000	34.49454	12.55499	116.1206
1200.000	40.32761	14.67810	125.6953
1300.000	46.50684	16.92712	135.1440
1400.000	53.01743	19.29675	144.4722
1500.000	59.84055	21.78015	153.6865
1600.000	66.96021	24.37158	162.7930
1700.000	74.36288	27.06392	171.7964
1800.000	82.03525	29.85840	180.7017
1900.000	89.96252	32.74365	189.5142
2000.000	98.13391	85.71777	198.2378